NTNU

Norwegian University of
Science and Technology

Study of Long Range Transported Pollutants in Arctic Soil

Carolin Elisabeth Huber

Environmental Toxicology and Chemistry
Submission date: May 2017
Supervisor: Øyvind Mikkelsen, IKJ
Co-supervisor: Eiliv Steinnes, IBI

Norwegian University of Science and Technology
Department of Chemistry

Preface

This thesis was carried out in the *Environmental Chemistry and Toxicology* (ENVITOX) program from the autumn semester 2015 until the spring semester 2017. Field work and sampling was performed in July 2016 in Longyearbyen and Ny Ålesund. The field work was funded by Forskingrådet. The project can be found at the RIS database with the number 10425.

The analysis of background soil samples from Svalbard has also been performed by two other NTNU students, Katarina Halbach (2016) and Marit Elisabeth Fors (2014). While those previous works focused mainly on elemental analysis, this work aims to point out occurring correlations on different sampling sites and also works on the analysis of Polychlorinated Biphenyls.

Trondheim, 2017-05-10

signature

Carolin Elisabeth Huber

Acknowledgment

I would like to thank the following persons for their great help during the time of accomplishing this work:
My main supervisor Øyvind Mikkelsen, for guidance throughout the project and helpful feedback on the results and for support during sampling in Svalbard. Rudolf Schmidt for the guidance through the GC-MS part. I also thank Syverin Lierhagen for the ICP-MS analysis.
Dorien Dunnebier for the helpful suggestions during the last weeks of writing.

C.H.

Abstract

In this master thesis, levels of Polychlorinated Biphenyls (PCBs), total organic carbon (TOC) and potentially long range transported inorganic elements (Cd, Hg and Pb) in surface soil and vegetation have been studied for samples from Svalbard (Norwegian Arctic). 74 soil and 35 vegetation samples were taken at six different sampling sites which provide background levels.

For measurement of PCBs in soil a method had been developed for the use of accelerated solvent extraction and gas chromatography coupled with tandem mass spectrometry. Different cleanup methods have been tested.

Results maintained from a certified laboratory showed abundance of PCB 52 in soil and vegetation samples with a mean of 3,0 ± 1,2 ng/g in soil and 5,9 ± 2,5 ng/g in vegetation. PCB 180 was found for sample sites in Leinstranda (Ny Ålesund). PCB 28 was found in two vegetation samples. Other measured congeners (101, 118, 138, 153) were under the limit of quantification (LOQ= 1 ng/g).

A mean concentration of Hg of 155 ± 83 ng/g in soil and 97,4 ± 32,8 ng/g in vegetation was obtained, with significant higher results for sample sites close to Longyearbyen. Hg significantly correlates with S and Cl in soil. Measured Pb levels in soil show a mean of 31,5 ± 10,6 μg/g and seem to result from the soil parent material. Cd levels (mean 0,489 ± 0,295 μg/g in soil) were high correlated with TOC. Higher levels and variation was found for Cd in vegetation samples (0,595 ± 0,371 μg/g).

Acronyms

ACP Arctic contamination potential

AMAP Arctic monitoring and assessment program

ASE Accelerated solvent extraction

CBz Chlorobenzene

CLTRAP Convention on long range transboundary pollution

DDE Dichlorodiphenyldichlorethene

DDT Dichlorodiphenyltrichlorethane

DL/ NDL Dioxin like/ non-dioxine like

FA Factor analysis

GC Gas chromatography

Globo-POP Global distribution model of persistent organic pollutants

HCB Hexachlorobenzene

HCH Hexachlorohexane

ISTD Internal standard

RSTD Recovery standard

SIM Single ion monitoring

SOM Soil organic matter

TOC Total organic carbon

K$_{AW}$ Partition coefficient between air and water

K$_{OA}$ Partition coefficient between octanol and air

K$_{OC}$ Partition coefficient between solid (organic) phase and water

K$_{OW}$ Partition coefficient between octanol and water

K$_{SA}$ Partition coefficient between soil organic matter and air

LOI Loss on ignition

LRAT Long range atmospheric transport

MS Mass spectrometry

MS/MS Tandem mass spectrometry

OC Organochlorines

PAH Polyaromatic Hydrocarbons

PBDE Polybrominated dipheyl ether

PCB Polychlorinated Biphenyls

PCA Principal component analysis

PCDD Polychlorinated dipenzo-p-dioxin

PCDF Polychlorinated dipenzo-p-furan

PFOS Perfluorooctanesulforic acid

POP Persistent organic pollutant

List of Tables

List of Figures

Contents

Chapter 1

Introduction

The Arctic, as well as the Antarctic, is no longer a pristine environment. Anthropogenic contaminants, like organic compounds, heavy metals, radionuclides and inorganic acids, have found their way through atmospheric transport or marine currents and the marine food chain up to the furthest places on the Earth. Industrial activities, especially since the Second World War, have affected the remote environmental systems of our planet. The first observation of human impact in the Arctic occurred in the 1950s with the observation of Arctic haze by Mitchell[53]. Since then, the observations and publications of human influences in the Arctic regions by air transported pollutants increased and are now (end 2016) described by over 16.700 publications [1].

Since 1979, political efforts have been made to protect the global environment from air pollution. The emissions of contaminants had been gradually reduced thanks to the ratification of international agreements like the Aarhus protocol (1998) or the Stockholm convention (2001). Global monitoring projects, like the *Arctic Monitoring and Assessment Program* AMAP (founded in 1991), provide information on the status of pollutant levels in Arctic regions and scientific advice to governments [5]. Rising levels of organic pollutants, as well as mercury in the Arctic food chain, raises the concern to the human health of Inuit populations, which are linked to a traditional high consumption of marine predators. This brings the topic to an ethical level since human communities are influenced by the environmental effects to which they had not contributed in the industrialization and did not profit from the use of those chemicals.

[1] Number of found publications by a ProQuest database search of the words "*Arctic*" and "*pollutant*" in December 2016. A search of the words "*Arctic*" and "*PCB*" revealed over 3.500 entries

The U.S. State Department has termed the problem of persistent organic pollutants (POPs) in 1996 as *"one of the great environmental challenges the world faces"* [84]. Difficulties in acting fast with global regulations on new emerging long-range transported pollutants are still occurring [31].

Polychlorinated Biphenyls (PCBs) were one of the first industrial POPs which occurred as a global environmental problem. A strong decrease of PCBs in the environment (air and sediment) was measured after they were restricted in the 1980s in several countries [26]. Nonetheless, observation and research on background levels of PCBs around the globe and in the Arctic environment are still interesting and the distribution pattern of the pollutant can solve some unanswered questions.

The archipelago Svalbard (74-81°N) is favored for measurements on background levels of pollutants in the Arctic since only a few local sources are present [38]. Long-term observations of air pollution in Ny-Ålesund in the time of 1993-2006 have shown a decline in the levels of PCBs measured in air [35]. However, temporal fluctuation has been observed[41]. A higher volatilization rate for several volatile POPs due to climate change was assumed to be a reason [44]. Soil-air exchange should therefore be investigated for high latitude monitoring sites since a change of the partitioning coefficient is influencing the concentrations measured in the air samples. The contamination of background soils in Arctic regions could be released during the Arctic summer, resulting in seasonal changes in the atmosphere. Annual changes caused by soil re-emission have already been observed at lower latitude [75].

PCBs as an organochlorinated compound, released to the environment in a high amount over a long period, can be used as an interesting study case of pathways, environmental partitioning and degradation processes in the environment. Examinations of the transport pathways and burden to the Arctic ecosystem will give us better opportunities to predict the fate of new anthropogenic pollutants. The environmental compartment soil holds a high reservoir capacity [79] of organic pollutants and is an important medium influencing the persistence of PCBs in the ecosystem.
Therefore monitoring of Arctic soil and vegetation levels contributes significantly to global modeling efforts to understand the ultimate fate and time to the elimination of these compounds [5].

Overall, level of traditional POPs like PCBs, restricted in 2004, show a declining trend in the environment [26, 35]. The regulation and restriction of those POPs have resulted in a fundamental reduction of the environmental exposure.

This study intends to determine the current burden of background pollution of PCBs and long-range transported inorganic pollutants (Cd, Hg, Pb) in Svalbard soil. Therefore samples in remote areas in Svalbard were taken and analyzed at a certified laboratory. A method applicable at NTNU was developed and tested.
Additionally, there is an interest in finding correlations to soil organic matter and inorganic elements in soil, which can explain the occurrence of spatial variation in the total PCB concentration and different ratios between the congeners between different sampling sites. Therefore a data set was constructed by bringing together geographical data, level of PCBs and inorganic contaminants, as well as soil characteristics, like the soil organic matter.

Chapter 2

Background

2.1 Persistent organic pollutants

Persistent organic pollutants (POPs) are a group of man-made chemicals, which were intentionally and unintentionally released to the environment during their usage. Main chemicals classified as POPs have been defined in 2001 by the Stockholm convention and their prohibition got ratified in 2004 [80]. All POPs have in common to show toxic effects and an accumulation in the food chain (bioaccumulative) with a long lifetime in the environment (persistence). They also undergo long-range atmospheric transport. The main groups of POPs are pesticides and insecticides (e. g. dichorodiphenyltrichloroethane (DDT)), industrial chemicals (e.g. hexachlorobenzene (HCB) and polychlorinated biphenyls (PCBs)), by-products (e.g. polychlorinated dibenzo-p-dioxins and -furans, (PCDD/Fs)) and later added groups such as brominated flame retardants (e.g. polybrominated biphenyls and polybrominated diphenyl ethers (PBDEs)) and fluorinated compounds (e.g. perfluorooctanesulfonic acid (PFOS)). More chemicals, which are not mentioned in Stockholm Convention, but are still in the focus of research (e.g. polyaromatic hydrocarbons (PAH))[22] are often also referred to POPs.

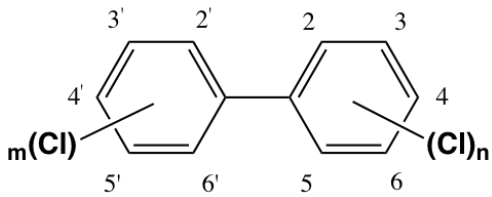

Figure 2.1: Molecular structure of Biphenyl and labeling of the chlorination positions

2.2 Polychlorinated biphenyls

Polychlorinated Biphenyls (PCBs) are a group of 209 congeners, which consist of a biphenyl main structure, where several hydrogens are replaced by chlorine atoms. During synthesis, the biphenyl main structure reacts with chlorine and iron(III)chloride as a catalyst. The degree of chlorination varies with the reaction conditions. After reaction, the mixture is distilled for fractionation[57].
All congeners are numbered in range of their chlorination by a system proposed by Ballschmiter and Zell 1980, which had been approved by the International Union of Pure Applied Chemists (IUPAC). This nomenclature will also be used during this work. The congeners are also often categorized in 10 different groups depending on the degree of chlorination (from mono- to decachlorinated biphenyls) [8].
Concerns about PCBs in the environment, especially in the Arctic, arise from the fact that most of the congeners, especially those with five or more chlorine atoms, are biomagnified in food chains because of their great biological stability and lipophilicity [9].

PCBs, that have been produced by Monsanto Co. (USA) are estimated to contribute to nearly 50% to the total world production. They are named Aroclor mixtures with a 4 digit number, representing with "12" the type of a chlorinated biphenyl and the last two numbers representing the percent of chlorine by weight. Mainly used technical mixtures produced contain chlorine between 21% (Aroclor 1221) and 68% (Aroclor 1268) [13]. Further commercially names are Clophen (Bayer, Germany) and Phenoclor (Prodelec, France), which are estimated to contribute both with around 10% to the total world production, and Sovol (USSR and West Germany), Delor (Czechoslovakia) among several other names [13, 37].

Congeners, which are chlorinated in the non-ortho-positions, are defined as coplanar. Noncoplanar PCBs are slightly more reactive than coplanar PCBs [57]. Also, the biological behavior and the resulting toxic effects can be distinguished between different

structures. Coplanar congeners show a similar structure with Polychlorinated dibenzo-p-dioxins PCDDs and therefore act similar to PCDDs as an antagonist of the aryl hydrocarbon receptor. Therefore, both groups are also named as dioxin like (DL) and non-dioxin like (NDL) groups. Noncoplanar congeners are more in focus of affecting the nervous and immune system if they are abundant in higher concentrations. Diorthochorinated biphenyls can interfere with the signaling pathways that are important for the Ca^{2+}- homeostasis [69].

The physical properties of PCBs are characterized by high chemical, thermal and biological stability, high dielectric constants, high electric resistivity, high density, hydrophobicity and lipophilicity- which are increasing with a higher degree of chlorination[57].

The total global production and usage of PCBs have been estimated to be over 1.3 million tons, where 97% is suggested to occur in the northern hemisphere. [13]. There are also estimations that nearly 31% of the total world production has been released to the global environment [74]. PCBs have been widely used for several technical applications like transformer and capacitor oils, hydraulic and heat exchange fluids, lubricating and cutting oils, coolant fluids, carbonless copy paper, and plasticizers agent in rubber sealants [9, 3]. The first concerns about their toxic behavior were revealed already in 1937 by Cecil K. Drinker [18] and the environmental effects of persistence and bioaccumulation in 1966 by Søren Jensen[39]. A whole decade later, in the 1970s, the usage, distribution and production got banned by many countries and PCBs got included in the Stockholm Convention in 2001 [80]. The main historical steps leading to a worldwide prohibition of PCBs are summarized in table 2.1.

Table 2.1: Summary of main facts about PCBs invention, usage and ban during history. Information is collected from several sources. If no source is given, data is collected from[31].

1881	First publication of the synthesis of PCBs by Schmidt and Schultz [66].
1929	PCB mixtures get first commercially available.
1937	First toxic effects are observed on rats [18].
1966	Jensen publicizes first observations of unknown molecules in sea eagles in Sweden [39].
1968	A contamination of rice oil with PCBs in Japan poisons 1200 people. First observations of toxic effects on humans are made.
1969	Jensen identifies the unknown molecules as PCBs, revealing the first proof of persistence and bioaccumulation effects of PCBs [40].
1970s	PCBs found in blubber tissue of seals, effects on reproduction are estimated [63].
1972	Japan government bans the production and use of PCBs.
1973	Sweden bans the open and dissipative use of PCBs.
1979	Second accident of rice oil contamination with PCBs in Taiwan.
1979	US congress decides to ban PCB production [78].
1980s	First observations of PCBs in human breast milk [86].
1981	Prohibition of PCB synthesis and PCBs in new equipment in the UK.
1998	Aarhus Protocol on POPs gets added to the Geneva Convention on Long-Range Transboundary Air Pollution (CLTRAP), mentioning PCBs among other POPs.
2001	Ratification of the Stockholm convention [80].
2003	Monsanto is forced to pay 700 million Dollars to residents of West Anniston, Alabama due to contamination of the area by manufacturing and dumping PCBs [25].
2004	Stockholm convention entered into force, banning PCBs by 128 parties [80].

2.3 Long-range transport of persistent organic pollutants

Several pathways of pollutants entering Arctic ecosystems have been observed. Among, ocean currents, pelagic organisms and migratory birds, transpolar icepacks and large Arctic rivers, the atmospheric transport is the most important long-range transport pathway for volatile and semivolatile pollutants [5]. Those chemicals have an air-octanol partitioning coefficient of log K_{OA}<10, are mobile in the environment and have a propensity for *long-range atmospheric transport* (LRAT). Involatile chemicals (log K_{OA}> 10) get mainly deposited with atmospheric particles before reaching the Arctic[10].

Transport or air masses to the Arctic

Especially during meteorological conditions appearing in winter in the northern hemisphere, the transport of air masses from southern source regions to the Arctic can take place in short time periods. Low pressures over the northern Pacific (Aleutian Low) and Atlantic Ocean (Icelandic Low) and high-pressures over the continents tend to a flow of air masses, resulting in a net transport from Eurasia across the Arctic towards North America. During summer, the continental high pressure cells disappear and the ocean low weakens, which leads to a lower south- north transport. The polar front builds a meteorological barrier[5].
Warm temperatures in lower latitudes favor evaporation, while colder temperatures in higher latitudes favor deposition due to a temperature dependence of adsorption and the vapor pressure of POPs. Thus, only a small fraction of POPs released in the source regions are conveyed to the Arctic, but POPs show a higher persistence in the Arctic environment, due to lower bacterial activity (see chapter 2.6) and less photooxidation in the winter time [5].

Influence of exchange processes on the LRAT

Exchange of contaminants during their transport between the atmosphere and the surface of the Earth includes dry deposition of particles and wet deposition, as well as gas exchange [45]. Precipitation is a scavenger of aerosol and gasses from the atmosphere and leads to a deposition of pollutants. Correlations of black carbon and POPs have been observed during second releases of POPs at biomass burning events [19] and their influence as a transport medium of pollutants has been discussed [55].

Evidence has shown that POPs have the tendency to undergo multiple cycles of evaporation and deposition between air, water, ice, vegetation and soil, based on the fact that most of them show a high volatility[84]. The storage capacity and the exchange of pollutants with the continental surface is high variable and also undergo seasonal changes [75]. The temporal variability implements a potential for second release. This re-evaporation, often driven by seasonal temperature changes, allows also semi-volatile POPs to reach Arctic regions. The process of re-emission, transport and deposition of POPs has been termed the *grass-hopper effect* or *multi-hopping effects* [56]. Since primary emissions of several POPs (especially PCBs after restriction) has declined in the last years, the second re-emission are more likely to affect global trends and fate of those pollutants [35].

Global fractionation

Beside temporal changes in the concentration of POPs in the atmosphere, also spatial variations have been observed for different POPs, as well as different PCBs congeners, which are explained by an effect called *global fractionation*[52], where different pollutants are getting transported to the north depending on their volatility (see figure 2.2). Due to this effect, pollutants with a high vapor pressure like Benzo(a)pyrene B[a]P are more abundant in their area of emission and therefore more occurring as local emissions, while semivolatile pollutants, like DDT, and volatile pollutants, like HCH and HCB, undergo the LRAT process. High volatile components, like chlorofluorocarbons (CFCs) and chlorinated hydrofluorocarbons (CHFCs), are even able to enter higher air layers of the atmosphere, which leads to a reduction of the ozone layer by catalytic photochemical reactions [84].
Since the physical properties of PCBs are depending on their degree of chlorination, the vapor pressure of PCB mixtures varies over a wide range. Therefore, PCB mixtures undergo a global fractionation during their LRAT. Model simulations have been performed to predict the global fractionation in the compartments air and soil of PCB mixtures[85]. While some studies have found evidence for this model [52], not all studies underlined this model[51].

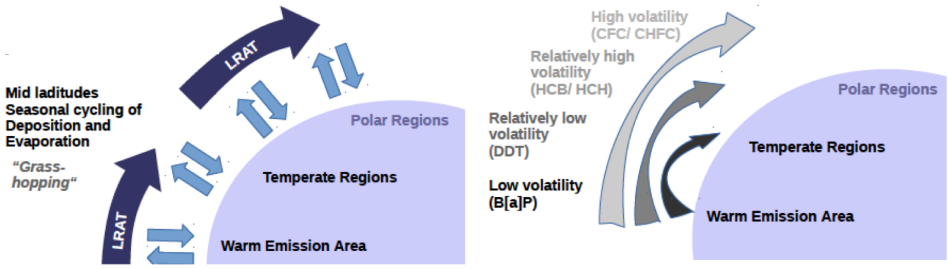

Figure 2.2: Schematic description of LRAT with the occurring grasshopper effect (left) and global fractionation (right). Due to several evaporation and deposition steps, POPs can be transported over longer distances. Hereby a fractionation of different pollutants occurrs depending on their volatility (*global fractionation*). Both graphics are adapted from [5] and [84] and individually modified.

Model approaches

Several models have been introduced to asses LRAT of POPs. Hereby, the models are based on a simulation of the dispersion of air pollution[77] (using either a gridded structure in the Eulerian approach or using trajectories in the Lagragian approach) or calculated by a multimedia box model, for example, fugacity based [10].
The potential of POPs for transport and deposition in remote regions can be studied by calculating the *Arctic contamination potential* (ACP). An intermediate and long term ACP is defined as the fraction of pollutants of the total amount present in the global environment (in exception of the atmosphere) that is transported to the Arctic in 1 or 10 years. Most air-emitted POPs have an intermediate ACP between 0.8 and 1.8% [83]. The calculations are based on the *Global Distribution Model (Globo-POP)*. The chemicals are mainly characterized by their partitioning between air, water and octanol (see chapter *Partitioning of POPs in the Environment*).

2.4 Partitioning of POPs in the environment

There is an exchange of POPs between different environmental media [67, p.55], like air, water, organic matter, mineral solids, and biota. By assuming equilibrium conditions, environmental factors, like partitioning can be quantified for organic pollutants. Compound properties like partitioning coefficients (between octanol-air (K_{OA}) or air water (K_{AW})) can be found in the literature, for example Mackay et al. 2006 [46].
Many studies can be found on the soil-air partitioning of pollutants. For background soils, this is the only estimated pathway for the occurring pollution. As several of those studies [14, 7, 56, 82, 88] have shown, the soil- air equilibrium is mostly influenced by the parameter SOM and soil temperature. Soils on different background sampling sites in lower latitude have shown a partition ratio close to equilibrium with an annual net direction to soil deposition. However, second source potential is partially given, especially for high volatile POPs, e.g. HCH [15].
The maximum reservoir capacity for soil to hold POPs is large, researches have shown that the top millimeter of soil has an air column higher than 1000 m to equilibrate with the soil [79]. Therefore, soil deposition of POPs is an important factor influencing the lifetime via degradation, atmospheric transport and environmental distribution of POPs.

The chemical space model

With the assumption, that the mutual solubility in water/octanol does not influence the partitioning ($K_{OW} = \frac{K_{OA}}{K_{AW}}$), the chemical space can be mapped in two dimensions and is displayed in figure 2.3. A chemical space model shows primary environmental compartments for hypothetical chemicals (with the assumption that they are steady emitted to the environment over 10 years and posses a long term persistence). Chemicals with properties of such as high $log\ K_{OA}$ tend to bind onto atmospheric particles, soils, and other solid phases, whereas chemicals with a high $log\ K_{AW}$ and low $log\ K_{OA}$ are more likely to remain in the atmosphere. The partitioning properties for PCBs, PCDDs and PCDFs as well as for Chlorobenzenes (CBs) are colored in the graph. The partitioning properties in this model are the main influence factors on the ACP. Additionally, the ACP has been shown to be significantly smaller if the emission occurs into water or soil, in comparison to an air emission [83].

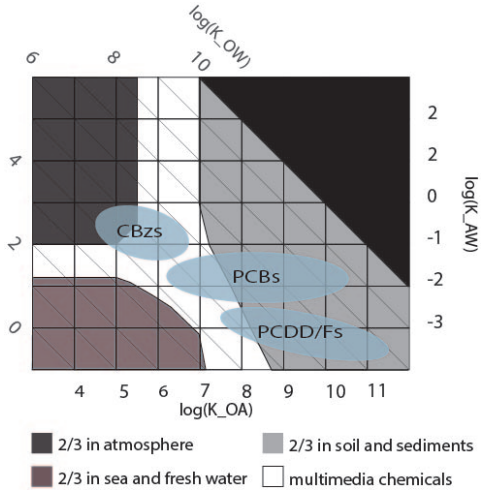

Figure 2.3: Primary environmental compartments for chemicals defined by their partitioning properties. The partitioning is based on calculations with the Globo-POP model assuming 10 years of a steady emission. (Graph adapted and modified from [83]). The graph and the model shows limitations for chemicals with $K_{OW} > 10$.

Agricultural soils are often contaminated by pesticides and industrial sites can contain pollutants from accidental releases. Therefore, those land-sites act as primary sources of pollutants into the air. Additionally, soil can act as a secondary source. This already described as the effect of *grasshopping*, mostly occurs for chemicals with $log\ K_{OA}$ around 8 and $log\ K_{AW}$ of around -2 [83].

2.5 Adsorption mechanism of POPs in soil

Contributors to the adsorption process in environmental soils

Soil organic matter (SOM) is seen by most researches as the main adsorbent of organic contaminants in the soil column and therefore influence their transport, reactivity and bioavailability [59]. Calculations show a dominance of SOM in the adsorption of weakly polar hydrophobic compounds in soils (if the organic carbon content is higher than >0,01%) [47]. Clay minerals have also shown a potential to bind hydopholic compounds [36]. Thus, due to a high abundance of water in the soil environment, their surfaces have to be considered as coated with multiple layers of water molecules, so that mineral-surface-interactions are strongly hindered and their contribution to the whole process in wet soils is negligible [47].
Dissolved organic matter (DOM) also has to be considered to play a part in the adsorption of hydrophobic pollutants, not only influencing the partitioning coefficient between soluble and surface-sorbet phase, K_{OC}, but also transport and bioavailability of the pollutants. Magee et al. [48] introduced a three-phase system between solid phase-bonded, DOM- bonded and soluble organic contaminants. DOM in soil can show a variety of compounds with a range of molecular weight, from low-molecular fragments of polysaccharides to high molecular colloids of humin[50].

Composition of soil organic matter

The bulk of SOM consists of humic substances, which can be composed of fluvic acid (water soluble), humic acid (soluble only at high pH), and humin (insoluble), which comprises more than half of the total SOM. In addition, SOM also contains recognizable amounts of lipid-soluble materials, proteins and carbohydrate fragments [59]. SOM is usually bound to mineral particles in different ranges. The variability of humus components and structure has been shown to influence the adsorption of hydrophobic organic pollutants and the K_{OC} values only in a small manner [50]. The surface of SOM is not well defined, revealing in the formation of humic acid colloids with a Gaussian concentration gradient from the edge to the center [59].

Observations of the adsorption process

Evidence for an existing hydrophobic interactions can be found in laboratory experiments, where the K_{OC} decreased with the polarity of the organic sorbent and can be influenced by pH and a higher ion concentration [50].
Pignatello is differentiating between two mechanisms: One fast (surface interaction) and one slow (diffusion controlled transport into the inner cavities of the sorbent)[59]. Thus, other researchers also describe the slow diffusion processes of organic pollutants as irreversible. If the macro-structure changes during absorbance, the process can be seen as irreversible, which reveals in the formation of unextractable residues[50].

Influence on sorption to environmental fate in Arctic areas

For Arctic areas, it can be concluded that the soil layer is mainly low developed and therefore shows a low depth. Therefore, mixing of the soil and transport of pollutants into deeper levels and therefore removing them from the air-soil exchange can be neglected. In conclusion, for Arctic areas, only the partitioning into SOM can be seen as a factor for removing pollutants from the active exchange. The process of incubation into the humic matrix of SOM results in a long-term exclusion of the pollutant from further volatilization [5].

2.6 Degradation processes of PCBs in soil

Observations of aerobic biodegradation by Arctic soil micro-organisms

Natural degradation processes of PCBs and POPs occur to be slow in a time order of decades. Therefore, they are influenced by a lot of other factors, like bioturbation and carbon burial/ sequestration [5]. Microoganisms are known to be mainly responsible for degradation and aging of PCBs and other organic pollutants in soil and sediments. The first observations of the capability of microbial degradation processes of PCBs in cold climate areas were made by Mohn in 1997[54]. Hereby, the degradation by microorganisms is simulated in laboratory studies of extracted indigenous Canadian Arctic soil microorganisms exposed to the commercial polychlorinated biphenyl mixture Aroclor 1221. An intrinsic potential for biphenyl mineralization was found for Arctic soil. The isolated microorganisms were either psychrophilic or psychrotolerant in the degradation process of biphenyl. Psychrophiles are extremophilic organisms, that are capable of growth and reproduction in cold temperature. Psychrotolerant bacteria are growing at low temperatures ($< 10^{\circ}C$), but have an optimum growth at higher temperatures. Among the extracted microorganisms, the psychotolerant isolates (Sag-50A and Sag-50G, both Gram-negatives) removed 54-60% of the mixture Aroclor 1221. In comparison with temperate soils, the mineralization rate was similar.

Description of the biopathways occurring during biodegradation

The aerobic degradation of PCBs is mainly performed by co-metabolism processes. Therefore, PCBs are normally not used as growth substrate for soil microorganisms. Thus, bacteria are able to use the dechlorinated structure, biphenyl, as a carbon source. The metabolism is accomplished stepwise by using *biphenyldioxygenase, hydrolase* and *dioxygenase* enzymes. During this pathway, chlorobenzoic acid is formed, which can be degraded by chlorobenzoic- mineralizing bacteria [81]. An overview of the process is given in figure 2.4.

Reductive dechlorination of PCBs can also be performed in water-logged soils by anaerobic bacteria and micromycetes, which are able to switch to the process of dehalorespiration. PCBs are acting as electron acceptors and undergo reductive dechlorination. The rate of dechlorination in sediments usually decreases from high- to low-chlorinated congeners [81].

As in the study of Mohn[54] mentioned, the degradation time is highly dependent on the degree of chlorination. The low degradation activity for highly contaminated soils can be explained by the formation of highly toxic PCB metabolites, like chlorinated dihydroxyphenyls or chlorocatechols [58]. Additionally higher chlorinated PCBs have a higher hydrophobicity, which leads to an accumulation of the pollutants in cytoplasmic and intracellular membranes of cells. This maintains a reduction of the accessibility to the enzymes and, at higher concentration, causes liquefaction and degradation of the membranes [81].

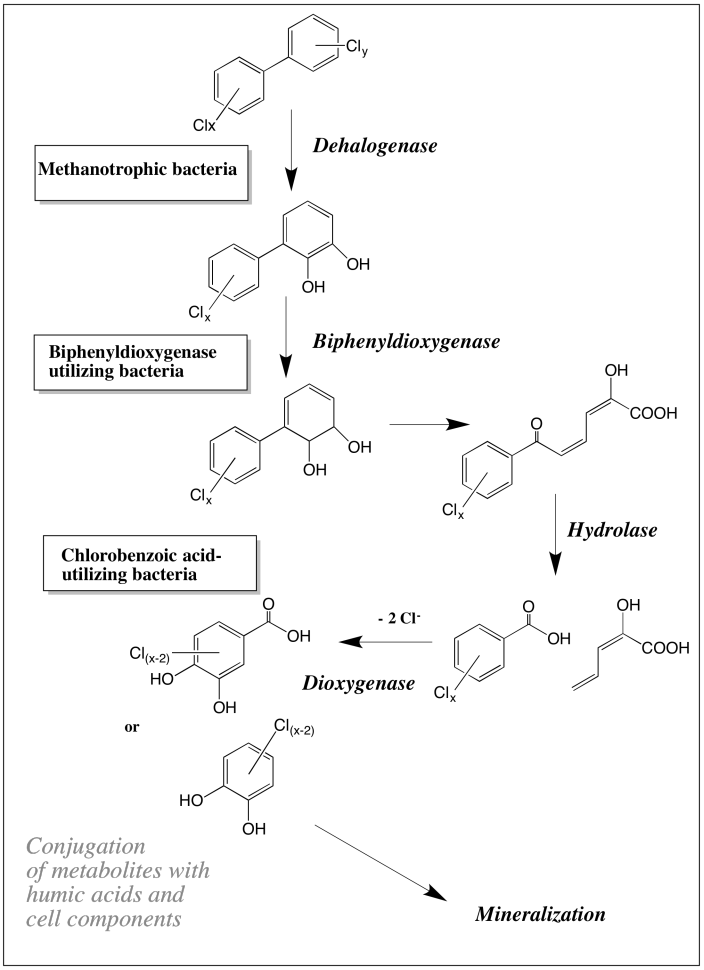

Figure 2.4: Schematic presentation of main pathways of PCB biotransformation. Adapted in a simplified version from [81].

2.7 LRAT of inorganic pollutants

Inorganic pollutants can origin from anthropogenic, but also from soil parent material (lithogenic sources) [4]. Input from sources, such as deposition of long-distance and atmospherically transported aerosol particles from fossil fuel combustion and other sources, can be found also in Arctic regions. However, local sources, like mining activities and fuel combustion, are also abundant and should be also taken into account for interpretation of occurring levels [28].
Long-range transport of mercury (Hg), cadmium (Cd), copper (Cu), lead (Pb), arsenic (As) and zinc (Zn) had been reported [4]. At the Zeppelin station (Ny Ålesund, Svalbard), a statistically significant decline of lead levels measured in the atmosphere between 1994 and 2010 had been reported. Heavy metals like As, Cd, Cu and vanadium (V) showed also a decrease in the atmosphere. Changes in the lead levels during the year can be explained by increased LRAT in the winter times (see chapter 2.3) and therefore gives evidence for lLRAT as a source [1].
Mercury has been in focus as a problem for the Arctic environment for a long time, especially since it is accumulating in the Arctic food chain. It is distributed over greater geographical ranges and to a greater extent long-range transported than other heavy metals [1]. It can occur in several states, in elemental form (Hg^0) in oxidized and soluble form (Hg^{2+}), and methylated (methylmercury MeHg and dimethylmercury Me_2Hg) [61]. Especially in spring, elemental Hg gets transformed by sunlight into reactive components, which are more taken up by animals and plants and are getting deposited from the atmosphere.
The main bulk of human emissions occurs from fossil fuel combustion for power and heating. Additionally, a high amount of Hg gasses are released by artisanal and small scale gold production. More than 65% of the emissions are occurring in Asia [6].
The natural Hg cycling in the Arctic ecosystem contains several pathways, like the release of Hg by weathering, and the transfer of Hg from soils, sediments and vegetation into aquatic systems through volatilization, fires, dust and sediment resuspension [61]. Measurements of Hg at the Zeppelin station appear to not show a declining trend since 2000 [1].
Differences in the pathways of inorganic pollutants versus POPs are resulting from higher water solubility. This influences ocean deposition as well as the faith of deposition on snow cover, which will mainly be transported by melting water instead of deposition in soil. In addition, leaching water is playing a role for mobilization of inorganic pollutants [4].

2.8 Characteristics of Arctic soils

Arctic tundra and soil covers approximately 5% of the Earth's land surface [90]. Chemical and biological processes, which lead to a soil development, are slow due to the Arctic climate. Soils formed under permafrost conditions are cryosols, which are defined by the Food and Agriculture Organization (FAO) [11]. The structure of cyrosols is defined by three layers: 1. An active layer, which undergoes frequent freeze-thaw and wet-dry cycles, 2. the transition layer and 3. the permafrost layer. The thickness of the active layer depends on several factors which vary in the terrain, like air temperature, vegetation, drainage, rock type, water content and degree and orientation of slope. In Svalbard, the active layer thickness ranges from 0,8–2,5 meters, with a permafrost temperature from -2,3 to -5,3 ^{o}C [11].

Cryoturbation occurs due to the periodical freeze-thaw cycles in the active layer and leads to the formation of ice lenses, which are melting in summer. This leads to the formation of earth hummocks which are characterizing the landscape. It also effects chemical properties such as the distribution and turnover of soil organic matter (SOM), nitrogen, iron and manganese redox relations and hydrogeochemistry of seasonal flow regimes. Cryoturbation is only occurring in soils with a deep active layer[12].

Arctic soils can be also classified in generic groups, such as lithosols, regosols and Arctic brown (which are formed under drained conditions) and tundra and bog (which are formed under impeded drainage). Lithosols and regosols are low developed soils. The are grading toward Arctic brown soil, especially at stabilized places. Here, the depth of thaw increases and allows the soil to establish a soil profile. Tundra and bog thaw only on a small layer on the surface and have a high water content. Arctic soils are characterized by a relatively low SOM. This is related to the low degree of vegetation as well as oxidation processes [76].

2.9 Trends of PCBs in the Arctic

Due to the previously described LRAT transport (see chapter 2.3) PCBs and other POPs can be found in Arctic environment and biota [41], even though the bulk of emission took place in a lower latitude. Several studies have been performed on that topic, and a summary of the current state is described in the AMAP report of 2002 [5]. A small summary of some publicized contamination levels of PCBs in different Arctic environmental medias is given in table 2.2. Only a few soil studies have been found concerning the Arctic. A detailed summary of studies of soil in Svalbard is given in chapter 3.1, since they are used for comparison to the occurring levels in this study.

Table 2.2: Levels of PCBs in selected publications from different media in the Arctic. This table gives an overview of previous studies. Comparability between the studies is limited due to different methods and publication of resulting values. Moreover, it shows the range of occurring levels. Moss levels[1] are taken from *Racomitrium lanuginosum*.

Sample area	Media	Level	Publication
Zeppelin station	**air**	mean $\sum_{32}$ 8,8 pg/m^3	Aas et al. 2016 [2]
Ny Alesund	**+ aerosol**	mean $\sum_{7}$ 3,34 ng/L	
Lomonosovfonna	**glacial**	max. 748 pg/L.	Hermanson et al. 2013
Svalbard	**ice**		[29]
Ny Alesund	**snow**	$\sum_{31}$ 2 pg/L	Kallenborn et al 2010
			[41]
Lake Ellasj øen	**lake**	max. $\sum_{18}$71,8 ng/g (dw)	Evenset et al. 2007 [26]
Bjørnøya	**sediment**	(1422 ng/g OM)	
Taymir, Russia	**moss**[1]	$\sum_{22}$ 1,07 ± 0,68 ng/g (dw)	Ford et al. 2000
Alaska	**moss**[1]	$\sum_{22}$ 0.61 ±0.21 ng/g (dw)	Ford et al. 2000
Alaska	**soil**	$\sum_{22}$ 13,2 ± 12,4 ng/g	Ford et al. 2000
Taymir, Russia	**soil**	$\sum_{22}$ 0,02 ± 0,02 ng/g	Ford et al. 2000
North Norway	**soil**	$\sum_{27}$ 242-5146,6 ng/g	Ockenden et al. 2002
			[52],[5]
Bjørnøya	**soil**	$\sum_{27}$ 17,2-4,4 ng/g	Ockenden et al. 2002
			[52],[5]

The distribution of PCBs in the Arctic environment is influenced by the hydrophobic character of the compounds. Therefore highest levels of PCBs can be found in hydrophobic media, e.g. biota, sediment and soil. A comparison of measured variations between soil and plant contamination in Ny Ålesund showed a higher variation in the plants, because the contamination of POPs is more influenced by uptake of plants via aerosol deposition from the air on the plant surface [88]. The uptake of the contaminants via roots of the plant from the soil is unflavored, because the hydrophobic character of POPs hinders a transport trough the vascular system of the plant.

Longterm monitoring of PCBs in Svalbard is performed at the Zeppelin station for air pollutants in Ny Ålesund. An overview of the annual mean concentrations measured in the last 20 years is given in figure 2.5. In this graph, a decline of PCBs abundant in the air is visible for the years 1998 to 2003.
Trichlorinated congeners dominated the profiles at Zeppelin station as well as in Alert (Canadian Arctic), [35]. This can be explained by the fact, that trichlorinated biphenyls were the most produced homologues.

Figure 2.5: Trend of PCBs ($\sum_{10}$ AMAP) in air and aerosols at Zeppelin station, Ny Alesund. Data was collected for the years 1998-2006 from [35], data for later years has been calculated from the raw data available from the EMEP database (http://ebas.nilu.no), and can be compared with the EMEP report for 2014 [2]. A trendline has been added.

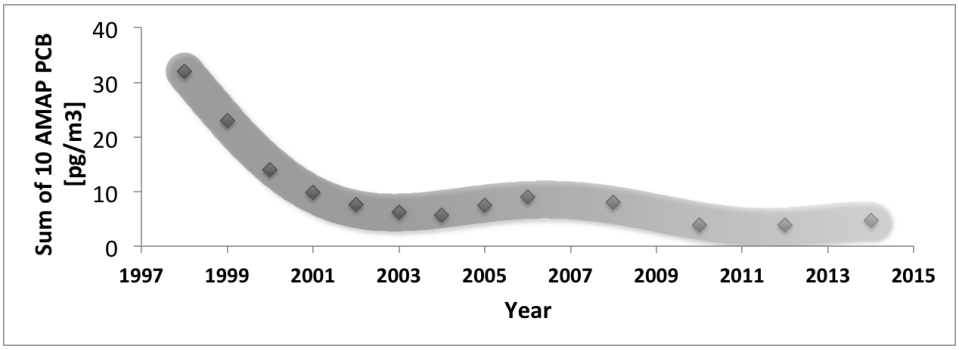

Chapter 3

Sampling

3.1 Study area

Svalbard is an archipelago with a land mass of 61.000 km^2, located between 74º and 81º North and 10º and 35º East (see figure 3.1). More than over 60% of the land mass is covered by glaciers [41]. The climate is shaped by low, but still due to influences of the West Spitzbergen current for the latitude moderate air temperatures. Therefore, winter temperatures in Svalbard with an average of -14°C in January are up to 20 °C higher than similar latitudes in Russia or Canada. The landscape is characterized by permafrost and tundra.
The largest settlement is Longyearbyen, with approx. 2000 inhabitants, followed by the Russian settlement Barentsburg. The northernmost settlement Ny Ålesund is only populated by researchers.

Svalbard has been used for several research projects and publications concerning background pollution of POPs, especially in biota [41]. The Zeppelin station in Ny Alesund is measuring several POPs in air and aerosols since 1998 as part of the European monitoring program (EMEP). As one of four long-term monitoring stations in the Arctic the station is also important for the AMAP [35]. A summary of PCB studies in soil performed in Svalbard is given in table 3.1.

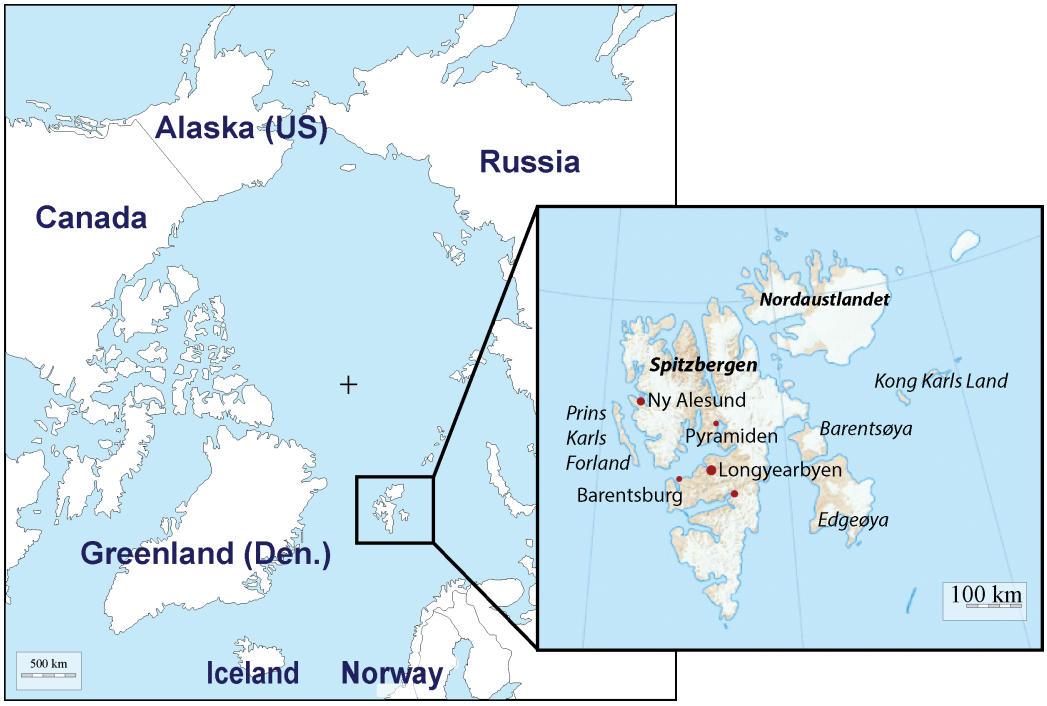

Figure 3.1: Location of Svalbard in the Arctic

Table 3.1: Studies of PCBs in surface soil at Svalbard. Sample size (n) is given for each study.

Study & Method	Area	n	Level of PCB [ng/ g (dw)]
Schlabach et al. 1999 [65]			
upper 2-3cm	Nordauslandet	1	$\sum_7$ 0,175
humus layer	Kongsfjord, Ny Alesund	3	$\sum_7$ 0,233-0,483
Soxhlet extraction	Longyearbyen	3	$\sum_7$ 0,410-0,784
GC-HRMS			
Eggen et al. 2011 [20]			
0-10cm surface soil	Prins Karls Forland	2x6	$\sum_7$ 3,13- 5,45
ASE extraction			(estim.)
HRGC/HRMS	St. Johnsfjorden	2x6	$\sum_7$ 1,55- 1,68
			(estim.)
Zhang et al. 2015 [91][88]			
ASE , GC-ECD	Ny Alesund	12	mean $\sum_8$ 6,72
GC-MSMS	London Island		(range 2,76-10,8)
Breedveld 2000 [41]			
	Platåfjellet	7	$\sum_7 < 0,4$
	Longyearbyen		
Harris et al. 2008 [41]			
	Nordauslandet	4	$\sum_7 < 1$

Samples from Schlabach et al. [65] showed a high organic content (70-80%). The most remote station, Nordaustlandet, shows the lowest concentration for nearly all congeners with exception of the hexa- and heptachloro PCBs, which exhibited at least comparable or slightly higher concentrations for samples around Ny Ålesund. Eggen et al. [20] found an estimated median for the sum of seven PCB which is four to six times higher than in the study of Schlabach.
Besides this background pollution studies, a high local contamination of PCB in soil can also be found close to Arctic settlements. PCB profiles from fjords with Russian settlements had a higher proportion of lower chlorinated congeners compared to fjords with Norwegian settlements, probably because of local pollution and the different PCB products used in each community[5]. Rose et al. (2004) studied 21 different lake sediments along the whole island archipelago on several pollutants (Pb, PAH, and Spheroidal carbonaceous particles). Five of the taken cores were also analyzed for PCBs. Of these, the highest PCB concentrations were found in the lake Tenndammen, which is located between Longyearbyen and Barentsburg [64].
An NGU report from 2008 concluded, that outdoor paint used in in Barentsburg, Colesbukta, Grumant, Isfjord Radio and Longyearbyen act as a primary source and results in local contamination [21]. Especially of interest were electrical equipment like transformers or capacitors that had been used and were left behind. A release of PCBs and associated contaminants into the soil and the total environment took place. High local contamination resulting from an improper disposal of equipment or products and unintentional releases are observed for example in Pyraminden, Barentsburg and Longyearbyen in Svalbard [38].

3.2 Sampling method

There were in total 84 soil and vegetation samples from 42 sampling sites in 7 different areas collected in Adventdalen (near Longyearbyen) and around Ny Ålesund (Kongsfjorden). All coordinates of the sample sites can be found in table A.1 in the appendix. On each sampling site, approx. 5 samples were taken at different areas. Each area got marked with a number. For each area (number) two equivalent samples (named A and B) were taken in a maximum distance of ca. 10m. The samples were cut with a knife and sampled together with the vegetation cover. Separation of vegetation and soil layer got performed later in the laboratory. The samples were kept in a rectangle shape and two times wrapped with aluminum foil (see figure 3.2). The samples got sent by post to NTNU Trondheim for further treatment.

Figure 3.2: Samples were wrapped in aluminum foil and labeled (left). On the right, soil temperature in comparison to the air temperature and GPS coordinates and attitude were determined.

The vegetation and soil of Svalbard is shaped by the long winter periods, leading to a soil layer with a low depth, which contains a high amount of uncombusted material. A cut of the top layer of soil can be seen in figure 3.3. The thickness of the vegetation layer varies from 0,5 to 3 cm. The organic soil layer varies in a thickness from 0 to 3 cm. Main appearing vegetation is moss, which leads to an accumulation of several old moss layers over each other, with a high root fiber content.

To find good soil samples appropriate for analysis, low vegetation content in the soil is preferred. Therefore it was not always possible to follow the planned sampling strategy, most sample areas had to be adapted to the soil conditions in the field. The samples were taken in a way that covered a high spatial variance but also approved statistical routines. In the laboratory, 10 samples were excluded due to low organic soil layer content.

Figure 3.3: Profile of the top soil in Svalbard. Vegetation and organic layer horizon (O) was sampled together and later separated in the laboratory. A sampling of inorganic soil layer (A) was avoided.

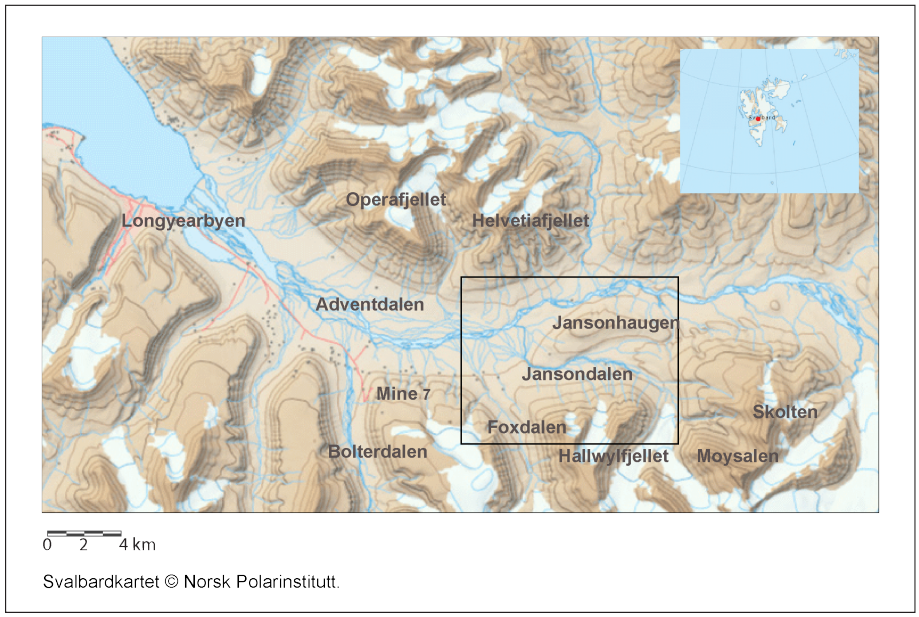

Figure 3.4: Overview of Longyearbyen and Adventdalen, sampling area described in figure 3.5 is highlighted with a square.

3.2.1 Sampling around Adventdalen (Longyearbyen)

All sampling sites were reached by foot, where several rivers had to be crossed. Accessing the sampling sites took the main time of the field work, which had been performed in 3 days. All sampling sites are in more than 15 km linear distance to Longyearbyen and 5-10 km linear distances to the last infrastructure (Mine 7). From previous fieldwork [30], Foxdalen had been known as an area with good soil development. Further places had been chosen by maps of vegetation coverage. An overview of the sampling sites in comparison to closest infrastructure is given in figure 3.4. All sampling points can be found in figure 3.5.

All three sampling sites (Foxdalen, Janssondalen, Jansonhaugen) have not been in contact with any industrial use. Only private cabin visitors and tourists access the area. The traffic by snowmobiles is prohibited for the main season (starting in March) in the whole sampling area. In conclusion, the chosen sampling sites are the best possible areas for measuring background pollution, reachable in the given time frame.
Foxdalen showed high soil development, which spread along the riverbed. In Jansondalen, the ground is merely glacial influenced and lithoidal with a low soil development.

Therefore, the chosen sampling sites are not spread around the valley. As additional sampling site, Jansonhaugen was chosen, where a good soil development was observed on the north face of the mountain.

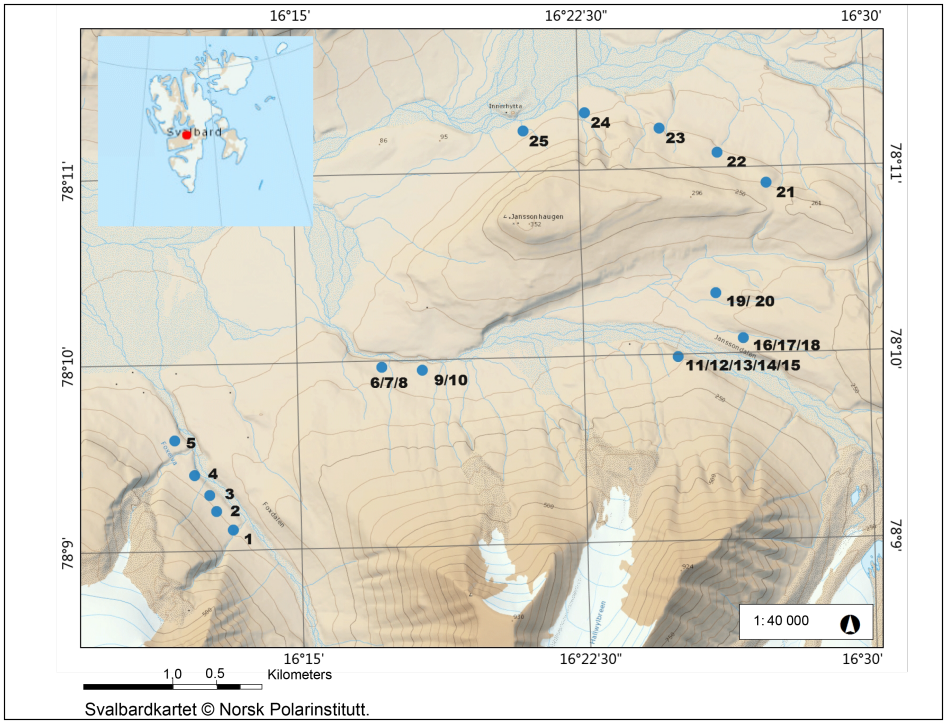

Figure 3.5: Map of sampling sites near Longyearbyen, which is located approx. 15km to the west. Last infrastructure (Mine 7) which can be approached by a road is located ca. 5km to the west. The points can be clustered to the areas Foxdalen (1-5), Jansondalen (6-20) and Jansonhaugen (21-25).

3.2.2 Sampling around Ny Alesund

The sampling in Ny Ålesund took place in 5 days. The area around Ny Ålesund is often used for measurements of background pollution. Several mining activities in the area took place during the last years and have also been taken into account. An overview of the sampled areas is given in figure 3.6. Sampling took place around Gasebu, on the feet of Knudsenheia and east and west of Bayelva river. All sampling sites showed a lower soil development than in Longyearbyen with a higher sand content.

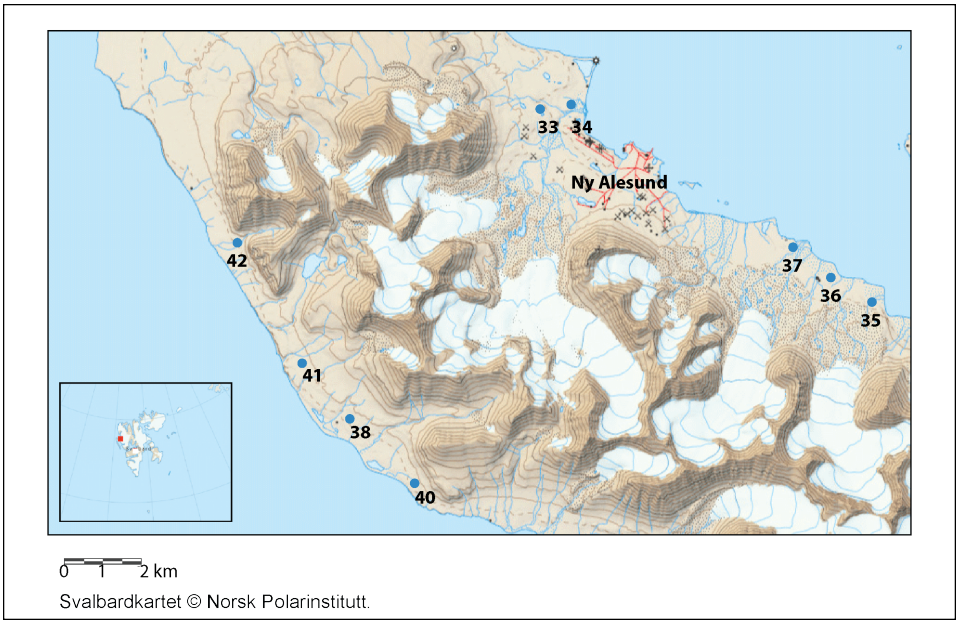

Figure 3.6: Sampling sites around Ny Ålesund, which can be clustered into Gåsebu (26,27,35- 37), Bayelva (28-36) and Leinstrandodden (38-42).

To achieve a more unaffected sample environment, additional sampling took place in Leinstranda, which could be reached by boat and showed a good soil development on the feet of the mountain range. All sampling sites are close to shore, therefore a different influence can be estimated in comparison to the samples in Longyearbyen. Soils around Ny Ålesund have silty clay and sand gley soil that has a thin organic soil cover [90].

Chapter 4

Materials and Methods

4.1 Pretreatment of soil samples

All samples were set aside at room temperature for first drying. To prevent any contamination of the samples from dust, the samples were kept in one piece and covered all around in aluminum foil, with a small gap on the sides, which allowed air exchange. Samples with high thickness and therefore a high weight (>1000 g), were cut into two pieces to accelerate the drying process.

After the samples showed an insignificant loss of weight (<5%) in 3 days they were further treated. On each side of the sample, ca. 0,5 cm of soil matter was cut away, the vegetation layer was removed and the sample was mixed and transferred to a cleaned aluminum box. Stones and thick roots were removed with forceps. The samples were kept at room temperature for further drying. Some samples appeared to show no further loss of weight but still remaining water was visible in the consistence. This sticky and moisture substance made it impossible to use those samples for further treatment (milling). To avoid this, all samples from Ny Ålesund were freeze dried to achieve fully dried samples.
Comparability can be assumed trough comparison of freeze drying and drying at room temperature in the literature [87]. There, no significant difference in the results between air and freeze drying for PCB levels in soil samples was found.

Freeze Drying was performed with an Alpha 1-2 LDplus by Martin Christ. Samples were first frozen at -25 °C. The samples were kept in a glass beaker and dried under a pressure of 0,94 mbar for 24 hours in the freeze dryer. The average loss of water during this drying step was around 290 g per kilogram of sample weight.

All dried soil samples were homogenized by milling with a standardized homogenizer (Retscher SM100). A sieve of 3 mm was used. The first homogenization fraction was removed to avoid cross-contamination by the machine.
The removed vegetation layer was separated from remaining soil and freeze dried and homogenized in a similar way. All samples were kept frozen at -25°C till they were used for further analysis.

4.2 Analysis strategy of samples

Due to a too low soil content some samples had to be excluded. Not all 84 samples could be used for further analysis since a sufficient weight for homogenization (>300 g) had not been reached. In total, 74 soil samples and 34 vegetation samples were pretreated and available for analysis. All soil and vegetation samples got analyzed for inorganic elements by ICP-MS. For all soil samples, total organic carbon (TOC) was determined by loss on ignition. For analysis of PCBs, a smaller selection of samples had to be chosen to achieve best possible information within a given budget. Therefore, from each of the 7 sampling areas (defined in the previous chapter and displayed in figure 3.5 and 3.6) an appropriate amount of samples (2-5 samples) and a total amount of 25 were sent to a certified laboratory (Sintef Molab). Additionally, 15 vegetation samples were also sent there for analysis.
Analysis of PCBs in soil and vegetation was performed at NTNU and tested on 7 soil and 2 vegetation samples, representing all sampling areas. For comparison and method validation, all samples were analyzed in parallel to the laboratory. A table of the sampling and analysis strategy is given in the appendix in table A.1.

4.3 Determination of soil organic matter by loss on ignition

Loss on ignition (LOI) is a semi-quantitative method to determine the TOC, which refers to the SOM content[62].
An amount of the sample (3-4g) was weighted into a crucible and dried in a compartment dryer at 105°C overnight. The ignition of the sample was performed in an incineration oven (L3/12 by Nabertherm). The sample was heated at 505°C for 3 hours. The loss on ignition (in percent) can be calculated by the mass of the soil before $M_{dry}(Soil)$ and after $M_{final}(Soil)$ the ignition:

$$LOI(\%) = \frac{M_{dry}(Soil) - M_{final}(Soil)}{M_{dry}(Soil)} \cdot 100 \tag{4.1}$$

Errors in this method can result from different temperature programs or incorrect weighting of the probes. Additionally, errors can result from structural water loss and decomposition of soil carbonates [33]. Carbonates can be removed by a treatment with acid, but this has been neglected for this work. Reproducibility was determined by igniting three aliquots of each soil sample.
For comparison, 2 samples were also ignited in a different oven (Carbolite ELF 11/6) and 3 samples were decomposed on higher temperature (650 °C), but no significant differences appeared.

4.4 Analysis of inorganic pollutants by inductively coupled plasma mass spectrometry (ICP-MS)

Inductively coupled plasma mass spectrometry (ICP-MS) was used for the analysis of elements in soil samples. The heated sample extract gets ionized in an argon- methane plasma. The produced ions get accelerated and separated by the mass to charge ratio under a magnetic and electric field. ICP-MS is a well-established method at NTNU. Specification of the instrumentation is given in table 4.1. The analysis of different elements was performed at three different resolutions to avoid interferences. All samples were digested in the method described below. Two blank samples were treated in the same manner and all results were corrected for the mean levels measured in the blanks. The instrumental detection limit (IDL) and blank detection limit (BDL) are given in table 4.2. The IDL results from the concentration yielding to 25% of relative standard deviation at three scans and were calculated for the used sample amount. Accuracy of the method was determined by extracting two parallels of the Reference Material Soil GBW 07408. The precision of the method was determined by the standard deviation of three parallel analysis of the same sample. Results can be also found in table 4.2.

Table 4.1: Specification of the ICP-MS instrumentation and extraction

Instrument	ICP-HR-MS Element 2 (Thermo Scientific)
Sample introduction system	Auto-sampler - SC2 DX
Gas flow	Splitting of sample gas, 10% methane in Argon
Analysis resolution	low (400)
	medium (5500)
	high (10 000)
Extraction	UltraCLAVE (Milestone)
	High-pressure digestion unit

Table 4.2: Instrumental and blank detection limit (IDL, BDL) for the analyzed elements in [μg/g (dw)]. No BDL is given if levels in blank had been under IDL. Comparison of the measured levels at NTNU with the certified levels reported for the reference material and the resulting accuracy (A). The relative standard deviation (RSD) is calculated for the analysis of 3 parallel analyzed samples.

Element	**IDL**	**BDL**	Ref. Material	Certified	A (%)	RSD(%)
Al	0,090	28,24				1,9
As	0,011		11,2 ± 0	12,7 ± 1,1	88	1,7
Cd	0,005		0,117 ± 0,004	0,13 ±0,02	90	2,8
Cr	0,002	0,064	54,6 ± 0,6	68±6	80	3,8
Cu	0,005	0,017	20,0 ±0,3	24,3 ±1,2	82	2,8
Fe	0,009	21,53				2,0
Hg	0,001		0,017 ± 0,000	0,017 ± 0,003	100	6,8
K	2,2	11				2,2
Mn	0,003	0,195	566 ±10	650 ± 23	87	5,3
Mo	0,009					1,8
Na	4,3					0,2
Ni	0,006		28,2 ±0,3	31,5 ± 2	89	1,9
P	0,17	2,1	694 ± 9	775 ± 25	90	1,7
Pb	0,001		13,7 ± 0,4	21 ±2	65	5,2
S	4,3					4,5
Sb	0,001		0,060 ± 0,003	1,0 ±0,2	6	6,0
Sn	0,004		0,464 ± 0,048	2,8± 0,5	17	10,1
W	0,001		0,015±0,007	1,7 ±0,2	1	22,1
Zn	0,017	0,090	57,9 ± 0,6	68 ± 4	85	1,7
Br	1,3	4,8				6,8
Cl	43					10,2

Digestion Method

For digestion, 200-300 g of prepared soil sample material (see chapter 4.1) was weighted into PFA vessels (18 mL volume) and 9 mL of 50% nitric acid was added (Ultra Pure grade, distilled by Milestone SubPur unit). After digestion, the sample was diluted to an total volume of 108 mL prior to analysis.

For analysis of the vegetation samples, 300-500 g of the material was used, 6 mL of 50% nitric acid was added, the sample got digested and afterwards diluted to an total volume of 60 mL.

4.5 Analysis of PCBs by gas chromatography coupled with mass spectrometry (GC-MS)

4.5.1 Chemicals and material

Standard materials and solutions

The used standard method with an isotopically labeled internal standard (ISTD) was chosen in correspondence to U. S. EPA method 1668 A. All purchased solutions are listed in table 4.3. The available fluorinated PCB- congener solutions are listed in table 4.4.

Table 4.3: Suppliers and purchased concentrations of the standard solutions. Congeners marked with an asterisk are $^{13}C_{12}$ isotopically labeled.

Solution	PCB congeners	Purchased conc.	Supplier
Calibration solution- (CEN PCB Congener Mix) 1	18, 28, 31, 44, 52, 101, 118, 138, 149, 153, 180, 194	10 μg/mL	Supelco (USA)
Internal standard	28*, 52*, 101*, 118*, 138*, 153*, 180*	1000 ng/mL	Cambridge Isotope Laboratories (USA)
Recovery standard (EN-1948-4)	70*, 111*, 170*	100 ng/mL	Cambridge Isotope Laboratories (USA)

Table 4.4: Suppliers and purchased concentration of the used Fluorinated PCBs for recovery standard.

Compound	purchased concentration	Supplier
3'-F-PCB 28	100 μg/mL	CHIRON AS
5'-F-PCB 118	10 μg/mL	CHIRON AS
5'-F-PCB 190	51 $\pm$ 1 μg/mL	CHIRON AS

Chemicals used for extraction
Acetone, ACS Grade, VWR Chemicals
Acetone (for cleaning), Technical Grade, VWR Chemicals
Hexane, ACS Grade, Fisher Scientific
Diatomaceous Earth, Fisher Scientific and Sigma-Aldrich
Ethyl acetate, ACS Grade, VWR Chemicals
Copper powder, particle size <425μm, 99,5% trace metal basis, Sigma-Aldrich
Aluminum oxide, pore size 58Å, pH= 7,0±0,5 (in H_2O), Sigma-Aldrich
Nitrogen, 5.0, AGA AS

Chemicals used for sulfuric acid cleanup
Sulfuric acid, 96.5%, ACS Grade, VWR Chemicals
Millipore water, ELGA-DV 25, conductivity 0,055μS/cm

Materials
Hamilton microliter syringe, 10μL, 100μL
Disposable Glass Pipettes, VWR
Centrifuge glasses, Gerresheimer
Volumetric flask for preparing standard solutions
Sample vials (2 mL), screw top vials, with 250μL inserts and screw cap (PTFE/RS), Agilent Technologies
Collection vials (clear glass), 60 mL, Thermo Scientific

4.5.2 Formulas for calculation

Limit of detection and quantification

The limit of detection can be defined by the occurring signal to noise ratio and was set to:

$$S_{LOD} = 3\frac{S}{N} \tag{4.2}$$

S is the height of the signal and N the height of the noise band. All signal to noise ratios were calculated automatically by the software. Signals below the ratio for the limit of quantification were not integrated and reported as not quantified.

The limit of quantification LOQ is reported as:

$$S_{LOQ} = 10\frac{S}{N} \tag{4.3}$$

Linearity test and calibration curve

The calculation of the response factor f_i is given by [23]:

$$f_i = \frac{A_s(i)}{c(i)} \tag{4.4}$$

Here is $c(i)$ the concentration of the analyte i in the injected sample and $A_s(i)$ the area of the signal in the chromatogram of the analyte i .

The relative response factor (RFF) or f_r is defined as $f_r = \frac{f_i}{f_{ISTD}}$ and can be calculated by:

$$f_r = \frac{c(ISTD) \cdot A_s(i)}{c(i) \cdot A_s(ISTD)} \tag{4.5}$$

Here is $c(ISTD)$ the concentration and $A_s(i)$ the area of the signal of the internal standard (ISTD).

If f_r is given, the amount of analyte M_i in the analyzed sample can be calculated from the ratio of the area of the analyte and the area of the ISTD via conversion of the formula:

$$M(i) = \frac{M(ISTD) \cdot A_s(i)}{A_s(ISTD) \cdot f_r} \tag{4.6}$$

$M(ISTD)$ is the amount of the ISTD in the analyzed sample. Since the volume is the same for $c(ISTD)$ and $c(i)$, the calculation can be done with the total amounts $M(ISTD)$ and $M(i)$.

Recovery range

In an analogous manner to the response factor described in the previous section, the response factor of the ISTD relative to the recovery standard RSTD, f_{rr} can be defined as [23]:

$$f_{rr} = \frac{c(RSTD) \cdot A_s(ISTD)}{c(ISTD) \cdot A_s(RSTD)} \tag{4.7}$$

Here is $c(RSTD)$ the concentration of the RSTD in the injected sample and $A_s(RSTD)$ the area of the signal in the chromatogram of the RSTD.

The surrogate recovery $R(\%)$ is then defined as:

$$R(\%) = \frac{M(RSTD) \cdot A_s(ISTD) \cdot 100}{M(ISTD) \cdot A_s(RSTD) \cdot f_{rr}} \tag{4.8}$$

Here is $M(RSTD)$ the amount of the RSTD in the analyzed sample.

4.5.3 Method development

Strategy of method development

Building a robust and applicable analysis method was one part of this thesis. Results of the method development are described in detail in this chapter. Figure 4.1 gives an overview of the order of steps performed inspired by literature [34].
First, an instrumental method was developed for analysis of the target compounds. Final setup can be found in table 4.10. The temperature program was modified to achieve best peaks for the target compounds. Then, retention times were identified and the setup of the mass spectrometer was developed. First, single ion monitoring was performed and later experiments were made in a tandem mode to increase the selectivity and reducing the limit of quantification. Method blanks were run to determine the contamination during the extraction and workup procedure in the laboratory.
Different concentrations of the injected solution were tested to determine the best possible concentration with an optimum of the signal to noise for internal standard and target compound. Different recovery standards had to be tested for use due to economical and logistical reasons.

The linearity range of the method was determined by performing analysis of a parallel set of spiked samples. Cleanup methods were tested to achieve a lower linearity range. The complete final analysis setup was tested for application by analyzing three parallel samples of a certified reference soil material. For application on background soil samples, 7 soil and 2 vegetation samples were analyzed.

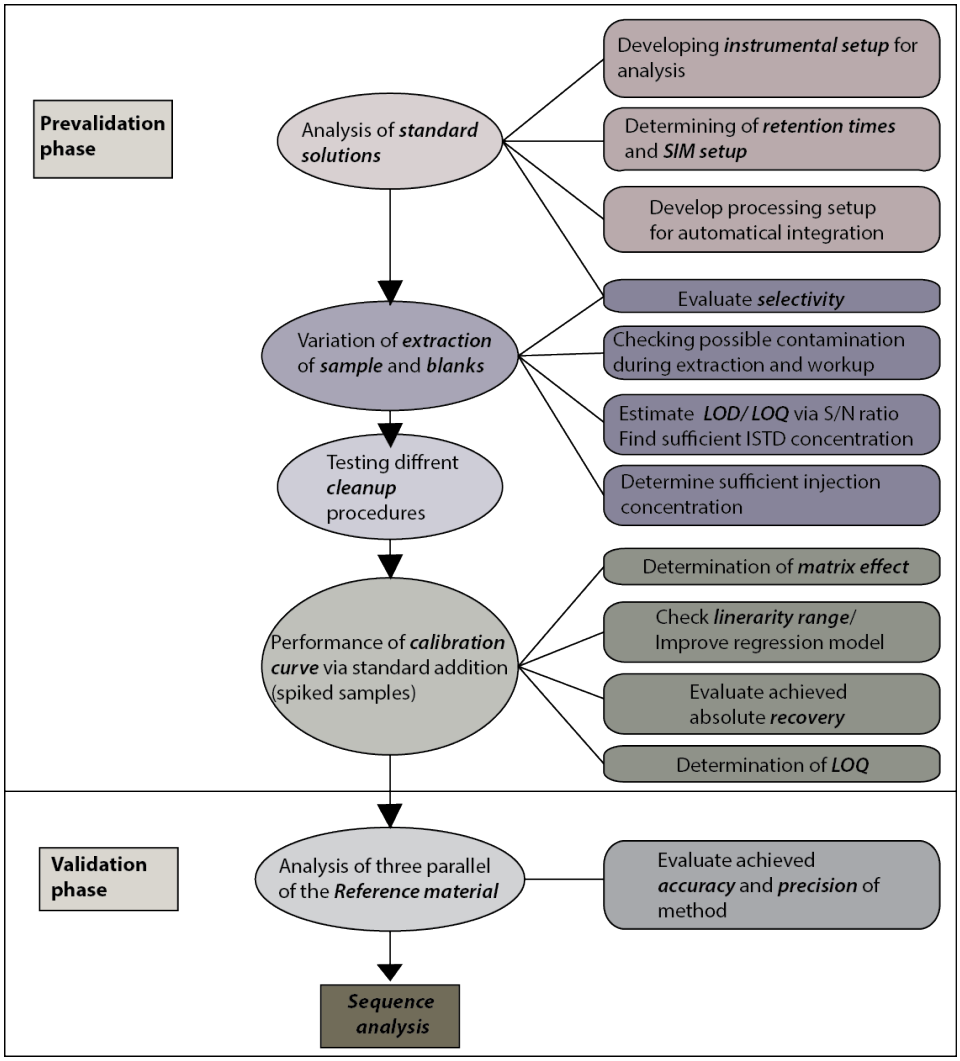

Figure 4.1: Overview of performed steps for quality assurance of the applied quantification method

Determination of retention times and temperature program

To determine the retention times on the chosen DB-5ms column, a calibration solution of 12 PCB congeners (see chapter 4.5.1) spiked with the ISTD was used.
The congeners 18, 28, 31, 44, 52 101, 118, 138, 149, 153, 180 and 190 were identified. The congeners 180, 118, 52 and 28 were identified by coelution with the peaks of the ISTD mixture.
The elution order of the pentachlorinated congeners 101 and 118 as well as 138 and 153 had to be determined by literature [16], since both congeners were in the ISTD solution. The congener 149 could be identified, since it is the only hexachlorinated congener in the standard solution, which is not included in the ISTD. The peak of 190 occurred in a time window (RT>24min) were a high column bleeding was observed. It occurred in general with low intensity and was therefore excluded from analysis. The congener 18 and 31 are described in the literature [71] to co-elute on a DB5-ms column.

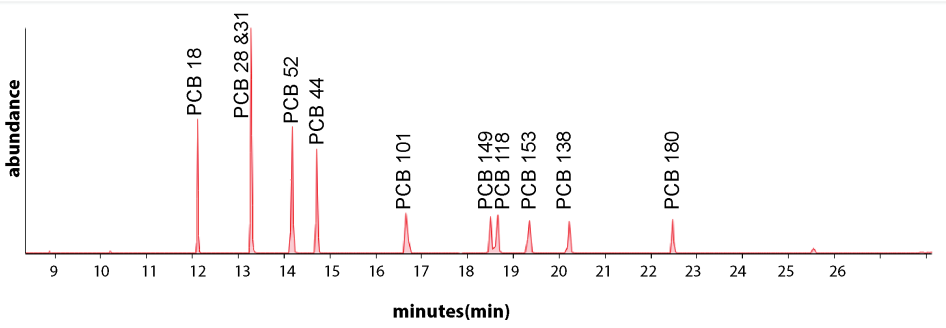

Figure 4.2: Chromatogram of CEN PCB congener mix 1 with ISTD revealing on a DB5-ms column. The MS was used in the SIM mode. The concentration of the used solution is 200 ng/mL.

Table 4.5: Retention times [min] which revealed under the temperature program (see table 4.10) for all analyzed PCBs on the DB5-MS column.

PCB	18	28 (& 31)	52	44	101	149	118	153	138	180
RT	12.0	13.1	14.0	14.5	17.4	18.3	18.5	19.1	20.0	22.3

Table 4.6: Retention times [min] which revealed under the temperature program (see table 4.10) for the recovery standard mixture.

***PCB**	70	111	170
RT	16.0	16.5	23.4

Internal standard

The developed method was performed in analogy to EPA Method 1668A. The different chlorinated congeners are measured as the ratio against the isotopically labeled internal standard (ISTD). Specifications of the purchased solution can be found in chapter 4.5.1. The usage of isotopically labeled ISTD allows quantification for compounds with a different analytical response and allows a distinct identification of the signals in the chromatogram. This method is generally known under the term *isotope dilution quantitation* [42].
Since the limit of quantification was higher with the instrumentation used here than on high-resolution mass spectrometry (HRMS), the sufficient concentration for ISTD had to be higher than in the EPA method. The amount of ISTD added to samples used in the SIM mode was 20 ng (on a total volume of 250 μL of the extract solution) and 10 ng for samples prepared for the MS/MS mode.

Testing of cleanup methods

In accordance with published extraction techniques for sediment samples[60], alumina was added to the extraction cell on the bottom (see chapter 4.5.5). This cleanup did not achieve sufficient removal of sample matrix for analysis of PCB concentrations below 10 ng. The introduction of further cleanup methods reduced the advantage of a low time-consuming method resulting from using ASE. Therefore, the application of the sulfuric cleanup was tested but not preferred to use in the final routine method. First trails were performed in accordance with EPA Method 3665A (1996). In that method, 50% sulfuric acid was used for solvent-solvent extraction. It was also tested to use concentrated acid in accordance with a procedure described in the literature [89], which yielded better cleanup results.

Procedure
First, acetone was mostly removed from the extraction mixture by the use of the TurboVap (Biotage TurboVap LV Evaporator). Then, 5 mL of concentrated sulfuric acid was added to the concentrate (5 mL) and got mixed for 2 min. The sample was kept in the freezer for one hour to achieve a sufficient separation of the layers. The sulfuric acid layer was removed with a glass syringe and washed with 5 mL of hexane two times. The hexane layer was washed one time with distilled water and all hexane layers were combined and further concentrated in the TurboVap.

Problems and repeatability
Since soil can contain different amounts of humic and fluvic acids, both layers emulsified for some samples. Therefore, a separation was in some cases not possible. The sulfuric acid layer contained several black residues, which were difficult to separate from the hexane layer. A simple analysis of four parallel samples (two with cleanup and two without) showed a successful reduction in the extraction matrix (full scan analysis). However, a high variation in the recovery of the ISTD was observed.

Test of fluorinated PCBs as recovery standard

Due to economical reasons, fluorinated PCBs were tested as recovery standard (RSTD), and were introduced instead of the isotopically labeled PCB congeners 70, 111 and 170. Tested fluorinated congeners are listed in table 4.4 and 4.7. For a possible use, quality control criteria had to be fulfilled when using the compounds as RSTD. First, solutions with a concentration of 1 μg/mL in ethyl acetate were prepared and run for identification of retention times and preferable mass numbers.
The suitable concentration of fluorinated recovery standard (F-RSTD) for quantification in the SIM- mode was determined by testing different concentrations (10, 50 and 250 μg/mL).
Then a mixture of all fluorinated congeners was spiked to a blank sample of ethyl acetate and to an extracted sample, to evaluate interferences with the sample matrix. For that, ca. 150 μL of extracted sample solution (reused from the testing of clean up methods) was spiked with 10 μL of each RSTD-F-PCB solution with a concentration of 1μg/mL, to an injected concentration of 56ng/mL.

Additionally, a sample without F-RSTD was tested for interfering masses and the RSTD-F-PCB solution was tested for possible interference with the ISTD and the target compounds.
Since for the detection of F-PCBs, two more masses had to be added to the SIM program, the sensitivity of the detector got reduced. Therefore, the scan time was increased by using two microscans.
The selectivity of all F-PCBs occurred to be too low for quantification (to high signal to noise ratio for the chosen masses). Since a higher concentration in the RSTD did not result in better chromatograms, tandem mass spectrometry (MS/MS) was chosen to perform better results. Here, only F-PCB 118 was finally used, since this congener did not coelute with other peaks of ISTD or target compounds and could be analyzed in its own time window. F-PCB 118 was then used as recovery standard for all analyzed samples, while the isotopically labeled recovery standard mixture was used for all calibration measurements.

Table 4.7: Summary of tested fluorinated PCBs as RSTD. Retention times (RT) and observed mass numbers (M+ and [M+2]+) in the SIM analysis.

Compound	**RT**	**MW** [g/mol]	**M+**	**[M+2]+**
3'-F-PCB 28	13,0	275,55	274	276
5'-F-PCB 118	17,8	344,44	342	344
5'-F-PCB 190	22,3	413,33	412	414

4.5.4 Extraction technique

Accelerated solvent extraction (ASE) is a relatively new extraction method. The extraction time and the solvent use can be here reduced in comparison to a conventional Soxhlet extraction by the possibility of working with temperatures above the boiling point of the solvent. The extraction process is enhanced due to increased analyte desorption and diffusion from the solid matrix.
Comparison of different extraction techniques in the literature showed comparable results and a good recovery range for the extraction of PCBs in soil [72]. Several publications had been found for ASE application on soil samples [32, 72, 43, 89], which all revealed comparable results on soil samples. The flush of two cycles showed a full extraction of the sample contamination on PCBs [32]. Therefore, ASE can be favored for extraction, due to its time efficiency and high repeatability due to the high automatization of the extraction.

The extraction was performed according to Dionex application note 316 [17] and therefore meet the requirements for U.S. EPA Method 3545 [24].

Table 4.8: Conditions for accelerated solvent extraction performed on soil samples

Parameter	**Value**
Instrument	Dionex ASE 150 by Thermo Fisher
System pressure	1,4MPa
Oven heat up time	5 min
Static time	5min
Oven temperature	100°C
Sample size	10 g
Cell size	22 mL
Cell type	stainless steel
Filter	
Collection vial	60 mL
Dispersing agent	Diatomaceous earth
	2,5g
Cleanup Agent	Alumina
	2g
Solvent	n-hexane:acetone 1:1 (v:v)
Flush volume	60%
No. of cycles	2
Nitrogen purge	1MPa

4.5.5 Description of standard extraction procedure

All used equipment was precleaned, heated in the oven at 105° C and rinsed three times with acetone after each use. The extraction cells were rinsed three times with water and soap and before use with acetone followed by nitrogen flushing.
The dried soil sample (10 g) was weighed into a glass beaker and spiked with 200 μL of an ISTD solution with a concentration of 100 ng/mL in ethyl acetate (using a Hamilton syringe). The sample was stirred with a cleaned spatula and the sample was kept until a complete evaporation of the solvent was visible. 2,5 g of activated diatomaceous earth (Thermo Fischer, purity, heated for 4 hours at 440° C) were added and mixed with the sample.
A 22 mL stainless steel cell was equipped with two filters (pore size) at the bottom and closed hand tight. Activated aluminum oxide (Sigma-Aldrich, purity, heated at 440° C for 16 hours, 2 g) was added to the cell. It was used to retain non-polar lipids during the extraction and to avoid further cleaning procedures. The layer was separated with one filter from the sample. The sample was poured into the cell using a stainless steel funnel. The mixture got packed into the cell by tapping and closed hand tight.
Between each extraction, the Dionex ASE 150 by Thermo Fisher Scientific was equipped with a cleaning cell and rinsed 3 times with the solvent mixture. The extraction was performed by the conditions listed in table 4.8.
The extract was reduced in the vial to 2 mL by a Biotage TurboVap LV Evaporator under a nitrogen stream and a bath temperature of 40° C. To avoid precipitation, a solvent exchange was made to ethylacetate. The vial was rinsed twice with three pipettes of ethyl acetate and the volume got reduced to 2 mL. The volume got further reduced (1 mL) and stepwise transferred to a GC vial equipped with a 0,2 mL inlet and reduced under a gentle nitrogen stream. Finally, the extract got spiked with 0,05 mL of the recovery standard solution (1μg/mL of F-PCB 118). The sample was stored in the at -5° C until analysis.

4.5.6 Instrumentation setup of GC-MS

All analysis and data treatment were preformed with the computer software: Thermo Xcalibur, version 2.1 (2009). For integration of the peaks in the chromatogram, the processing setup had been used. The peaks were identified by the method *Genesis*. For MS/MS- chromatograms, 5 smoothing points per peak had been used to improve the peak shape. The retention times were used in accordance with table 4.5, with a time window of 30 seconds. The instrument specifications for gaschromatography can be found in table 4.10. All specifications for the mass spectrometer are listed in 4.9. Chromatograms pictured in this thesis were taken with OpenChrom Community Edition (Aston), an open source software for chromatography and mass spectrometry.

Table 4.9: Instrument specifications and conditions for mass spectrometer

Parameter	Value
Mass spectrometer	
Instrument	ITQ 1100 Ion Trap Mass Spectrometer
	(Thermo Fischer Scientific)
Type	Quadrupole ion trap
Ionization technique	Electron ionization (EI), external ion source
Ionization voltage	
Ion source temperature	200°C
Electron multiplier offset	300
Start time	8.00
Stop time	24.00
Scan mode	SIM and MS/MS
	program see table 4.12
Microscans	2 (6 ions) -3 (4 ions) for SIM
	1 for MS/MS
Scan event time	0,94 sec

Table 4.10: Instrument specifications and conditions for gas chromatography

Parameter	Value
Injection	
Injection system	TriPlus Autosampler (Thermo Fischer Scientific)
Injection syringe	10 μL (HamiltonMicroliter 701)
Injection mode	Splitless
Split Flow	15 mL/min
Splitless Time	4,5 min
Temperature	280°C
Purge flow	Constant septum purge
Injection volume	1,0 μL
Washing solvent	Ethyl Acetate
Glas inlet	Liner TQ, 5 mm, splitless with glass wool (Thermo Fischer Scientific)
Column	
Chromatograph	TRACE Ultra Gas Chromatograph (Thermo Fischer Scientific)
Column type	DB-5ms fused silica capillary column (Agilent J& W)
Dimension	30m x 0,25mm x 0,25m film
Film	5% Phenyl/95% methyl siloxane
Carrier gas	Helium
Flow control mode	Constant flow
Linear velocity	1 mL/min
Temperature program	
Initial temperature	70°C, hold time 3,50 min
Ramp 1	25°C/min, 180°C
Ramp 2	5 °C/min, 300°C, hold time 4,00 min
Running time	35min (46min with Prep. Run)
Transfer line temperature	300°C

4.5.7 Single ion monitoring

First, analysis results were obtained by performing a single ion monitoring (SIM). For each congener, two ions as identification points were observed. Therefore, two identification points are given for each congener. The mass numbers observed were chosen inside the chlorine cluster. The observation of fragments was influenced by the sample matrix. The chosen masses are listed in table 4.11. The analysis time was subdivided into different segments, each one is screening for congeners with a different degree of chlorination, based on the retention times, which had been identified in the full scan mode. The segments are listed in table 4.12. The segments were chosen to limit the number of observed ions to a maximum of 6 ions per segment.

Table 4.11: Summary of the molecular weight and important ions for mass spectrometry. All mass numbers were used in the SIM with a window of 1 mass.

Group	Congener	MW	M+	[M+2]+
Native PCBs				
trichlorinated	18, 28,31	257,55	256	258
tetrachlorinated	44, 52	291,99	290	292
pentachlorinated	101, 118	326,44	324	326
hexachlorinated	138, 149, 153	360,88	360	362
heptachlorinated	180	395,33	394	396
$^{13}C_{12}$ **labeled PCBs**				
trichlorinated	28	267,55	268	270
tetrachlorinated	70,52	301,99	302	304
pentachlorinated	101, 118, 111	336,44	336	338
hexachlorinated	138, 153	370,88	370	372
heptachlorinated	170, 180	405,33	406	408

Table 4.12: Segments used in the single ion monitoring. The used mass numbers are found in table 4.11.

Segment	**1**	**2**	**3**	**4**	**5**	**6**	**7**
RT Start	8.00	13.80	16.00	18.10	18.90	20.50	21.50
PCB	tri	tetra	penta	penta	penta	hexa	hepta
					hexa		
mass no.	256	290		324	324	360	394
for	258	292		326	326	362	396
target	268	302		336	336	370	406
compound	270	304		338	338	372	408
and					360		
ISTD					362		
mass	274		342				412
for	276		344				414
F-RSTD							

4.5.8 Tandem mass spectrometry

Tandem mass spectrometry (MS/MS) involves multiple steps of mass selection, which leads to a higher selectivity and therefore a better signal to noise ratio. It was applied after a too high LOD and LOQ was obtained for the SIM mode. However, in the MS/MS mode in comparison to the SIM, the sensitivity for one ion mass gets somewhat reduced.
In the first step of mass spectrometry (MS1), ions are formed by external ionization and separated by mass to charge ratio in the ion trap. *Precursor ions* are selected and are fragmented by a pulsed dissociation mode in the ion trap (Advanced Pulsed Q Dissociation PQD, Thermo Scientific). In the second step (MS 2), the product ions are separated and detected. An overview of the instrumentation parts is given in figure 4.3.
Several papers have been published on analysis of PCBs, where one study also used an ion trap mass spectrometer for analysis [49].
Precursor and product ions were chosen in accordance with literature [42] and are listed in table 4.13. Only one MS1 scan per target compound could be performed and therefore only one precursor ion had been analyzed. Further explanation can be found in the discussion.
The ITQ 1100 is equipped with an automated collision energy (ACE), which automatically calculates an estimated optimal collision energy based on the operating parameters of the scan. ACE runs three energies in a single scan to ensure optimal fragmentation and product ion production [68]. Since a high sensitivity is preferred over a high variety of fragment ions, the collision energy was kept under the automatically chosen minimum.
The figure 4.4 and 4.5 show the chromatogram for a spiked soil sample in the SIM mode and in the MS/MS mode, respectively. In the SIM mode, a high noise level and a shift of the baseline is visible, especially for the segments of the lower chlorinated congeners. This can be successfully avoided by the use of MS/MS.

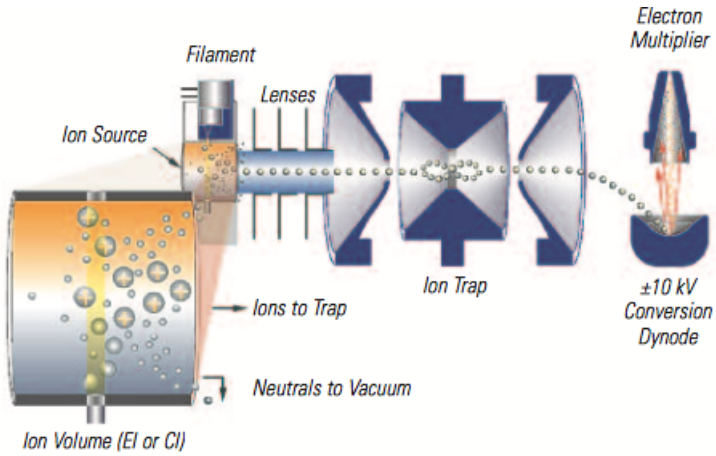

Figure 4.3: Ion trap and external ionization in the mass spectrometer ITQ1100 (Themo Scientific). Figure was taken from the product description [68].

Table 4.13: Observed precursor and product ions in the MS/MS mode for the analysis of 10 PCB congeners and isotopically labeled standard. The window of the Retention time (Rt) is listed each observation.

PCB	**Precursor**	**Product**	Segment	Rt
trichlorinated	256	186	1	8-13,8
trichlorinated (ISTD)	26	198	1	8-13,8
tetrachlorinated	290	220	2	13,8-16,5
tetrachlorinated (ISTD)	302	232	2	13,8-16,5
pentachlorinated	324	254	4	18,1-18,9
pentachlorinated (ISTD)	336	267	4	18,1-18,9
hexachlorinated	358	290	5	18,9-21,5
hexachlorinated (ISTD)	370	302	5	18,9-21,5
heptachlorinated	392	322	6	21,5-24,0
heptachlorinated (ISTD)	404	336	6	21,5-24,0
F-PCB118	342	274	3	16,5-18,1

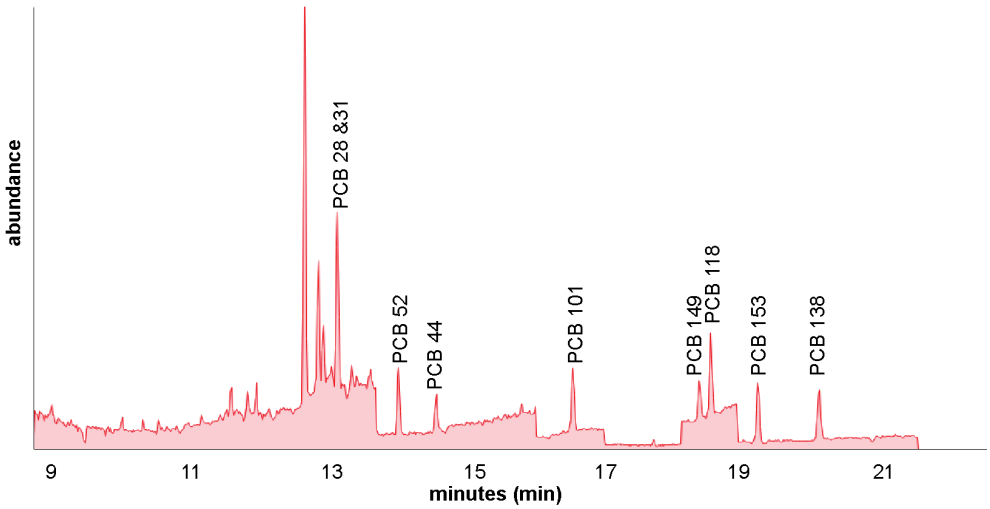

Figure 4.4: Chromatogram under the used SIM mode (see table 4.12) for an extracted soil sample (10 g) spiked with 200 ng of calibration solution.

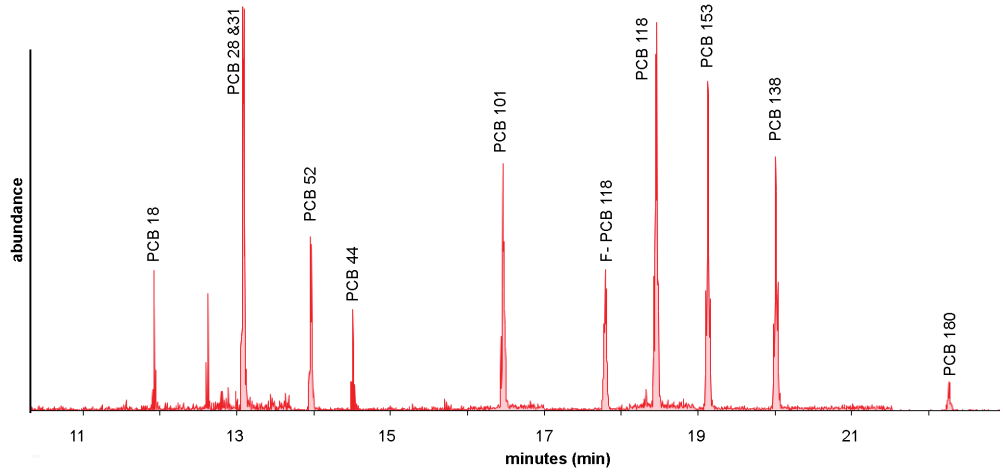

Figure 4.5: Chromatogram under the used MS/MS mode for a extracted soil sample (10 g) spiked with 200 ng of calibration solution.

4.5.9 Quality assurance

Evaluation of method blanks

Method blanks were performed to assure no contamination during the handling in the laboratory. The first extractions revealed no contamination of PCBs (when measured in the SIM mode). Yet, later extracted method blanks showed a contamination, especially for higher chlorinated congeners, which were possible to quantify in the MS/MS mode. The concentrations of PCBs measured in the method blank are listed in table 4.14. The increase of the blank level and its assumed causes are described in the discussion.

Table 4.14: Levels of PCBs revealed by using MS/MS in the method blank samples after several usage of the extraction cells.

PCB congener	concentration [ng]
18	ND
28	0,1
52	ND
44	ND
101	ND
118	6,1
138	2,4
153	1,1
180	7,2

Method validation

Several steps were made for method validation. In total 5 blanks were run during the analysis sequence (two during method validation, one inside of the analysis sequence of the reference material, and two in each analysis sequence of the samples). For a first evaluation of the method, three parallel extractions and analysis of the reference material had been performed (certified reference material, in accordance with ISO Guide 34:2009 and ISO/IEC 17025:2005, SQC068, PCB congeners in soil, purchased from Sigma-Aldrich). To achieve a better comparability of the analysis of the reference material with the analyzed samples, half of the amount (5 g) of the material was used in comparison to the routine method for background samples. Measured levels in comparison to the certified levels of the reference material for 6 PCB congeners are given in table 4.15. Results are further discussed in chapter 6.

Table 4.15: Certified levels of PCBs in the reference material SQC068. Relative standard deviation (RSD) for 3 parallel extracted samples. Recovery (R) is reported as surrogate recovery according to equation 4.8.

PCB	**Confidence Range** [ng/g]	**measured level** [ng/g]	RSD(%)	mean R(%)
28	82,5-218	90	33,8	84
52	24,0-63,4	45	18,2	111
101	51,4-136	105	40,2	97
118	141-373	368	154,4	87
138	56,7-149	95	37,6	88
153	172-452	194	169,7	90
180	89-236	245	120,3	89

Analysis of spiked samples for calibration

To determine the response factor, LOD/LOQ, the recovery range of the extraction method, and the influence of the sample matrix on the analysis, standard addition was performed. Therefore, material of one sample was spiked with a different amount of calibration solution (0.5, 1, 2, 10, 50, 100 and 200 ng) and analyzed by the routine method. The mean response factor of each congener, as well as the coefficient of determination of the linearity response and the relative standard deviation of the response factor are given in table 4.16. For comparison, the response factors calculated from the analysis of calibration solutions without sample matrix are given in table 4.17.
For graphical visualization, the response factors for all PCB congeners are plotted against the spiked concentration (figure 4.6). The upper plot shows the results calculated from the SIM analysis. There are high deviations in the response factors visible for different spiked concentrations. Therefore, no linear response of the detector is given. The results in the MS/MS mode show better results, although is the deviation higher than 10%. For very low concentrations (1 ng and 2 ng) the response of the detector is higher than expected. For comparison and determination of the influence of the matrix, the same plot was also established for the calibration solution (figure 4.7) and for three samples treated with sulfuric acid for cleanup (figure 4.8). All plots are further discussed in chapter 6.

Table 4.16: Mean response factor (f_r) calculated from samples spiked with calibration solution (10-200 ng, n=4), the coefficient of determination (R^2) for the linearity response and relative standard deviation the response factor (RSD) given. The recovery (R) is the mean recovery of all spiked samples and was calculated with the used ISTD relative to PCB 70, 111 and 170. The standard deviation of the recovery SD(R) between the four samples is given.

PCB	f_r	$\mathbf{R}^2$	RSD(%)	R (%)	SD(R) (%)
18	0,0949	0,9494	44,4	98,6	25,7
28	0,2139	0,9831	19,7	98,6	25,7
44	0,2401	0,9907	34,5	98,6	25,9
52	0,1145	0,9934	5,5	98,6	25,9
101	0,1311	0,9901	34,6	117.5	34,9
118	0,2412	0,9740	26,8	98,7	28,4
138	0,1017	0,9935	30,5	97,8	25,4
153	0,1248	0,9750	14,9	102,2	35,3
180	0,0982	0,9892	4,9	98,39	28,9

Table 4.17: Mean relative response factor calculated from calibration solutions (25-150 ng, n=4), coefficient of determination for the linearity response and relative standard deviation of the response factor are also given.

PCB	f_r	$\mathbf{R}^2$	RSD(%)
18	0,0629	0,9231	12,6
28	0,2101	0,9540	19,8
44	0,1577	0,9441	18,6
52	0,0761	0,9944	17,5
101	0,1591	0,9583	20,1
118	0,1228	0,9592	12,7
138	0,0183	0,9616	17,0
153	0,1075	0,9933	9,3
180	0,0046	0,9196	22,5

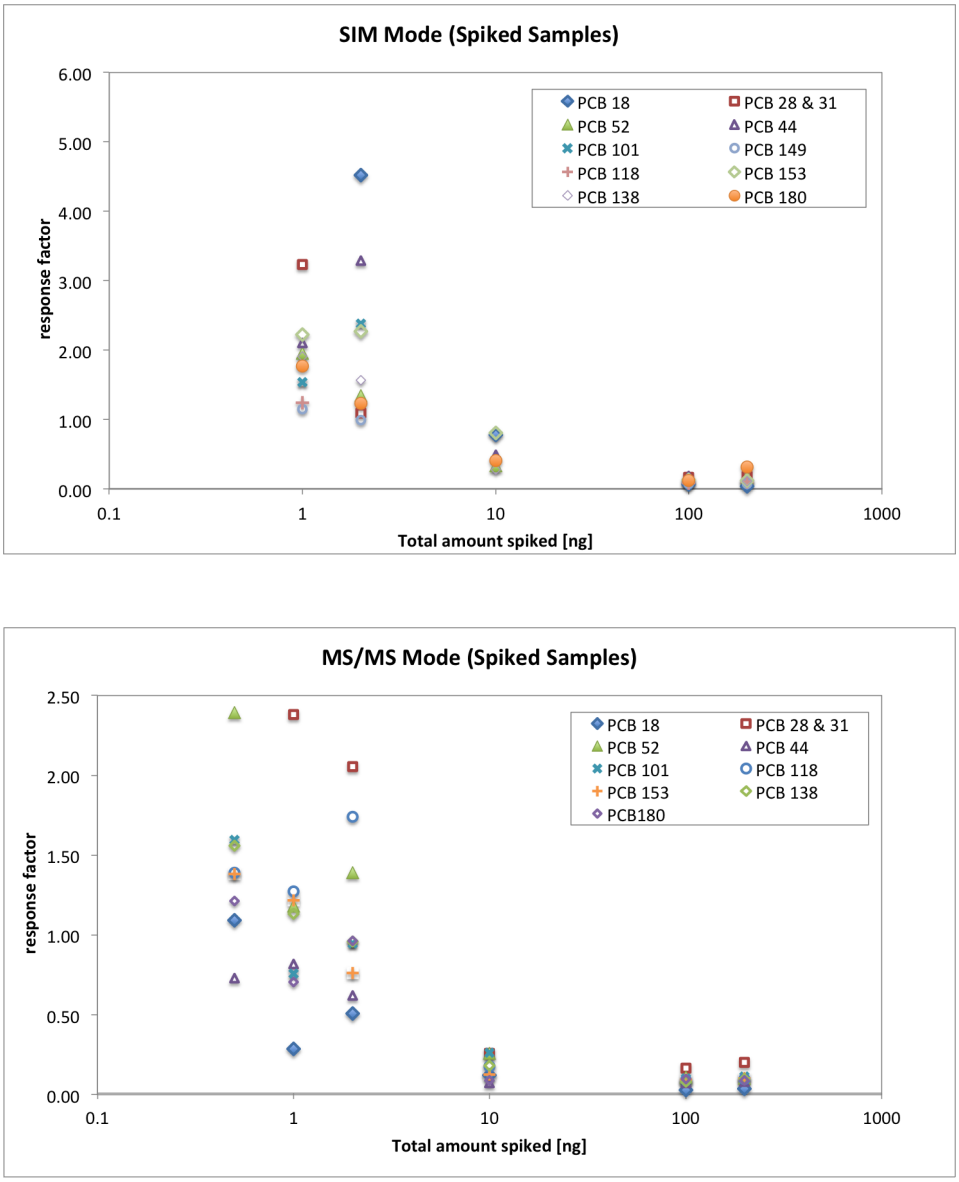

Figure 4.6: Response factors for all spiked samples (0.5, 1, 2, 10, 100 and 200 ng) used for calibration. Calculated from the analysis in the SIM (top) and MS/MS (bottom) mode.

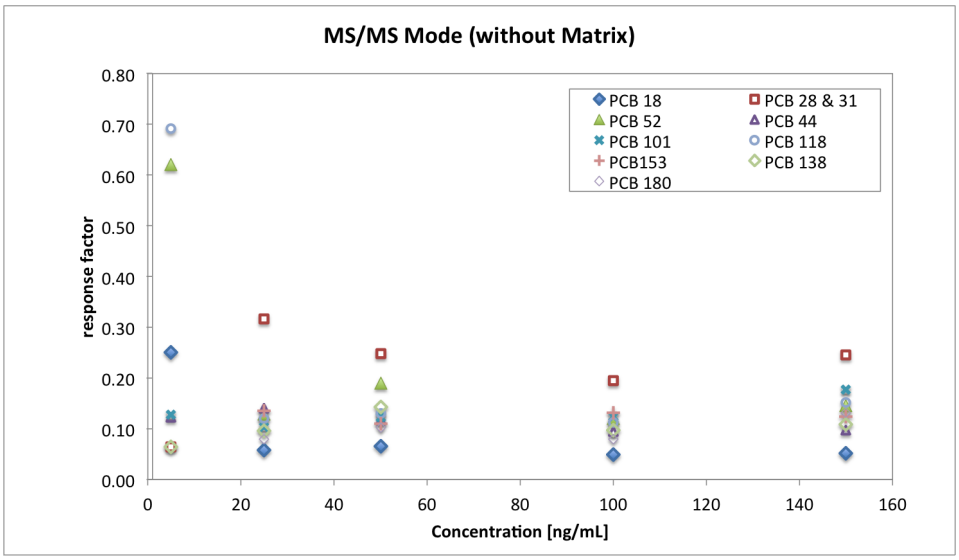

Figure 4.7: Response factors for calibration solutions without sample matrix. Calculated from analysis in the MS/MS mode.

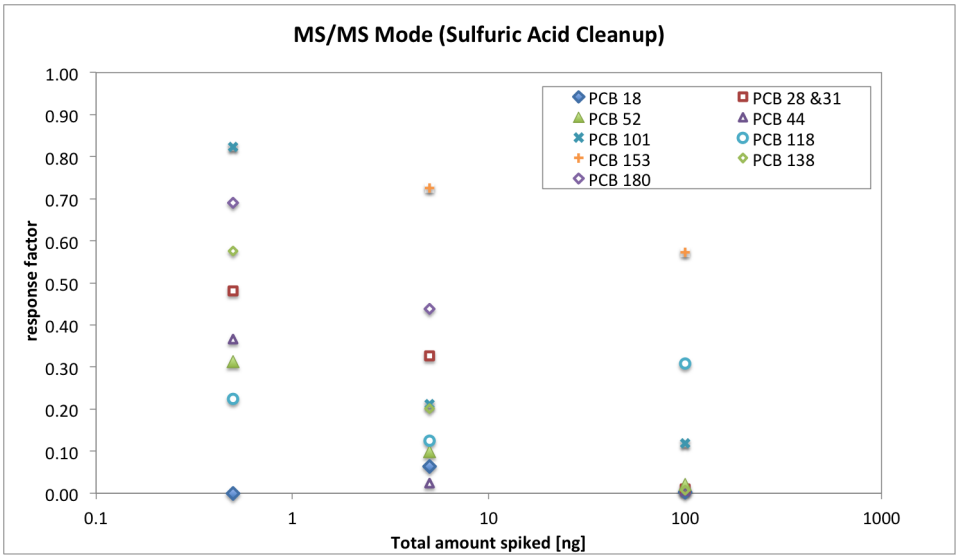

Figure 4.8: Response factors for spiked samples (0.5ng, 5ng and 100ng) and treated with sulfuric acid before analysis. Calculated from analysis in the MS/MS mode.

4.6 HYSPLIT analysis

The Hybrid Single-Particle Lagrangian Integrated Trajectory (HYSPLIT) model can be used to create backward trajectories for given starting locations. It has been developed by the National Oceanic and Atmospheric Administration (NOAA) [73]. For a simplified use, the Real-time Environmental Applications and Display sYstem (READY) has been used. The trajectories have been calculated for the sampling sites in Adventdalen, Kongsfjorden and Leinstranda. Since this model is based on global meteorological data, local weather phenomenon are not included in the data, and therefore the model is assumed to be inaccurate for close sampling sites (like Gasebu and Bayelva as well as Foxdalen, Janssondalen and Janssonhaugen) and no differentiation has been made. For this comparison, 72-hour backward trajectories are calculated for 30 days in July 2016, with starting a new trajectory every 6 hours. The coordinates used for calculation are given in table 4.18.

Table 4.18: Used coordinates and elevation above ground level (AGL) for the calculation of three HYSPLIT scenarios for the area around Adventdalen (which includes all samples taken in Foxdalen, Janssondalen and Jansonhaugen) as well as Kongsfjorden (which includes Gasebu and Bayelva).

	Adventdalen	Kongsfjorden	Leinstranda
Elevation (m)	50	20	20
Coordinates	78°10’11"N	78°55’33"N	78°52’7"N
(DDMMSS)	16°16’35"E	11°54’49"E	11°37’1"E

4.7 Statistical approach

Statistical analysis was carried out using RStudio 1.0.136 as well as IBM SPSS Statistics version 24. Statistical tests were performed for validation of assumptions made on the graphical plots. The significance level for all tests was set at p<0,05 as not differently reported, and classified with * for p<0,005 and ** for p<0,0005.
Before applying tests, the data was also tested to see if the underlying assumptions are fulfilled. Shapiro-Wilk test was used to test for normal (and lognormal) distribution. Levene statistic was performed to test for homogeneity of variance.

The extent of relationship of variables was estimated by Person correlation for data with bivariate normal distribution and Spearman rank correlation for data with no normal distribution, but a monotonical association. Difference of the distribution of one element between six sample areas (Foxdalen, Jansondalen, Jansonhaugen, Gasebu, Bayelva, Leinstranda) was tested with one-way ANOVA (Kruskal-Wallis Test) and between Longyearbyen and Ny Alesund with Mann-Whitney U Test (MWU).

4.8 Principal component analysis/ Factor analysis

Principal component analysis (PCA) and the rotated version factor analysis (FA) are multivariate analytical tools and used to reduce a set of original variables and to extract a small number of components/factors for analyzing relationships among the observed variables.
In this study, it was used to examine in which way trace metals are more influenced by the soil parent material versus the LRAT input. It shows, in which way the trace metals are correlated with each other, and main factors influencing the measured levels can be identified in the rotated version.
The correlation matrix (Pearson) was tested for at least one linear association of the variable with another variable. If this criteria was not fulfilled, the variable got removed from the analysis.
Sampling adequacy was verified by the Kaiser -Meyer -Olkin measure (KMO) and reported for each PCA study. For all study cases, a KMO measure higher than 0,6 had to be achieved. Otherwise, variables were excluded from the study. Variables for exclusion were chosen by examination of the anti -image matrices. Variables with a low individual KMO measure were excluded until a high overall KMO had been achieved.
Bartlett's test of sphericity test had been performed to test the hypothesis that the correlation matrix is an identity matrix. The significance level for this measure had been set to $p<0.05$.
Rotation of the PCA was performed by Varimax with Kaiser normalization for FA. Missing values were left blank and excluded list wise.

Chapter 5

Results

5.1 Level of inorganic pollutants

The main focus is set on elements which are described as LRAT pollutants[4]. Descriptive statistics for all measured elements for soil and vegetation is given in tables A.3 and A.2 in the appendix. An overview of the measured levels in soil and vegetation samples for selected elements for different sampling sites is given in the appendix (see table A.4 and A.5). For this study, Cd, Hg and Pb are set as the main interesting pollutants. Figure 5.1 and 5.4 shows plots of the spatial variance for the sampling areas Foxdalen, Jansondalen and Jansonhaugen (which were reached from Lonyearbyen) and Gasebu, Bayelva and Leinstranda (which were reached from Ny Ålesund). The sample sites are plotted in figures 3.5 and 3.6 and grouped in the sample areas.
The boxplot in figure 5.1 and figure 5.4(a) shows the spatial variance for mercury. The measured levels for all sampling sites close to Longyearbyen were significantly higher (MWU-test, **) than for sampling sites measured in Ny Ålesund. The lowest mean of Hg in soil was measured in Leinstranda (mean= 0,0177± 0,0178 μg/g), highest levels were measured around Jansonhaugen, especially for vegetation (mean(soil)=0,0816± 0,0183 μg/g, mean(vegetation)= 0,130± 0,039 μg/g). The mean for vegetation showed to be higher than the mean measured in soil.
The graph in figure 5.2 and figure 5.4(b) shows the spatial variance for Cadmium.
The lowest mean of Cd was measured in soils from Gasebu (mean(soil)= 0,161± 0,164 μg/g), while the highest mean of Cd was found for samples around Bayelva river (mean (soil)= 0,318± 0,077 μg/g). The mean for the vegetation showed to be higher than the mean of the soil.

The graph in figure 5.3 and figure 5.4(c) shows the spatial variance for Pb. The highest levels of Pb in soil were measured in Jansondalen (mean(soil)= 15,9 ±3,5 μg/g), while lowest levels were measured in Leinstranda (mean(soil)= 9,1± 6,0 μg/g). The mean for Pb in soil is, despite Leinstranda, in all sample areas higher than the measured mean of the vegetation.

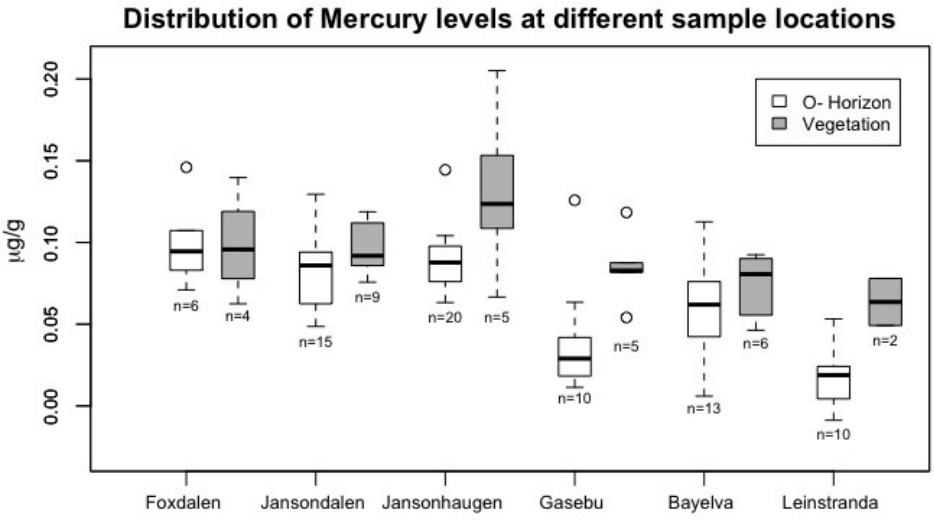

Figure 5.1: Boxplot for mercury in soil and the vegetation cover at six different sample areas. Different sample sizes (n) were taken at the different locations. The interquartile range (IQR) is marked by the box, the black line shows the median. The whisker is calculated by the 1st/3rd quartile ± 1.5 · IQR. Outliers are marked with a circle.

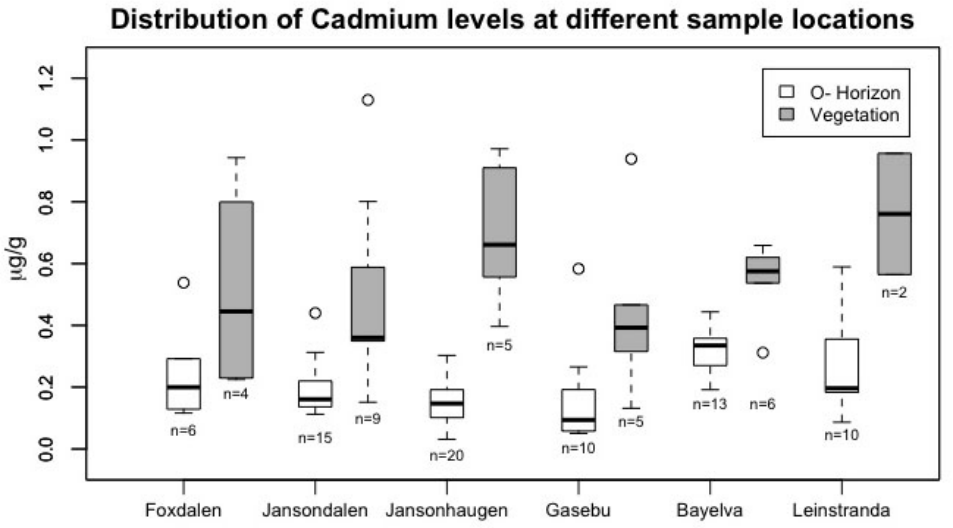

Figure 5.2: Boxplot for lead in soil and the vegetation cover at six different sample areas. Different sample sizes (n) were taken at the different locations. The interquartile range (IQR) is marked by the box, the black line shows the median. The whisker is calculated by the 1st/3rd quartile ± 1.5 · IQR. Outliers are marked with a circle.

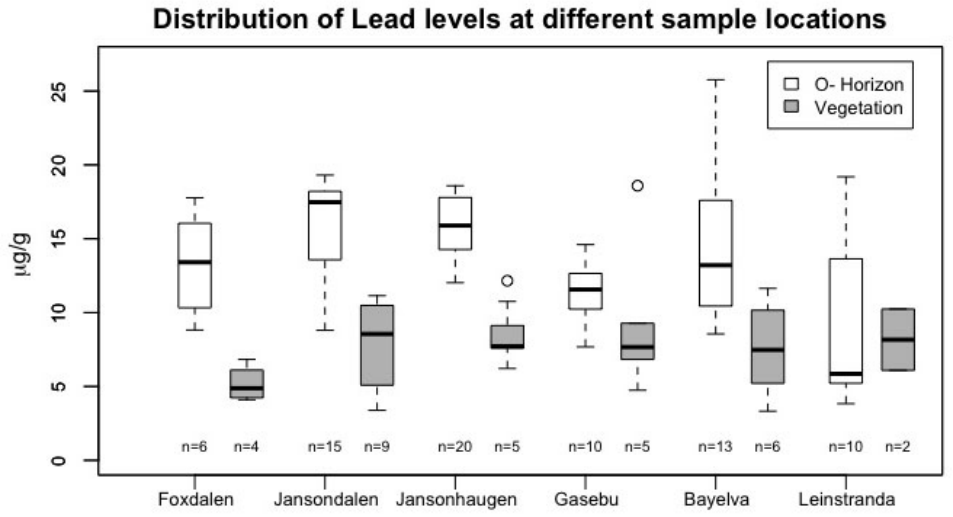

Figure 5.3: Boxplot for cadmium in soil and the vegetation cover at six different sample areas. Different sample sizes (n) were taken at the different locations. The interquartile range (IQR) is marked by the box, the black line shows the median. The whisker is calculated by the 1st/3rd quartile ± 1.5 · IQR. Outliers are marked with a circle.

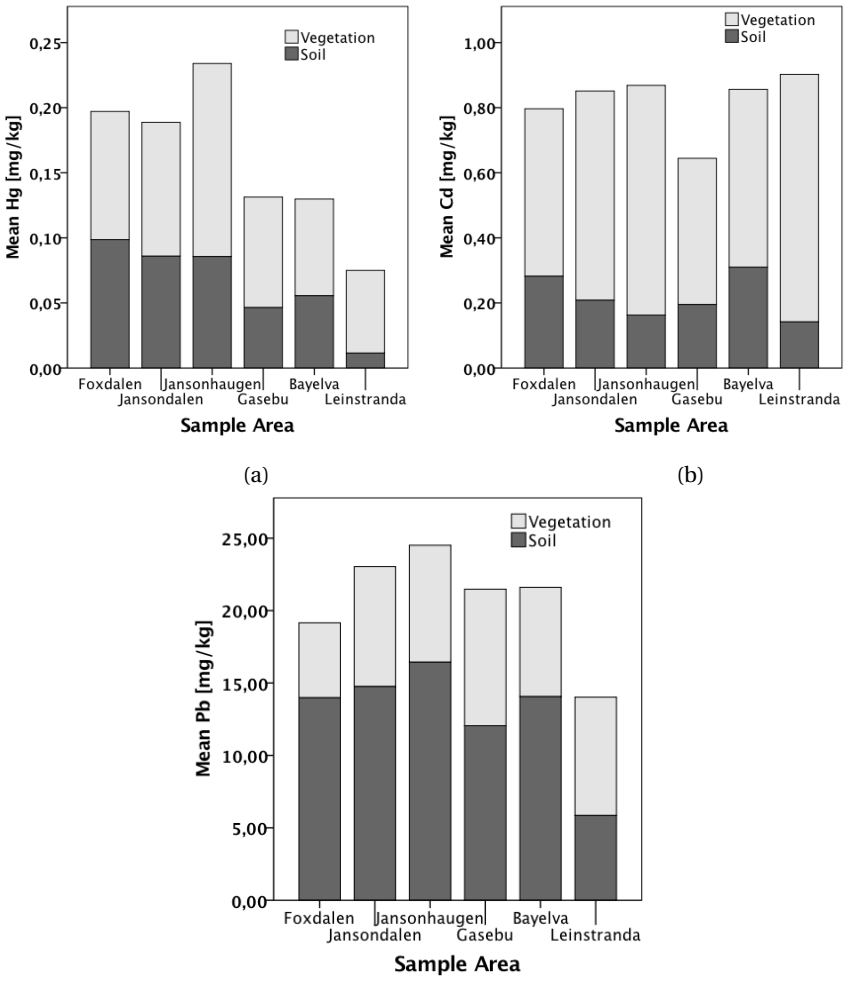

Figure 5.4: Mean levels of (a) mercury, (b) cadmium, (c) lead for the six different sampling sites, differentiated between vegetation and soil layer.

A closer examination of the U levels revealed outlier on the sample sites 35 A+B (Bayelva) and 36 A+B (Gasebu) for soil and vegetation. The on these sample site measured levels were 10 times higher than the measured mean (up to 15,8 μg/g, mean for other sample sites 1,10 μg/g in soil). Without the outliers, the sample sites Gasebu showed significant higher U levels in soil (ANOVA,**).

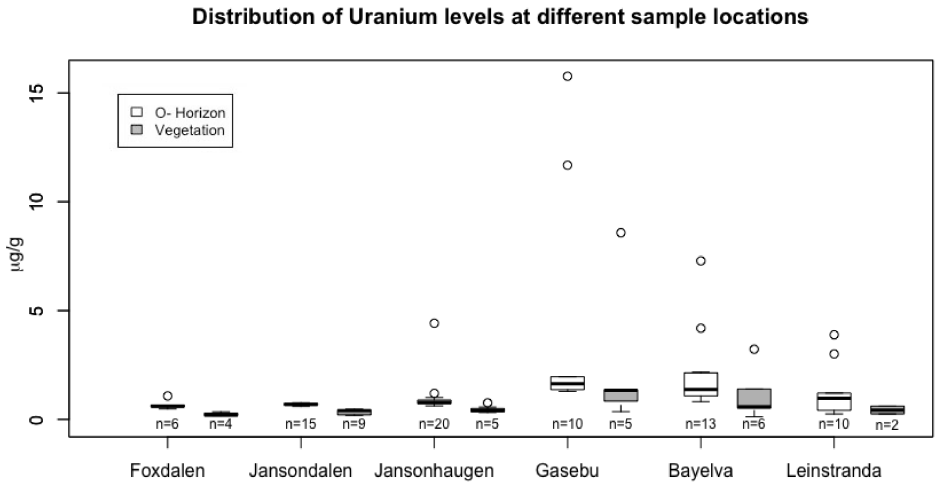

Figure 5.5: Boxplot for uranium in soil and the vegetation cover at six different sample areas. Different sample sizes (n) were taken at the different locations. The interquartile range (IQR) is marked by the box, the black line shows the median. The whisker is calculated by the 1st/3rd quartile $\pm$ 1.5 $\cdot$ IQR. Outliers are marked with a circle.

5.2 Level of PCB in Svalbard

For analysis of PCB at NTNU, no data of the samples got reported, since all measured levels were outside of the linear range of the method (see chapter 4.5 and 6.1 for further explanation). The levels presented here were reported by Sintef Molab.
The analysis was performed by an internally certified method. The method was reported with a relative standard deviation of 30%. The results are listed in table A.7 and A.6. In total 7 PCB congeners (28, 52, 101, 118, 138, 153, 180) were analyzed. Only four congeners exceeded the limit of quantification for this method (LOQ= 0,001).
Table 5.1 shows the descriptive statistics for the measured data. All quantified levels are visualized in the boxplots in figure 5.6 for soil and vegetation. The levels of PCB 52 were significantly higher for vegetation than for soil.
Figure 5.7 and 5.8 shows the measured data points in comparison to their geographical data. As it is clearly visible, almost all samples with measured PCB 52 are located close to Longyearbyen, while PCB 180 was measured at Leinstanda and west of Ny Alesund. No significant relationship was found between the distance to infrastructure and the measured PCB levels.

Table 5.1: Descriptive statistics for the results of 25 soil and 15 vegetation samples. Levels are presented in [$\mu g/g$]. Mean, median and standard deviation (SD) are calculated from the quantified data. The detection rate (DR) shows the number of samples over the limit of quantification LOQ. The minimum level (Min) was set to the LOQ. Max shows the maximum value in the data.

	Medium	**DR**	**Mean**	**Median**	**SD**	**Min**	**Max**
PCB 52	Soil	15/25	0,0030	0,0029	0,0012	<0,001	0,0055
PCB 52	Vegetation	7/15	0,0059	0,0056	0,0025	<0,001	0,0097
PCB 180	Soil	4/25	0,0049	0,0052	0,0009	<0,001	0,0056
PCB 28	Vegetation	2/15	0,0052	0,0052	0,0022	<0,001	0,0067

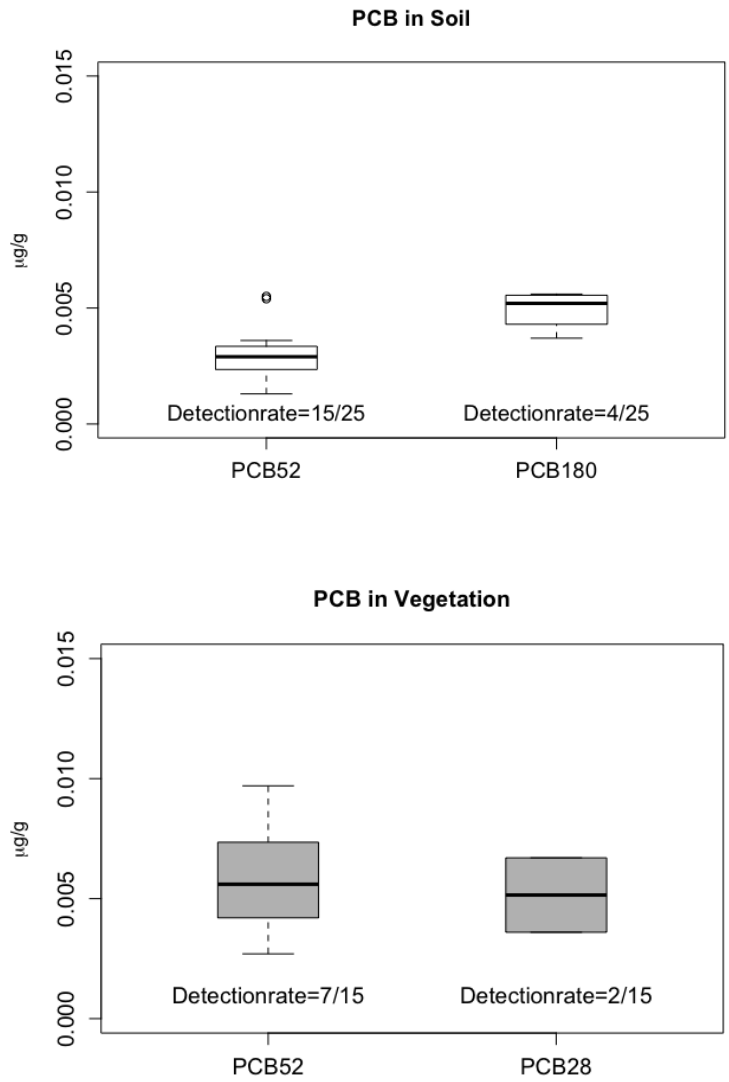

Figure 5.6: Boxplot for all measured PCBs in soil and vegetation. The interquartile range (IQR) is marked by the box, the black line shows the median. The whisker is calculated by the 1st/3rd quartile $\pm$ 1.5 $\cdot$ IQR. Outliers are marked with a circle. Additionally, the detection rate is given.

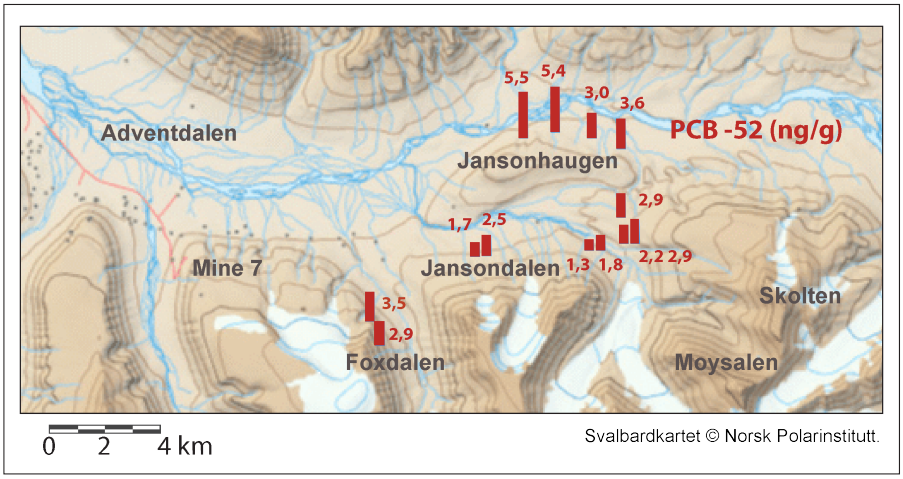

Figure 5.7: Visualization of the results received from the laboratory for the samples taken in around Adventdalen/ Longyearbyen. Only PCB 52 was over the limit of detection, all other PCB congeners are below 0,1 ng/g (dw). Reported uncertainty is 30% of the value.

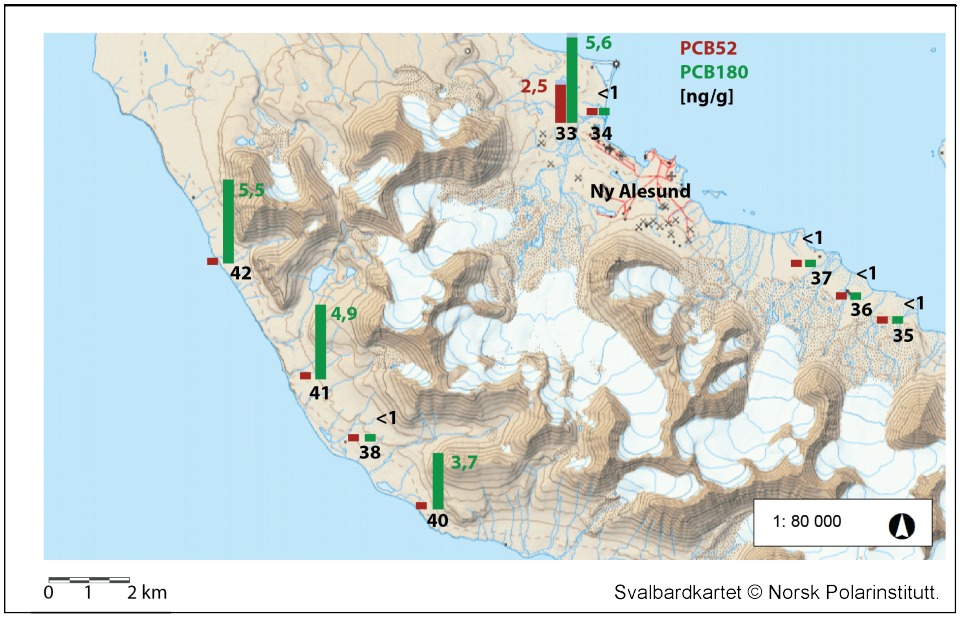

Figure 5.8: Visualization of the results received from laboratory for the samples taken in around Ny Ålesund. Only PCB 52 and 180 were over the limit of detection, all other measured PCB congeners are bellow 0,1 ng/g (dw). Reported uncertainty was 30% of the value.

5.3 Variation and influence of SOM

Figure 5.2 illustrates the total orgarnic carbon (TOC) in the surface soil samples, which refers to the SOM content of the soil. The TOC ranged between 5,0 and 70,9 % with a mean of 22,5% and a median of 19,0%. The standard deviation between the three replicates ranged from 0,02 to 2,7 % with a mean of 0,3%. Table 5.2 shows the mean TOC for all six sample areas and the boxplots in figure 5.9 visualize the data range for different sample sites.

Table 5.2: Total organic carbon for surface soils in Svalbard

Area	TOC [%]
Foxdalen	31,2±8,2
Jansondalen	19,1±8,7
Jansonhaugen	13,8±4,5
Bayelva	33,2±8,3
Gasebu	23,6±16,7
Leinstranda	21,8±26,3

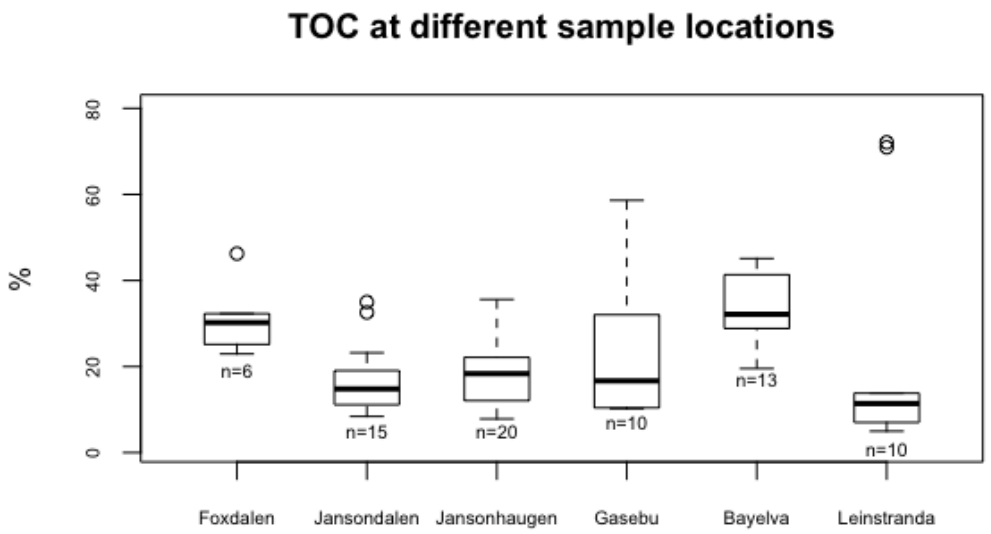

Figure 5.9: TOC determined by loss on ignition on different 6 different sampling locations. Different sample sizes (n) were taken at the different locations. The interquartile range (IQR) is marked by the box, the black line shows the median. The whisker is calculated by the 1st/3rd quartile ± 1.5 · IQR. Outliers are marked with a circle.

The measured levels of PCB 52 and PCB 180 were tested for correlation versus the TOC for all sample sites. Here, no significant correlation was found. Figure 5.10 shows the correlation only for the sample area Jansonhaugen with a significant correlation (Spearman's ρ= 0,943*). One sample point was marked as an outlier. Figure 5.11 displays the measured levels of Cd versus the TOC, which shows a positive correlation (Pearson r=0,728**, Spearman's ρ=0,652**). Furthermore, a moderate negative correlation was found for Pb and TOC (Pearson r=-0,339*, Spearman's ρ=-0,319*).

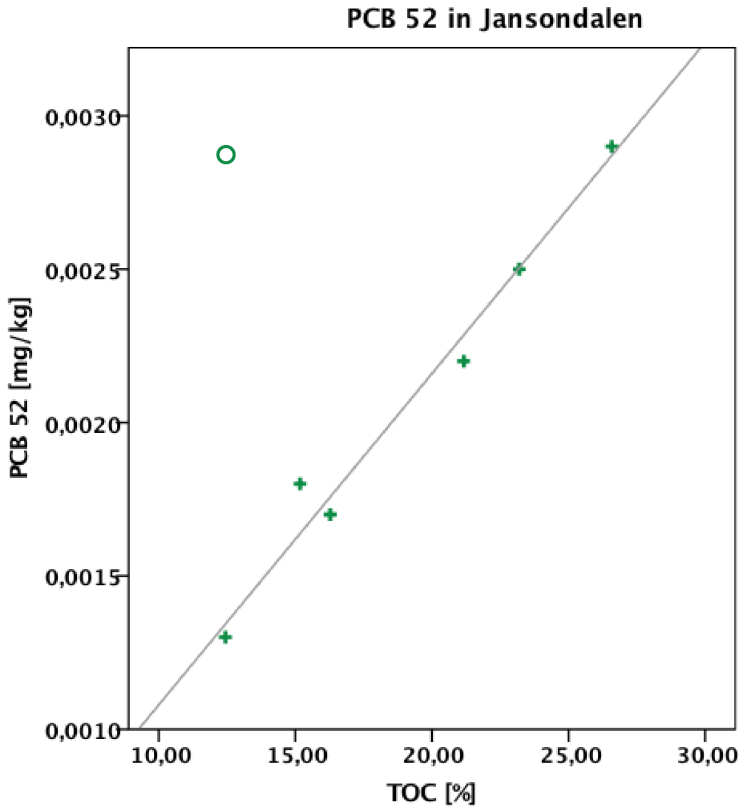

Figure 5.10: PCB 52 versus the measured TOC at the sample area Jansonhaugen. Outliers are marked with a circle. The fit line is given for the correlation (Spearman's ρ= 0,943*).

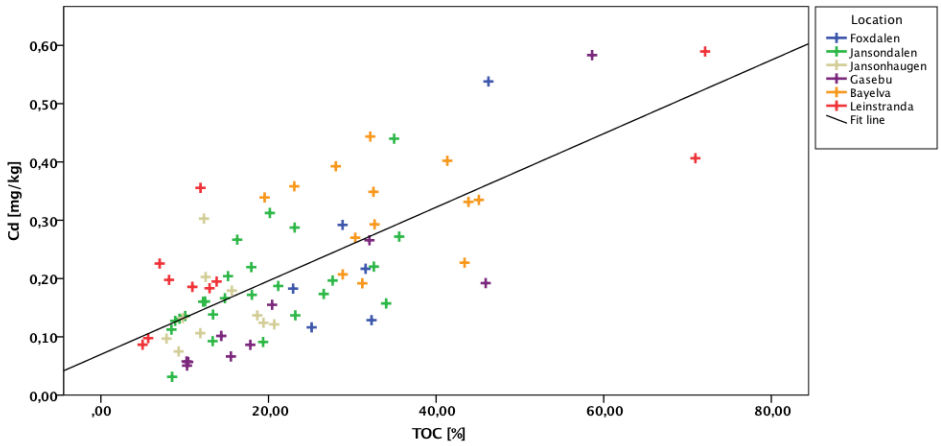

Figure 5.11: Cadmium versus the measured TOC at all sample sites. the fit line is given for the correlation (Pearson r=0,728**, Spearman's ρ=0,652**).

5.4 Principal component analysis and factor analysis

Three study cases have been performed:

(A) Factor analysis for all soil samples and all analyzed inorganic elements and TOC. The dataset contained 25 variables and 74 samples.

(B) Factor analysis with general soil characteristic measures (thickness of O-horizon, thickness of vegetation layer, temperature gradient between soil and air, attitude, TOC, ration between Al and Mg) as well as the results of the PCB analysis. The final datasets contained each 14 variables and 25 samples.

(C) Biplot for soil and vegetation samples (109 samples) for 18 elements of interest. Influence of the scores between soil and vegetation samples have been compared to evaluate the different correlation of elements in vegetation and soil.

Factor analysis for inorganic elements - study case (A)

In total, 7 components showed an eigenvalue higher than 1. However, three factors were extracted, since they could be interpreted. The loadings of the variables on the rotated components and the explained variance are given in table A.9. The main factor is explains 43,7% for three extracted factors. For this analysis, the KMO measure was determined by 0,771. Bartlett's test of sphericity showed a high significance ($p<0,0005$). The scree plot is given in figure A.1 in the appendix. The first 3 factors were used for interpretation (see chapter 6.3).
The score plot of all the used sample sites is given in figure 5.12. Here, three sample sites are clearly not clustering with the main bulk of samples. These sample sites are marked as outliers and are not included into the final factor analysis. Samples close to Longyearbyen (Foxdalen, Jansondalen, Jansonhaugen) cluster together and samples close to Ny Ålesund (Gasebu, Bayelva, Leinstranda) cluster together. Figure 5.13 shows the loading plot for all variables for the three main components. Further explanation of the plot is given in the discussion (chapter 6.3).

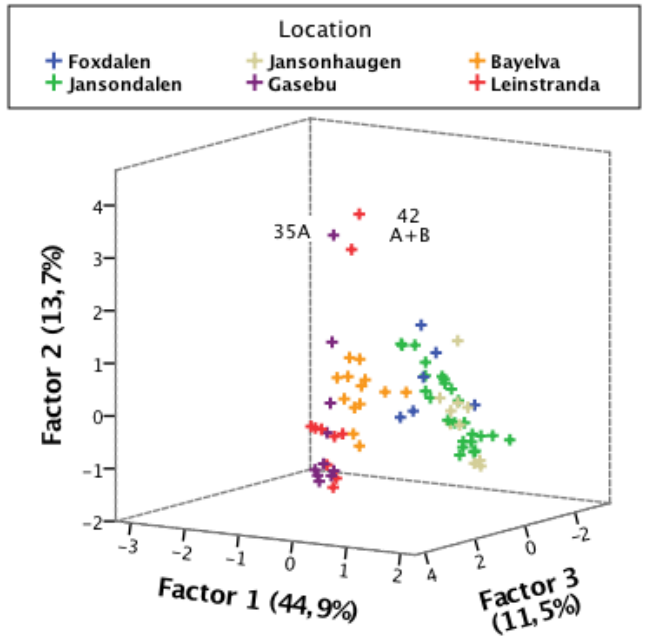

Figure 5.12: Score plot for all sampling sites in the study case (A). Outliers are marked with a text annotation of the sample number. Different sampling sites can be differentiated by the legend.

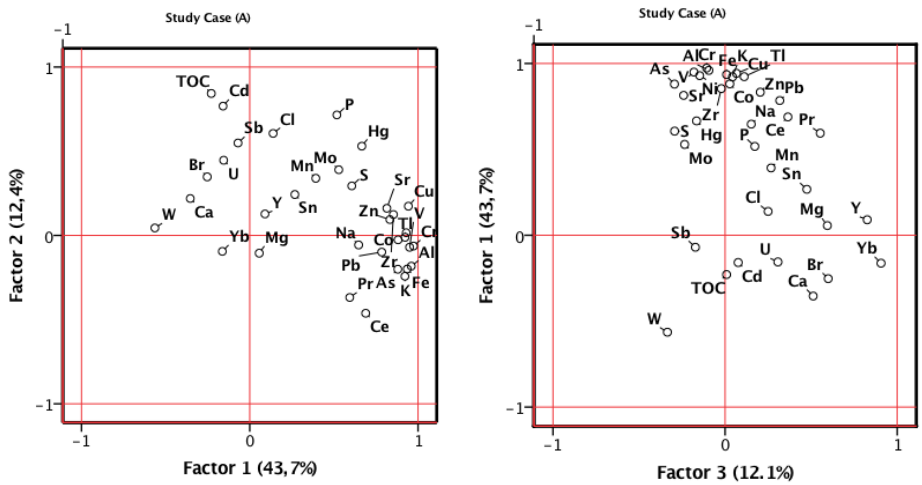

Figure 5.13: Loading plot for the first three factors for the study case (A). The explained variance is given for each factor.

Factor analysis for general soil characteristics and PCB- study case (B)

The PCB dataset has a low sample size and therefore limits the number of variables which can be introduced into the PCA/FA. For that reason,the same FA was performed first without the PCB variable, for each of the variables which show a same loading one of the variables got chosen (reducing redundancy in the set of variables). Then, the FA was performed with an amount of variables that show the best KMO (Kaiser Mayer Oklin sample adequacy). Since the main loadings of the variables did not changes while including the PCB variable, results can be seen as interpretable even though the KMO is lower for this analysis. The analysis with included PCB variable showed a low KMO (0,525). The same analysis was performed without the variable PCB and showed an acceptably KMO (0,645). Loadings between both PCA for all other variables were comparable. The analysis was performed with the variable PCB since this was in the main interest of this work. Bartlett's test showed a significance of p<0,0005. Due to the Eigenvalue criterion, 4 factors had been extracted. Scree plot is given in figure A.2 in the appendix. The loadings of the variables on these 4 factors are given in table 5.3 with the explained variance for each factor.
Figure 5.14 shows the loadings of all included variables on the first three factors. Those showed a cumulative explained variance of 69,9%. Figure 5.15 shows the score plot of all included samples. Different sample areas are marked with a different color. Further explanation of the plot is given in the discussion (chapter 6.3).

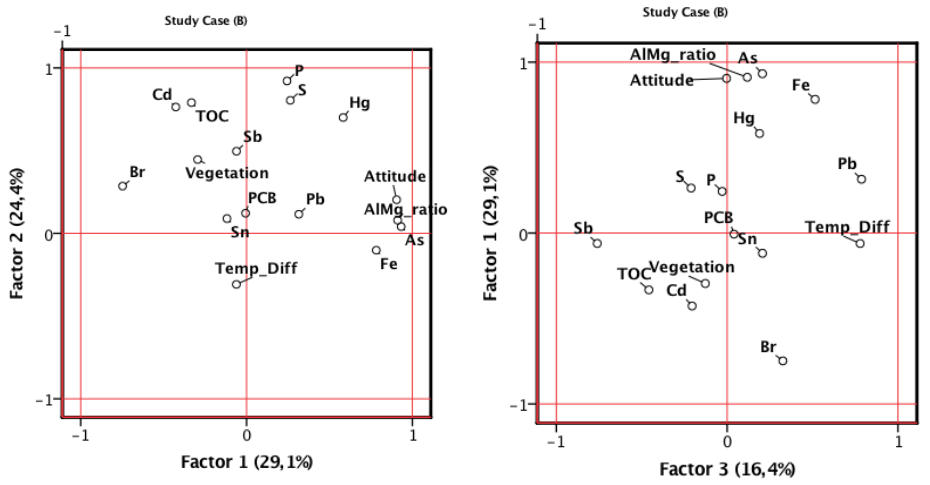

Figure 5.14: Loading plot for the first three factors for the study case (B): Soil characteristics, inorganic elements and PCB (52+180). The explained variance is given for each factor.

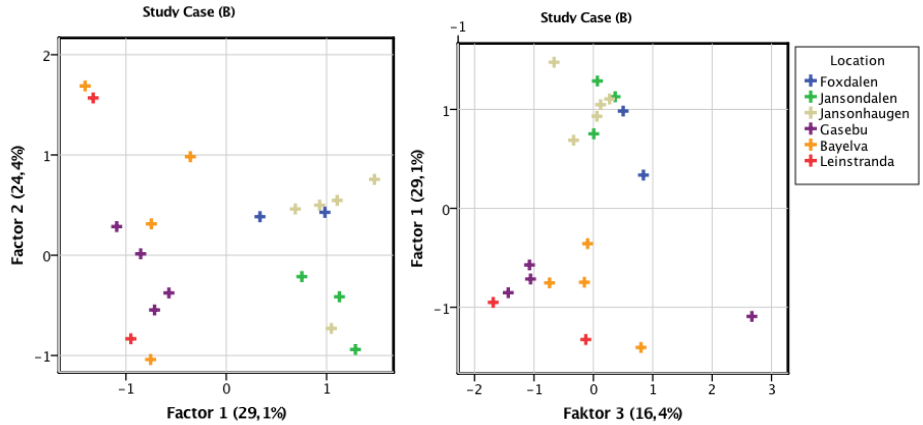

Figure 5.15: Score plot for all sampling sites in the study case (B). Different sampling sites can be differentiated by the legend.

Table 5.3: Factor loading (varimax rotated) for selected inorganic elements and soil characteristics for the first 4 loadings (marked positive loadings are higher than 0,4 and negative loadings lower than -0,4).

	Component			
	1	**2**	**3**	**4**
Variance [%]	**28,15**	**24,91**	**16,86**	**11,40**
Attitude	**0,905**	0,203	-0,003	0,116
Vegetation cover	-0,295	**0,446**	-0,128	-0,382
TOC	-0,332	**0,790**	**-0,458**	-0,006
Al/Mg-Ratio	**0,911**	0,079	0,118	0,064
Temperature	-0,061	-0,308	**0,779**	0,149
Br	**-0,748**	0,286	0,326	0,125
Cd	**-0,427**	**0,764**	-0,205	0,035
Sn	-0,118	0,089	0,207	**-0,908**
Hg	**0,582**	**0,700**	0,190	-0,017
Pb	0,315	0,116	**0,787**	-0,283
P	0,244	**0,921**	-0,029	-0,028
S	0,263	**0,804**	-0,211	0,058
Fe	**0,782**	-0,102	**0,515**	-0,059
As	**0,932**	0,041	0,207	0,205
Sb	-0,061	**0,496**	-0,760	0,102
PCB	-0,006	0,122	0,040	**0,886**

Biplot for soil and vegetation - study case (C)

Biplots show the relationships between variables (loadings as arrows) and observations (samples as scores). The biplot had been performed by CATPCA option in SPSS. Figure 5.16 shows the biplot with differentiation between the soil and vegetation samples in the scores. Further interpretation is given in chapter 6.3.

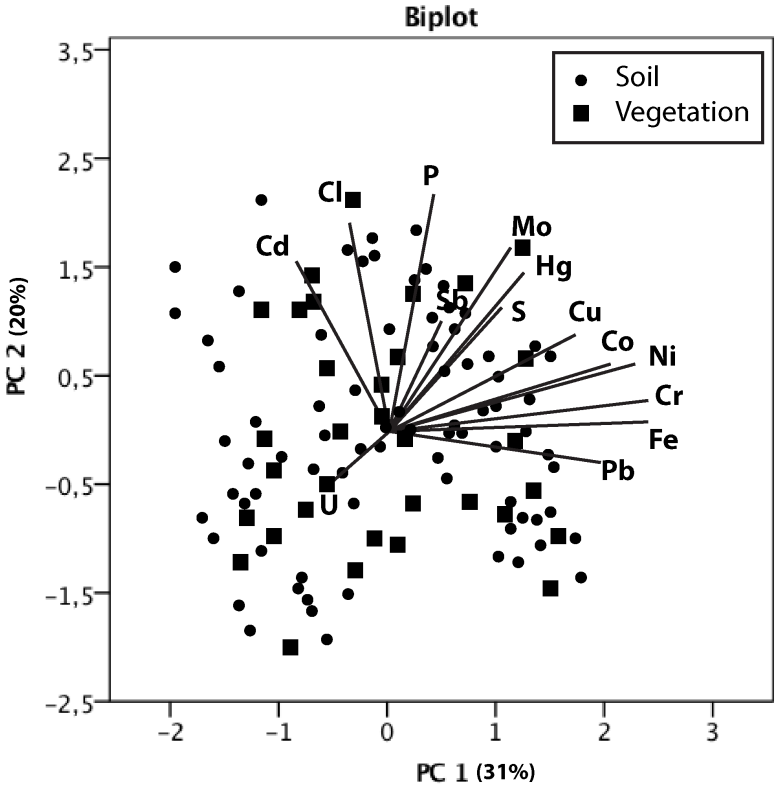

Figure 5.16: Biplot for soil and vegetation samples for 18 elements. The first dimension explains 31% of the variance while the second dimension explains 20%. The different sample material is plotted with different marker (see legend).

5.5 Correlations between selected elements

The correlation matrix for (Pearson correlation and Spearman's rank) are given in table A.3 and A.4 in the appendix. The results for Shapiro Wilk test for normal distribution is given in table A.8.

The Elements Hg, Pb and Cd were tested for correlation with other measured variables based on the results. Pearson correlation coefficients for all elements with calculated significance can be found in figure A.3 in the appendix. The sample size for this correlations is N=74.

Mercury showed high significant correlation with S (Pearson r=0,612**, Spearman's ρ =0,554**) and Cl (Pearson r=0,406**, Spearman's ρ=0,415**), which are displayed in figure 5.17 and 5.18. Similar correlation was also found in vegetation for Hg and S (Pearson r=0,583**, Spearman's ρ=0,662**). Additional correlation can be found between Hg and P (Pearson r=0,782**, Spearman's ρ=0,662**) and Hg and As (Pearson r=0,602**, Spearman's ρ=0,542**).

Positive correlation was found for Pb and Fe (Pearson r=0,774**, Spearman's ρ=0,774**), which is displayed in figure 5.19.

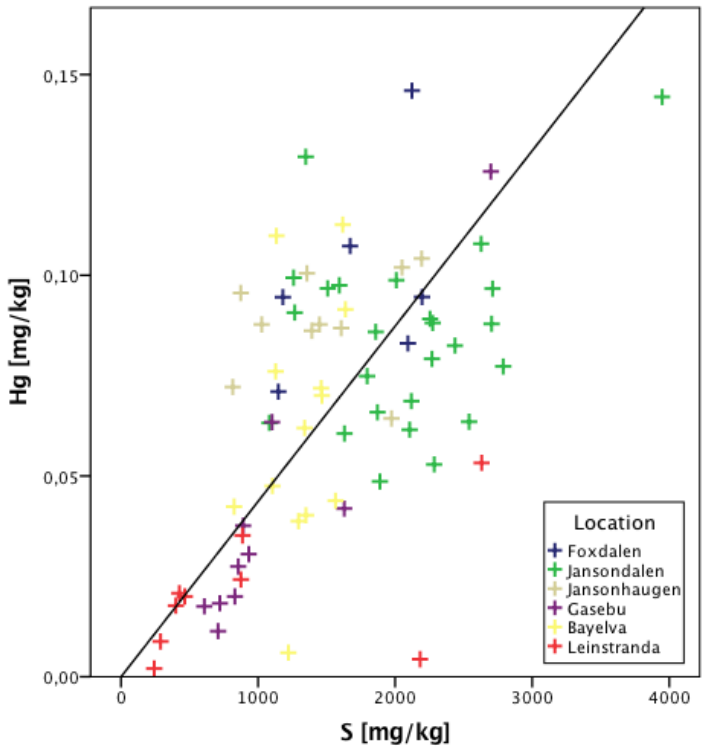

Figure 5.17: Plot of Mercury levels and Sulfur levels in surface soil (Pearson r=0,612**, Spearman's ρ=0,554**). Different sample sites are marked with different colors.

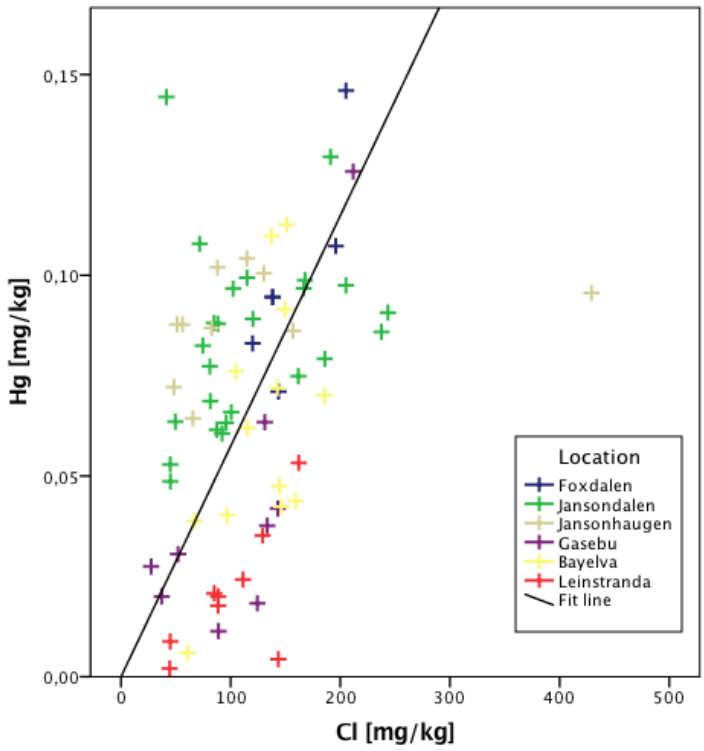

Figure 5.18: Plot of Mercury levels and Chlorine levels in surface soil (Pearson r=0,612**, Spearman's ρ=0,554**). Different sample sites are marked with different colors.

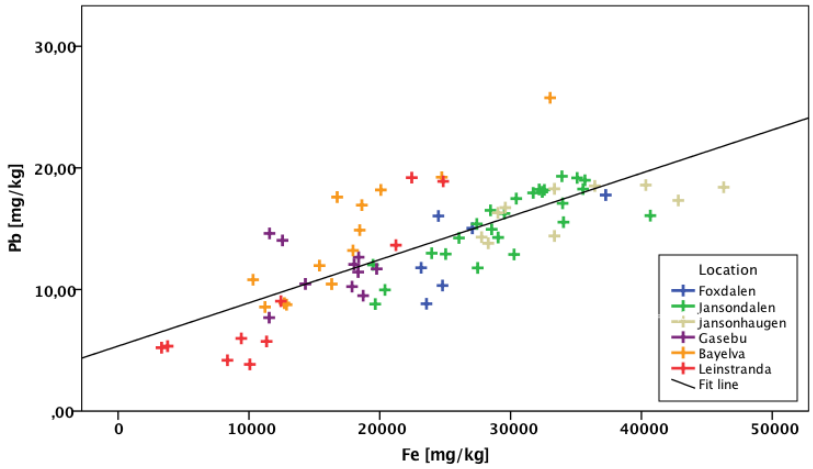

Figure 5.19: Plot of Lead levels and Iron levels in surface soil (Pearson r=0,774**, Spearman's ρ=0,774**). Different sample sites are marked with different colors.

5.6 HYSPLIT modeling of trajectories

Figure 5.20 shows the Frequency plot for the back trajectories calculated for Adventdalen, Ny Alesund and Leindstanda for August 2016. The trajectory frequency option starts a new trajectory from a single location and height every 6 hours and then sum the frequency that the trajectory passed over a grid cell and then normalize by the total number of trajectories. The used frequency grid resolution was 1 degree. A trajectory can intersect a grid cell several times but is just counted once in this calculation.

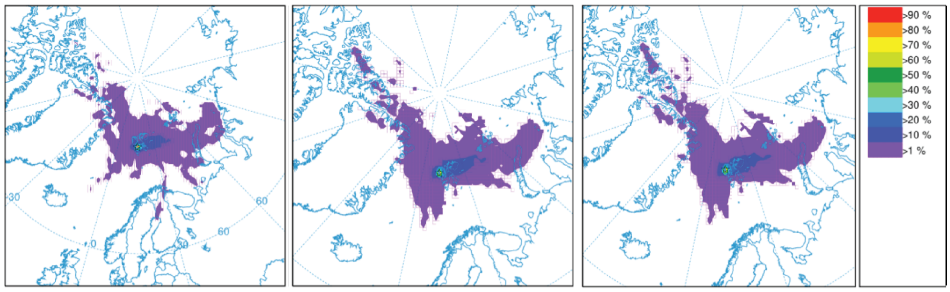

(a) Adventdalen (b) Kongsfjorden (c) Leinstranda

Figure 5.20: HYSPLIT Frequency plot of the trajectories for August 2016 calculated for three different starting points.

Chapter 6

Discussion

6.1 Assessment of the method development

Extraction and cleanup

Part of this thesis was the testing and evaluation of a newly purchased instrumentation for extraction (Dionex ASE 150 by Thermo Fisher) on soil samples. Regarding the achieved results, the ASE stands out with reproducible extraction results and a faster sample throughput than common used extraction techniques (like Soxhlet extraction). However, cleaning of the extraction cells proofed to be more important than expected. High method blank levels (see table 4.14) could be measured after an estimated number of ca. 30 extractions. This levels could have either occurred due to contamination of the extraction and workup solvents or due to contamination of the instrument. After a run of a new method blank with new deactivated diatomaceous earth, new solvent bottles and a cleaning of the cells with acetone in an ultrasonic bath (porous stainless steel filters removed from the cap of the extraction cell) the method blank levels could be reduced to the starting conditions (none of the analyzed PCB got detected). The disassembly of the cell caps is described in the instructions as not preferable to perform after every extraction since it harms the sealing of the cell. For further usage of the instrument, more work on a routine cleaning method of the instrument is recommended. During extraction, several leaks occurred in the instrumentation. This lead to a lower pressure in the extraction cell and therefore an inefficient extraction. Samples, which were extracted with a leakage, showed a recovery of 8-47% and were therefore repeated. The leakage could be stopped in the most cases by using a smaller filter size for the cellulose filter and changing the sealing of the cell.

Regarding the in-cell cleanup used, which had been described in the literature[60] for sediment samples, no efficient removal of influencing sample matrix could be achieved by the usage of copper and alumina in the cell. Since sulfur levels measured in the ICP-MS were low, the copper was not used during the routine method for soil samples. An additional removal of organic compounds by treatment of the extract with sulfuric acid achieved a lower linearity range (see figure 4.8). Thus recovery levels achieved with sulfuric acid cleanup were low (under 10%).

Limit of detection and quantification

The LOD was determined by the formula 4.2 described in chapter 4.5.2. Low noise levels occurred in the MS/MS mode and all peaks got reported with a high signal to noise ratio by the software. Table 6.1 shows the calculated LOD from a noise band occurring in a spiked soil sample (lowest concentration 0,5 ng of PCB calibration solution added) in the front of the retention time of the congener. The signal height was estimated to be proportional to the signal area (and therefore also to be proportional to the concentration of the compound).

Table 6.1: Comparison of LOD levels occurring in the SIM and MS/MS mode.

Congener	LOD_{SIM} [ng/g]	$LOD_{MS/MS}$ [ng/g]
28	0,7	0,59
31	2,6	0,10
44	3,9	0,03
52	4,6	0,03
101	1,4	0,09
118	2,0	0,14
138	1,6	0,13
153	1,1	0,16
180	2,7	NA

For the limit of quantification, the linearity range of the method, as well as the measured method blank levels have to be considered. In the SIM mode, high deviations of the response factors at different spiked concentrations had been measured (see fig-

ure 4.6). Therefore, no quantification results got reported. For the MS/MS mode, best results had been achieved by measuring calibration solutions without sample matrix (see figure 4.7). Also here, a high deviation of the response factor can be observed for the congeners 18, 28& 31, 51, 138, 118 for a concentration of 5 ng/mL. Since the total volume of the extract for GC analysis was around 250 μL, this refers to the same concentration in a sample extract of a sample spiked with 1.25ng of PCB. As a conclusion, also other factors than influencing sample matrix have to be considered.

As it can be seen in figure 4.6, the linearity range for the extraction is only valid until 10ng/g. All samples spiked with a lower concentration showed a higher response factor and therefore limited the linear range of the method.

Accuracy and precision of the method

Regarding the results of the reference material in table 4.15, only the level of PCB 180 was outside of the reported confidence range by the reference material supplier. However, a high deviation between three sample extractions for the congeners 118, 153 and 180 had been measured. This low precision can result from matrix effects, which lead to instable measurement results. Higher precision maybe could have been achieved by analyzing the sample extract three times and calculating the results from the mean of the three sample analysis.

Peak performance and integration in the MS/MS mode

The use of the MS/MS mode for an ion trap mass spectrometer is limited on the number of scan events which can be performed at the same time. An ion trap collects a maximum of ions and empties them towards the detector. The time of opening the trap for collecting the ions is determined by a prescan. Therefore the cycles of ejection of the trap towards detector are limited by the time needed for prescan, collection and ejection. A higher sensitivity can be reached with an ion trap by collecting a higher amount of ions in comparison to a triple quadrupole ion trap. This favors this instrument for MS/MS full scan modes. For MS/MS experiments, where only one or two fragment ions had to be observed, the higher duty cycle time limits its application. Since ions are reaching the detector only in batches, no continuously observation of the chromatogram can be reached. Due to the limited available time during the elution of a peak, the observation of ions had to be limited to a minimum (one precursor and one fragment ions for each target component and ISTD). The accuracy of the quantification

is limited by the accuracy resulting from the integration of the peaks.
In figure 6.1 and 6.2, the peak shape of an exemplary peak in the MS/MS mode is shown. As it is clearly visible in the red line, the measured ion density is fluctuating between the different time points. For a measurement of the peak with one microscan, the time resolution increases, but a higher fluctuation appears. The peak shape was smoothened by applying 5 smoothing points in the processing setup, which resulted in peak shape close to the ideal shape. However, this application can result in a higher error in the integration.

Identification criteria as used in the literature [42] for triple quadrupole instruments with two precursor ions could not be applied. The observation of two fragment ions, as explained in some works [49], could not be applied, since only one fragment ion with significant intensity was observed in a MS/MS- fullscan analysis. Observation of two fragment ions could not be performed for all PCB, since, especially for lower chlorinated PCBs, only one fragment ion was observed in the automatically mode. A manual change of the collision energy would have resulted in the observation of more fragment ions but was not preferred since this would also strongly lower the sensitivity of the detection.
Thus, GC-MS/MS delivers three identification points for each congener by retention time, filtering of the precursor ion and detection of the fragment ion. Publications with similar instrumentation reported a LOD of 0,1 pg for PCB in fish samples, with a repeatability and precision comparable to GC-HRMS measurements [49]. Also, high linearity was achieved in the range 0,1-500ng (R^2 over 0,9999). Unfortunately, these results could not be repeated in this work with soil samples.

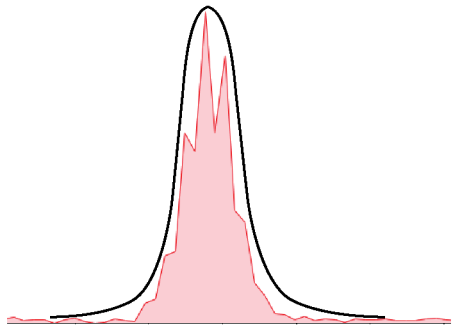

Figure 6.1: Peak shape appearing in the chromatogram (MS/MS mode) with 2 microscans. The peak is getting fragmented due to low time resolution. The approximately ideal peak shape is displayed by the black line.

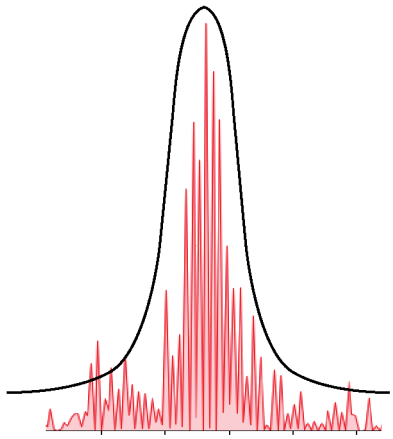

Figure 6.2: Peak shape appearing in the chromatogram (MS/MS mode), where the number of microscans had been reduced to one in comparison to peak in figure 6.1

General evaluation of the method

For application of the method, more efforts have to be done to achieve a lower deviation in the response factors for concentration lower than 10 ng/g of the target PCBs. It can be assumed, that a better cleanup procedure (for example size exclusion techniques like gel permeation chromatography) might result in a better linear response in the mass spectrometer.

For the use of MS/MS, the collision energy and ionization parameters should be modified to achieve a better peak shape as well as the possibility to observe two fragment ions for better identification criteria.

Coelution of 31/28 and 149/153 had been observed on a DB-5ms column. 149 and 153 could be separated by mass spectrometry due to a different degree of chlorination. Therefore a different column (like a DB1 column as described in the EPA method 1668) is recommended for the separation of this PCB congeners.
The use of F-PCB as recovery standard is not recommended if they are coeluting with a target compound on the used column since this will lead to more ions, which have to be observed in the same time. F-PCB 118 availed not to coelute on a DB5-ms column with the observed PCBs and was therefore be used as recovery standard. The use of three recovery standards (like in EPA method 1668) will deliver more robust recovery levels since different degrees of chlorination differ in their detector response.

6.2 PCB congeners found in Svalbard soils

As seen in figure 5.6, only two congeners (PCB 52/180 and PCB 52/28) are measured in soil and vegetation samples. All other congeners were under the LOQ (1ng/g). Levels from previous studies on PCB in Svalbard soils are listed in table 3.1.
In all found studies [88], [91], [65], [20] was the sum of analyzed PCB congeners close to 1ng/g and which profs the range of the here measured results. However, no study was found which showed high enrichment of PCB 52 in soils. A study of dechlorination pathways for Aroclor 1260 showed high enrichment of PCB 52 after microbial treatment [27]. Tetrachlorobiphenyls with unflanked chlorines (like PCB 52) are here described as a major product after microbial dechlorination.
Tri- and Tetrachlorinated congeners (like PCB 28 and PCB 52) are also more volatile than the other congeners, and therefore an occurrence in the Arctic is more likely. Overall studies of organochlorine compounds in soil have also assumed a different environmental path for those congeners [70].
The absence of PCB 52 in Ny Alesund cannot reveal from the fact, that samples from this area were freeze dried since also PCB 52 was found in vegetation, which was freeze dried.
Higher abundance of PCB 180 in Leinstranda and Bayelva can be explained by the fact, that those sample sites were close to the shore and are therefore higher influenced by the marine transport. Though, also a different air transport due to different main trajectories is possible.
During the treatment of the samples at NTNU, one blank was performed, but not analyzed in the external laboratory. Though, since not all samples showed measurable PCB 52 levels is a contamination during sample handling unlikely.
For a better discussion of PCB levels in Svalbard soil, a complete congener profiles of the 7 observed PCBs would be preferable.

6.3 Result of PCA/ FA- analysis

The first factor analysis (study case A) includes mainly variables which are influenced by the geomineral sources. Factor 1 shows a high variance (43,7%) and is influenced by the variance originating from the mineral soil. High loadings on factor 1 can be found for the elements Fe, Ni, Co Cu, Zn, Sr, V, As, Cr, Na and K. A strong clustering in the score plot between sample sites in Adventdalen with those taken around Ny Alesund (see figure 5.12) shows different soil parent material for both sample areas.
The second factor, which explains 12,4% of the variance shows high loadings of TOC, Cd, Sb, P, Hg, U, Cl, Br and S. It is therefore to some extent correlated with the soil development and the bioactivity on the sample site. Some elements (Cd, Sb, Hg, U) seem to accumulate carbon rich soils. Samples 42 A+B, which were excluded (see figure 5.12) showed high TOC (over 70%). The loading of U and Sb in the FA shows evidence that these elements might also be air deposited.
The third factor shows high loading of Y, Yb, Ce and Pr and therefore describes the geomineral influence of minerals which are containing these elements.
In conclusion, it can be said that Cd and Hg are most likely derived from atmospheric deposition and accumulate in the organic-rich soils and vegetation. Hg contributes to factor 1 and 2. Therefore a geochemical source for Hg in Svalbard could be also possible. However, Halbach [30] reported lower levels of Hg in mineral soil than in surface soil, which shows evidence for mainly air deposition contributing to the occurring levels.

In the second factor analysis (study case B), also the first factor is strongly influenced by the variance originating from the mineral soil. Attitude is also loading strongly on this factor. Cd is negatively correlated with this factor and therefore seems to not origin from the soil parent material. No joint effects could be found for the measured PCB levels. The variable PCB is only loading on the last extracted factor, which explains a low variance. Including the measured levels of PCB (congeners 52+180) into the analysis, strongly reduces the sampling size and therefore the sampling adequacy. This has to be considered by evaluating the results of this factor analysis.

The biplot in figure 5.16 shows the loadings for 14 elements as arrows and the scores for soil and vegetation samples. The angle between two arrows is a measure of the correlation between those variables. Pb has a low angle to Fe, while Cd and U show a wide angle to the other elements. Cd, P and Cl have high loadings on the second component PC2, while the metals Pb, Fe, Cr, Co, Ni and Cu have a high loading on the first component PC1. Hg shows a small angle to S and is loading on both components. U is loading negatively on both components.
Regarding the spread of scores for soil and vegetation, an even spread of both samples was found and no clustering occurred. This means, that the elements show to have similar correlations in soil and vegetation.

6.4 Evaluating the spatial differences between different sampling sites

At each sample point, two samples were taken in a radius of maximum 10 m. Between those samples, only a small variance occurred (mean of all elements 11%, with a maximum 24% for Mn and a minimum of 1% for Mg). Also, Cd and Hg showed a high variance (both around 21%).
Spatial variation was analyzed by comparison of six different sampling areas: Foxdalen, Jansondalen, Jansonhaugen close to Longyearbyen and Bayelva, Gasebu and Leinstranda around Ny Ålesund. Samples taken from one of this areas were clustering in the score plot of PCA analysis and therefore showed similar trends.
Higher Hg levels at sample sites close to Longyearbyen can result from the local source coal mining and coal combustion. Leinstranda also showed lower Hg levels than Gasebu and Bayelva. Correlation of sample sites with distance to Longyearbyen and Ny Ålesund was tested for PCB 52, Cd, Hg and Pb, but no significant correlation could be found.
Low levels of Cd in Gasebu can be explained by a low SOM, but low Cd levels in Leinstranda cannot be explained by SOM. Therefore, most sample sites in Leinstranda and Bayelva are higher than the linear trend between Cd and TOC (see figure 5.11).

In figure 5.20 different trajectory frequencies are plotted for three different starting points of the calculation. The violet range shows the area, where trajectories were passing during the calculation.It therefore shows the range in which an air parcel can be transported to the sample site within 72 hours. Some differences in the range can be seen between Adventdalen and Kongsfjorden. For Adventdalen one trajectory adumbrates coming from the mainland Norway.
For the measured U levels (see figure 5.5), local contamination around Ny Ålesund was assumed to be the reason.
All level are below the reported guidelines for soil quality and therefore are display background pollution[4].

6.5 Correlations of soil constitution and occurring pollutant levels

In comparison to the previous study by Halbach[30], a correlation between Hg and S could be found (see figure 5.17). A similar correlation was also found in vegetation. This can be explained by the importance of S as a ligand for Hg. Additionally, a high correlation could be found between Hg and Cl (see figure 5.18). This can be explained by the occurrence of the complex $HgCl_2$. No parametric significant correlation could be found between Hg and TOC for the whole dataset. Thus, correlation could be found for splitting the dataset into Ny Ålesund (Person r=0,533**, Spearman's ρ=0,690**) and Longyearbyen (Person r=0,359*, Spearman's ρ=0,330*). This underlines the thesis of local influences for samples close to Longyearbyen.
Strong correlation had been found between Cd and TOC. Cd levels measured in vegetation were significantly higher than in soil (see figure 5.1). Cd bioavailability is reported as relatively large, but varies and total soil Cd concentrations poorly predict Cd uptake [4]. Since no specification of the vegetation had been made, the high measured variation in the Cd levels in vegetation can occur from different species with different uptake of Cd. Zn is the chemical analog of Cd. This explains significant correlation of Cd and Zn in vegetation (Person r=0,615**, Spearman's ρ=0,488*).
Pb correlates with Fe (see figure 5.19) and clusters with soil metals in the Factor analysis. Therefore the levels measured are mostly revealing from soil parent material than by LRAT. Pb was significantly higher in measured soil than in the vegetation samples.

6.6 Comparison with previous studies

Halbach performed sampling of inorganic and surface soil in 2015 in Foxdalen and next to Bayelva river [30]. Nevertheless, sampling was performed in a different way than in comparison to this study. For analysis of surface soil, the vegetation layer was included into the soil sample. Therefore, higher levels for loss on ignition occurred (mean TOC 53,5 %, while in this study a mean of 22,5 % was measured). A combination of the measured levels in soil and vegetation for the same sample sites showed similar results. A comparison for 12 elements is given in table 6.2.

Table 6.2: Comparison of measured levels of previous studies [30] with the combined levels of soil and vegetation at Foxdalen and Bayelva in μg/g. The sample size (n) is given.

	Halbach [2015]	Huber [2016]
n	25	9
Al	$18{,}4 \pm 7{,}1 \cdot 10^3$	$17{,}7 \pm 0{,}9 \cdot 10^3$
As	$5{,}20 \pm 2{,}55$	$4{,}66 \pm 3{,}48$
Cd	$0{,}414 \pm 0{,}205$	$0{,}356 \pm 0{,}204$
Cr	$25{,}3 \pm 8{,}6$	$26{,}7 \pm 14{,}3$
Cu	$11{,}3 \pm 3{,}0$	$12{,}7 \pm 4{,}4$
Fe	$14{,}1 \pm 4{,}8 \cdot 10^3$	$14{,}7 \pm 5{,}3 \cdot 10^3$
Hg	$0{,}110 \pm 0{,}035$	$0{,}0803 \pm 0{,}0289$
Mn	201 ± 68	262 ± 52
Ni	$15{,}7 \pm 5{,}3$	$15{,}6 \pm 9{,}6$
Pb	$9{,}45 \pm 1{,}90$	$10{,}3 \pm 2{,}1$
S	$1{,}36 \pm 0{,}24 \cdot 10^3$	$1{,}54 \pm 0{,}46 \cdot 10^3$
Zn	$64{,}5 \pm 10{,}9$	$63{,}6 \pm 18$

Chapter 7

Conclusion

In this work, PCBs and LRAT inorganic elements (Hg, Cd, Pb) were investigated in soil and vegetation samples of Svalbard (Norway).
The method development for PCB analysis was performed but not applied in this work. The linearity of the method was not sufficient for an application on background samples. Further work on better clean up techniques can reduce the influence of the matrix on the measurement and lead to an application of this method on levels <10ng/g. The use of ASE extraction techniques was efficient and reliable. Concerning the instrumentation method, a different column is suggested for PCB analysis, since PCB 28 and 31 are coeluting. Tandem mass spectrometry showed a successful reduce of disturbing ions and showed the potential for a robust and applicable analysis technique.
In 25 soil samples and 15 vegetation samples measured for seven PCB in a certified laboratory, PCB 52, 28 and 180 could be quantified in some samples. Hereby was PCB 52 the most abundant congener with a mean concentration of 3,0 ng/g in soil and 5,9 ng/g in vegetation. Samples with PCB 52 were located close to Adventdalen (Longyearbyen). For further studies, high-resolution gas chromatography is recommended to reach lower LOQ and a complete congener profile. Studies on other POPs, like PFOS, PCDD/Fs or PAHs could be interessting to be included in further work.
Hg levels were higher on sample sites in Adventdalen than around Ny Alesund. This leads to the conclusion, that local sources in Longyearbyen are present and contribute to the measured background levels. Hg showed significant correlation with S and Cl for all sampling sites. Cd showed significant correlation with TOC and higher levels in vegetation than in soil. Pb levels measured in Svalbard soil are most probably occurring from the soil parent material.

Bibliography

[1] W. Aas, M. Fiebig, S. Platt, S. Solberg, and K.E. Yttri. Monitoring of long-range transported air pollutants in Norway. Annual report, Norwegian Institute for Air Research, NILU, PO Box 100, NO-2027 Kjeller, Norway, 2015.

[2] W. Aas, K. Aspmo Pfaffhuber, and P. B. Nizzetto. Heavy metals and pop measurements 2014. EMEP/CCC-report, Norwegian Institute for Air Research, PO Box 100, NO-2027 Kjeller, Norway, 2016.

[3] W.-R. Abraham, B. Nogales, P. Golyshin, D. H. Pieper, and K. N. Timmis. Polychlorinated biphenyl-degrading microbial communities in soils and sediments. *Current Opinion in Microbiology*, 5(3):246–253, 2002.

[4] B. J. Alloway, editor. *Heavy Metals in Soils: Trace Metals and Metalloids in Soils and their Bioavailability*. Springer Dordrecht, 3. edition, 2013.

[5] Arctic Monitoring and Assessment Programme (AMAP). Persistent organic pollutants in the Arctic. Assessment 2002, 2004.

[6] Arctic Monitoring and Assessment Programme (AMAP). Mercury in the Arctic. Assessment 2011, Oslo, Norway, 2011.

[7] C. Backe, I. T. Cousins, and P. Larsson. PCB in soils and estimated soil–air exchange fluxes of selected PCB congeners in the South of Sweden. *Environmental Pollution*, 128(1–2):59–72, 2004.

[8] K. Ballschmiter and M. Zell. Analysis of polychlorinated biphenyls (PCB) by glass capillary gas chromatography. *Fresenius' Zeitschrift für analytische Chemie*, 302(1):20–31, 1980.

[9] L. A. Barrie, D. Gregor, B. Hargrave, R. Lake, D. Muir, R. Shearer, B. Tracey, and T. Bidleman. Arctic contaminants: sources, occurrence and pathways. *Science of The Total Environment*, 122(1):1–74, 1992.

[10] A. Beyer, D. Mackay, M. Matthies, F. Wania, and E. Webster. Assessing long-range transport potential of persistent organic pollutants. *Environmental Science & Technology*, 34(4):699–703, 2000.

[11] J. G. Bockheim. *Cryopedology*, chapter Cryosols as a Three-Part System, pages 7–21. Springer International Publishing, Cham, 2015.

[12] J. G. Bockheim. *Cryopedology*, chapter Cryogenic Soil Processes, pages 53–63. Springer International Publishing, Cham, 2015.

[13] K. Breivik, A. Sweetman, J. M. Pacyna, and K. C. Jones. Towards a global historical emission inventory for selected PCB congeners - a mass balance approach: 1. Global production and consumption. *Science of The Total Environment*, 290(1-3):181 – 198, 2002.

[14] A. Cabrerizo, J. Dachs, and D. Barceló. Development of a soil fugacity sampler for determination of air soil partitioning of persistent organic pollutants under field controlled conditions. *Environmental Science & Technology*, 43(21):8257–8263, 2009.

[15] A. Cabrerizo, J. Dachs, K. C. Jones, and D. Barceló. Soil-air exchange controls on background atmospheric concentrations of organochlorine pesticides. *Atmospheric Chemistry and Physics*, 11(24):12799–12811, 2011.

[16] S. Chu and C.-S. Hong. Retention indexes for temperature- programmed gas chromatography of polychlorinated biphenyls. *Analytical Chemistry*, 76:5486–5497, 2004.

[17] DIONEX. Extraction of PCBs from environmental samples using accelerated solvent extraction (ASE). Application note 316, DIONEX, (USA).

[18] C. K. Drinker, M. F. Warren, and C. A. Bennett. The problems of possible systemic effects from certain chlorinated hydrocarbons. *The Journal of Industrial Hygiene and Toxicology*, 19:283–311, 1937.

[19] S. Eckhardt, K. Breivik, S. Manø, and A. Stohl. Record high peaks in PCB concentrations in the Arctic atmosphere due to long-range transport of biomass burning emissions. *Atmospheric Chemistry and Physics*, 7(17):4527–4536, 2007.

[20] O. A. Eggen, M. Jartun, and R. T. Ottensen. Bakgrunnsnivåer av PCB i overflatejord rundt forlandssundet på Svalbard. Rapport, Norges geologiske undersøkelse NGU, Postboks 6315 Sluppen, 2011.

[21] O. A. Eggen, M. Jartun, and R. T. Ottesen. PCB fra lokale kilder påSvalbard- overflatejord of produkter 2007-2009. Rapport 2010.038, Norges geologiske undersøkelse (NGU), Postboks 6315 Sluppen, 2010.

[22] E. Eljarrat and D. Barcelo. Priority lists for persistent organic pollutants and contaminants based on their relative toxic potency in environmental samples. *Trends in Analytical Chemistry*, 22(10), 2003.

[23] Environmental Protection Agency (EPA). *METHOD 8082A*.

[24] Environmental Protection Agency (EPA), Washington (USA). *Method 3545A, Revision 1*, 1998.

[25] EPA. Superfund program: Anniston site (monsanto co). https://cumulis.epa.gov/supercpad/cursites/csitinfo.cfm?id=0400123 (accessed 22.02.2017).

[26] A. Evenset, G.N. Christensen, J. Carroll, A. Zaborska, U. Berger, D. Herzke, and D. Gregor. Historical trends in persistent organic pollutants and metals recorded in sediment from Lake Ellasjøen, Bjørnøya, Norwegian Arctic. *Environmental Pollution*, 146(196-205), 2007.

[27] S. K. Fagervold, H. D. May, and K. R. Sowers. Microbial reductive dechlorination of Aroclor 1260 in Baltimore harbor sediment microcosms is catalyzed by three phylotypes within the phylum chloroflexi. *Applied and Environmental Microbiology*, 73(9):3009–3018, 2007.

[28] J. Ford, D. Landersb, D. Kugler, B. Lasorsad, S. Allen-Gil, E. Crecelius, and J. Martinsone. Inorganic contaminants in Arctic Alaskan ecosystems: long-range atmospheric transport or local point sources? *The Science of the Total Environment*, 160/161:323–335, 1995.

[29] O. Garmash, M. H. Hermanson, E. Isaksson, M. Schwikowski, D. Divine, C. Teixeira, and D. C. G. Muir. Deposition history of polychlorinated biphenyls to the Lomonosovfonna glacier, Svalbard: A 209 congener analysis. *Environmental Science & Technology*, 47(21):12064–12072, 11 2013.

[30] K. Halbach. Study of mercury and selected trace elements in soil in the Nowegian Arctic, Svalbard. Master's thesis, Nowegian University of Science and Technology, 2016.

[31] P. Harremoes, D. Gee, M. MacGarvin, A. Stirling, J. Keys, B. Wynne, and S.G. Vaz. The precautionary principle in the 20th century: Late lessons from early warnings. Report 1/2013, European Environment Agency EEA, 2013.

[32] V. Hodak-Kobasic, M. Picer, N. Picer, and T. Kovač. Application of ASE 200 extractor for extraction of pcb from soil samples. *Organohalogen Compounds*, 66, 2004.

[33] M . J . J . Hoogsteena, E . A . Lantingaa, E . J . Bakkerb, J . C . J . Groota, and P. A . Tittonella. Estimating soil organic carbon through loss on ignition: Effects of ignition conditions and structural water loss. *European Journal of Soil Science*, 66:320–328, 2015.

[34] P. Hubert, P. Chiap, J. Crommena, B. Boulanger, E. Chapuzet, N. Mercier, S. Bervoas-Martin, P. Chevalier, D. Grandjean, P. Lagorce, M. Lallier, M.C. Laparra, M. Laurentie, and J.C. Nivet. The SFSTP guide on the validation of chomatographic methods for drug bioanalysis: from the Washington Conference to the laboratory. *Analytica Chimica Acta*, 391:135–148, 1999.

[35] H. Hung, R. Kallenborn, K. Breivik, Y. Su, and E. Brorström-Lundén. Atmospheric monitoring of organic pollutants in the Arctic under the Arctic Monitoring and Assessment Programme (AMAP): 1993–2006. *Science of The Total Environment*, 408(15):2854–2873, 2010.

[36] S. Hwang and T. J. Cutright. Impact of clay minerals and DOM on the competitive sorption/desorption of PAHs. *Soil and Sediment Contamination: An International Journal*, 11(2):269–291, 2002.

[37] V. Ivanov and E. Sandeli. Characterization of polychlorinated biphenyl isomers in sovol and trichlorodiphenyl formulations by high-resolution gas chromatography with electron capture detection and high-resolution gas chromatography-mass spectrometry techniques. *Environmental Science & Technology*, 26(10):2012–2017, 1992.

[38] M. Jartun, R. T. Ottesen, T. Volden, and Q. Lundkvist. Local sources of polychlorinated biphenyls (PCB) in Russian and Norwegian settlements on Spitsbergen island, Norway. *Journal of Toxicology and Environmental Health, Part A*, 72(3):284–294, 2009.

[39] S. Jensen. Report of a new chemical hazard. *New Scientist*, 32(612), 1966.

[40] S. Jensen, A. G. Johnels, M. Olsson, and G. Otterlind. DDT and PCB in marine animals from Swedish waters. *Nature*, 224(5216):247–250, 1969.

[41] R. Kallenborn, R. T. Ottensen, and G. Gabrielsen. PCB on Svalbard. Report, Sysselmannen at Svalbard, 2011.

[42] D. Krumwiede and H.-J. Huebschmann. Analysis of pcbs in food an biologiacal samples using GC triple quadrupole GC-MSMS. Application note 10262, Thermo Fisher Scientific, Bremen, Germany, 2008.

[43] I. Krzemień-Konieczka and B. Buszewski. Determining polychlorinated biphenyls in soil using accelerated solvent extraction (ASE). *Polish Journal of Environmental Studies*, 24(5):2029–2033, 2015.

[44] J. Ma, H. Hung, C. Tian, and R. Kallenborn. Revolatilization of persistent organic pollutants in the Arctic induced by climate change. *Nature Clim. Change*, 1(5):255–260, 08 2011.

[45] R. W. Macdonald, L. A. Barrie, T. F. Bidleman, M. L. Diamond, D. J. Gregor, R. G. Semkin, W. M. J. Strachan, Y. F. Li, F. Wania, M. Alaee, L. B. Alexeeva, S. M. Backus, R. Bailey, J. M. Bewers, C. Gobeil, C. J. Halsall, T. Harner, J. T. Hoff, L. M. M. Jantunen, W. L. Lockhart, D. Mackay, D. C. G. Muir, J. Pudykiewicz, K. J. Reimer, J. N. Smith, G. A Stern, W. H. Schroeder, R. Wagemann, and M. B. Yunker. Contaminants in the Canadian Arctic: 5 years of progress in understanding sources, occurrence and pathways. *Science of The Total Environment*, 254(2–3):93–234, 2000.

[46] D. Mackay, W. Y. Shiu, K.-C. Ma, and S. C. Lee. *Physical-Chemical Properties and Environmental Fate for Organic Chemicals*, volume II- Halogenated Hydrocarbons. CRC Press, Taylor & Francis Group, 2006.

[47] B. T. Mader, K. U. Goss, and S. J. Eisenreich. Sorption of nonionic, hydrophobic organic chemicals to mineral surfaces. *Environmental Science & Technology*, 31(4):1079–1086, 1997.

[48] B. R. Magee, L. W. Lion, and A. T. Lemley. Transport of dissolved organic macromolecules and their effect on the transport of phenanthrene in porous media. *Environmental Science & Technology*, 25:323–331, 1991.

[49] J. Malavia, F. J Santos, and M.T. Galceran. Comparison of gas chromatography–ion-trap tandem mass spectrometry systems for the determination of polychlorinated dibenzo-p-dioxins, dibenzofurans and dioxin-like polychlorinated biphenyls. *Journal of Chromatography A*, 1186:302–311, 2008.

[50] B. Marschner. Sorption von polyzyklischen aromatischen Kohlenwasserstoffen (PAK) und polychlorierten Biphenylen (PCB) im Boden. *Journal of Plant Nutrition and Soil Science*, 162(1):1522–2624, 1999.

[51] S. N. Meijer, W. A. Ockenden, A. Sweetman, K. Breivik, J. O. Grimalt, and K. C. Jones. Global distribution and budget of PCBs and HCB in background surface soils: Implications for sources and environmental processes. *Environmental Science & Technology*, 37(4):667–672, 2003.

[52] S.N. Meijer, E. Steinnes, W. A. Ockenden, and K. C. Jones. Influence of environmental variables on the spatial distribution of PCBs in Norwegian and U.K. soils: Implications for global cycling. *Environmental Science & Technology*, 36:2146–2153, 2002.

[53] M. Mitchell. Visual range in the polar regions with particular reference to the Alaskan Arctic. *J. Atmos. Terr. Phys.*, pages 195–211, 1956.

[54] W. W. Mohn, K. Westerberg, W. R. Cullen, and K. J. Reimer. Aerobic biodegradation of biphenyl and polychlorinated biphenyls by Arctic soil microorganisms. *Applied and Environmental Microbiology*, 63(9):3378–3384, 1997.

[55] J. J. Nam, O. Gustafsson, P. Kurt-Karakus, K. Breivik, E. Steinnes, and K. C. Jones. Relationships between organic matter, black carbon and persistent organic pollutants in European background soils: Implications for sources and environmental fate. *Environmental Pollution*, 156:809–817, 2008.

[56] W. A. Ockenden, K. Breivik, S. N. Meijer, E. Steinnes, A. J. Sweetman, and K. C. Jones. The global re-cycling of persistent organic pollutants is strongly retarded by soils. *Environmental Pollution*, 121(1):75 – 80, 2003.

[57] Canadian Council of Ministers of the Environment. Polychlorinated biphenyls (total). Technical report, Canadian Soil Quality Guidelines for the Protection of Environmental and Human Health, 1999.

[58] D. H. Pieper. Aerobic degradation of polychlorinated biphenyls. *Applied Microbiology and Biotechnology*, 67(2):170–191, 2004.

[59] J. J. Pignatello. Soil organic matter as a nanoporous sorbent of organic pollutants. *Advances in Colloid and Interface Science*, 76–77:445–467, 1998.

[60] M. G. Pintado-Herrera, E. González-Mazo, and P. A. Lara-Martín. In-cell clean-up pressurized liquid extraction and gaschromatography–tandem mass spectrometry determinat on ofhydrophobic persistent and emerging organic pollutants in coastal sediments. *Journal of Chromatography A*, 1429:107–118, 2016.

[61] N. Pirrone and K. R. Mahaffey, editors. *Dynamics of Mercury Pollution and Global Scales: Atmospheric Processes and Human Exposures Around the World*. Springer Science, 2005.

[62] R.R. Ratnayake, G. Seneviratne, and S.A. Kulasooriya. A modified method of weight loss on ignition to evaluate soil organic matter fractions. *International Journal of Soil Science*, 2(1):69–73, 2007.

[63] P. J. H. Reijnders. Organochlorine and heavy metal residues in harbour seals from the wadden sea and their possible effects on reproduction. *Netherlands Journal of Sea Research*, 14(1):30–65, 1980.

[64] N. L. Rose, C. L. Rose, J.F. Boyle, and P.G. Appleby. Lake-sediment evidence for local and remote sources of atmospherically deposited pollutants on Svalbard. *Journal of Paleolimnology*, 31:499–513, 2004.

[65] M. Schlabach and E. Steinnes. Organic contaminants in natural surface soils from Svalbard. *Organohalogen Compounds*, 43:227–230, 1999.

[66] H. Schmidt and G. Schultz. Über benzidin (α-diamidodiphenyl). *Justus Liebigs Annalen der Chemie*, 207(3):320–347, 1881.

[67] R.P. Schwarzenbach, P.M. Gschwend, and D.M. Imboden. *Environmental Organic Chemistry*. John Wiley & Sons Inc, 2 edition, 2003.

[68] Thermo Fisher Scientific. Thermo scientific ITQ series quadrupole ion trap GC/MSn. booklet, Austin (USA).

[69] T. Simon, J. K. Britt, and R. C. James. Development of a neurotoxic equivalence scheme of relative potency for assessing the risk of PCB mixtures. *Regulatory Toxicology and Pharmacology*, 48(2):148–170, 2007.

[70] B. Škrbić and N. Đurišić Mladenović. Principal component analysis for soil contamination with organochlorine compounds. *Chemosphere*, 68(11):2144–2152, 8 2007.

[71] L. Somoano-Blanco, P. Rodriguez-Gonzalez, D. Profrock, A. Prange, and J. I. Garcia Alonso. Comparison of different mass spectrometric techniques for the determination of polychlorinated biphenyls by isotope dilution using 37Cl-labelled analogues. *Analytical Methods*, 7(21):9068–9075, 2015.

[72] S. Sporring, S. Bøwadt, B. Svensmark, and E. Björklund. Comprehensive comparison of classic soxhlet extraction with soxtec extraction, ultrasonication extraction, supercritical fluid extraction, microwave assisted extraction and accelerated solvent extraction for the determination of polychlorinated biphenyls in soil. *Journal of Chromatography A*, 1090(1–2):1–9, 10 2005.

[73] A.F. Stein, R.R Draxler, G.D. Rolph, B.J.B. Stunder, M.D. Cohen, and F. Ngan. NOAA's HYSPLIT atmospheric transport and dispersion modeling system. *Bulletin of the American Meteorological Society*, 96:2059–2077, 2015.

[74] S. Tanabe. PCB problems in the future: Foresight from current knowledge. *Environmental Pollution*, 50(1):5–28, 1988.

[75] Y. Tasdemir, G. Salihoglu, N. K. Salihoglu, and A. Birgül. Air–soil exchange of PCBs: Seasonal variations in levels and fluxes with influence of equilibrium conditions. *Environmental Pollution*, 169:90–97, 2012.

[76] J. C. F. Tedrov and J. V. Drew. Arctic soil classification and patterned ground. *Arctic*, 15(2):109–116, 1962.

[77] S. Ubl, M. Scheringer, A. Stohl, J. F. Burkhart, and K. Hungerbuhler. Primary source regions of polychlorinated biphenyls (PCBs) measured in the Arctic. *Atmospheric Environment*, 62:391–399, 2012.

[78] EPA United States Environmental Protection Agency. Polychlorinated biphenyls (PCBs). www.epa.gov/pcbs/learn-about-polychlorinated-biphenyls-pcbs (accessed 22.02.2017).

[79] M. Dalla Valle, E. Jurado, J. Dachs, A. J. Sweetman, and K. C. Jones. The maximum reservoir capacity of soils for persistent organic pollutants: Implications for global cycling. *Environmental Pollution*, 134:153–164, 2005.

[80] C. Vanden Bilcke. The Stockholm convention on persistent organic pollutants. *Review of European Community & International Environmental Law*, 11(3):328–342, 2002.

[81] G. K. Vasilyeva and E. R. Strijakova. Bioremediation of soils and sediments contaminated by polychlorinated biphenyls. *Microbiology*, 76(6):639–653, 2007.

[82] X.-P. Wang, J.-J. Sheng, P. Gong, Y.-G. Xue, T.-D. Yao, and K. C. Jones. Persistent organic pollutants in the Tibetan surface soil: Spatial distribution, air–soil exchange and implications for global cycling. *Environmental Pollution*, 170:145–151, 11 2012.

[83] F. Wania. Assessing the potential of persistent organic chemicals for long-range transport and accumulation in polar regions. *Environmental Science & Technology*, 37(7):1344–1351, 2003.

[84] F. Wania and D. MacKay. Peer reviewed: Tracking the distribution of persistent organic pollutants. *Environmental Science & Technology*, 30(9):390A–396A, 1996.

[85] F. Wania and Y. Su. Quantifying the global fractionation of polychlorinated biphenyls. *Ambio*, 33(3):161–168, 2004.

[86] T. M Wickizer and L.B. Brilliant. Testing for polychlorinated biphenyls in human milk. *Pediatrics*, 68(3):411–415, 1981.

[87] W. Wilcke, M. Krauss, and G. Barančíková. Persistent organic pollutant concentrations in air- and freeze-dried compared to field-fresh extracted soil samples of an eastern Slovak deposition gradient. *Journal of Plant Nutrition and Soil Science*, 166(1):93–101, 2003.

[88] P. Zhang, L. Ge, H. Gao, T. Yao, X. Fang, C. Zhou, and G. Na. Distribution and transfer pattern of polychlorinated biphenyls (PCBs) among the selected environmental media of Ny-Ålesund, the Arctic: As a case study. *Marine Pollution Bulletin*, 89(1–2):267 – 275, 2014.

[89] P. Zhang, G. Linke, Z. Chuanguang, and Y. Ziwei. Evaluating the performances of accelerated-solvent extraction, microwave-assisted extraction, and ultrasonic-assisted extraction for determining PCBs, HCHs and DDTs in sediments. *Chinese Journal of Oceanology an Limnology*, 29(5):1103–1112, 2011.

[90] T. Zhang, N.-F. Wang, H.-Y. Liu, Y.-Q. Zhang, and L.-Y. Yu. Soil pH is a key determinant of soil fungal community composition in the Ny-Ålesund region, Svalbard (High Arctic). *Frontiers in Microbiology*, 7:227, 2016.

[91] C. Zhu, Y. Li, P. Wang, Z. Chen, D. Ren, P. Ssebugere, Q. Zhang, and G. Jiang. Polychlorinated biphenyls (PCBs) and polybrominated biphenyl ethers (PBDEs) in environmental samples from Ny-Ålesund and London Island, Svalbard, the Arctic. *Chemosphere*, 126:40 – 46, 2015.

Appendix A

Additional Information

Table A.1: Sample Strategy for soil (s) and vegetation (v) samples. Samle areas are marked with 1=Foxdalen, 2=Jansondalen, 3=Jansonhaugen, 4=Gasebu, 5=Bayelva and 6=Leinstranda. Analysis was performed at an external certified laboratory and 7 samples were tested for analysis at NTNU. Loss on ignition was perfomed for all samples to determine the total organic carbon.

Sample	Area	Lattitude	Longitude	ICP-MS (s)	ICP-MS (v)	PCB (s)	PCB (v)
1B	1	78°09.105'	16°13.242'	x	x	x	-
3B	1	78°09.299'	16°12.635'	x	-	x	-
4A	1	78°09.405'	16°12.242'	x	x	-	-
4B	1	78°09.405'	16°12.242'	x	-	-	-
5B	1	78°09.518'	16°11.592'	x	x	-	-
6B	2	78°09.964'	16°17.204'	x	x	-	x
8A	2	78°09.966'	16°17.297'	x	x	-	x
9A	2	78°09.948'	16°18.282'	x	x	x	-
10A	2	78°09.948'	16°18.282'	x	x	-	-
10B	2	78°09.948'	16°18.282'	x	-	x	-
11A	2	78°09.989'	16°25.013'	x	x	x	x
11B	2	78°09.989'	16°25.013'	x	-	-	-
12A	2	78°09.989'	16°25.013'	x	x	-	-
12B	2	78°09.989'	16°25.013'	x	-	-	-
13A	2	78°09.989'	16°25.013'	x	x	-	-
13B	2	78°09.989'	16°25.013'	x	-	-	-
14A	2	78°09.979'	16°24.960'	x	x	x	-
14B	2	78°09.979'	16°24.960'	x	-	-	-
15B	2	78°09.979'	16°24.960'	x	-	-	-
16A	2	78°10.028'	16°26.569'	x	x	x	-
16B	2	78°10.028'	16°26.569'	x	-	-	-
17A	2	78°10.028'	16°26.569'	x	x	x	-
17B	2	78°10.028'	16°26.569'	x	-	-	-
18A	2	78°10.028'	16°26.569'	x	-	-	-
18B	2	78°10.028'	16°26.569'	x	x	-	x
19A	2	78°10.326'	16°26.001'	x	-	-	-
19B	2	78°10.326'	16°26.001'	x	x	x	x
20A	2	78°10.326'	16°26.001'	x	x	-	-
20B	2	78°10.326'	16°26.001'	x	-	-	-
21A	3	78°10.914'	16°27.405'	x	-	-	-
21B	3	78°10.914'	16°27.405'	x	-	x	-
22A	3	78°11.074'	16°26.116'	x	-	-	-
22B	3	78°11.074'	16°26.116'	x	x	x	x
23A	3	78°11.215'	16°24.600'	x	-	-	-
23B	3	78°11.215'	16°24.600'	x	x	x	-
24A	3	78°11.308'	16°22.658'	x	x	x	x
24B	3	78°11.308'	16°22.658'	x	-	-	-
25A	3	78°11.222'	16°21.049'	x	-	-	-
25B	3	78°11.222'	16°21.049'	x	x	x	-

26A	4	78°54.646’	12°03.982’	x	x	x	-
26B	4	78°54.646’	12°03.982’	x	-	-	-
27A	4	78°54.646’	12°03.982’	x	x	-	x
27B	4	78°54.646’	12°03.982’	x	-	-	-
28A	5	78°55.887’	11°49.707’	x	-	-	-
28B	5	78°55.887’	11°49.707’	x	x	x	x
29B	5	78°55.835’	11°49.269’	x	x	-	-
30A	5	78°55.775’	11°50.520’	x	x	x	-
30B	5	78°55.775’	11°50.520’	x	-	-	-
31A	5	78°55.738’	11°50.664’	x	x	-	-
31B	5	78°55.738’	11°50.664’	x	-	-	-
32A	5	78°56.405’	11°48.948’	x	-	-	-
32B	5	78°56.405’	11°48.948’	x	-	-	-
33A	5	78°36.281’	11°49.025’	x	x	x	x
33B	5	78°36.281’	11°49.025’	x	-	-	-
34A	5	78°56.250’	11°49.061’	x	x	x	x
34B	5	78°56.250’	11°49.061’	x	-	-	-
35A	4	78°53.954’	12°09.923’	x	x	x	x
35B	4	78°53.954’	12°09.923’	x	-	-	-
36A	4	78°54.156’	12°08.614’	x	x	x	-
36B	4	78°54.156’	12°08.614’	x	-	-	-
37A	4	78°54.518’	12°05.285’	x	x	x	x
37B	4	78°54.518’	12°05.285’	x	-	-	-
38A	6	78°52.164’	11°36.708’	x	x	x	x
38B	6	78°52.164’	11°36.708’	x	-	-	-
39A	6	78°52.164’	11°36.708’	x	-	-	-
39B	6	78°52.164’	11°36.708’	x	x	-	x
40A	6	78°51.426’	11°41.706’	x	-	x	-
40B	6	78°51.426’	11°41.706’	x	-	-	-
41A	6	78°52.849’	11°33.488’	x	-	x	-
41B	6	78°52.849’	11°33.488’	x	-	-	-
42A	6	78°54.172’	11°30.153’	x	-	-	-
42B	6	78°54.172’	11°30.153’	x	-	x	-
Sum				74	34	25	15

Table A.2: Descriptive statistic for all vegetation samples.

Element	mean	min	max	SD	RSD	median	geo mean
	[µg/g (dw)]				[%]		
Al	16200	1870	34800	10000	61,7	14.500	12800
Fe	11900	1620	27800	6740	56,6	11300	9810
K	6010	1750	13100	3040	50,6	5.680	5240
Mg	3430	1390	5050	938	27,3	3.500	3290
S	1720	742	3310	528	30,7	1.690	1640
P	802	413	1663	227	28,3	755	775
Na	255	111	404	81	31,9	253	242
Mn	246	78	699	131	53,1	200	222
Cl	226	84	470	105	46,3	195	203
Zn	75,9	33,8	125,5	18,8	24,8	75,6	73,5
Cr	22,5	2,8	52,4	14,1	62,6	19,5	17,8
Ni	20,9	2,8	66,9	14,5	69,2	19,8	15,6
Cu	11,6	4,7	23,1	4,2	36,2	12,3	10,8
Pb	7,78	2,40	18,59	3,19	41,0	7,65	7,15
As	5,98	0,32	17,66	5,21	87,0	4,14	3,72
Y	5,53	1,17	9,51	1,82	33,0	5,35	5,18
Br	1,48	0,15	2,51	0,85	57,5	1,67	1,13
U	0,783	0,126	8,578	1,448	185,0	0,420	0,463
W	0,687	0,003	9,695	1,933	281,4	0,020	0,047
Cd	0,595	0,132	2,161	0,371	62,3	0,560	0,505
Mo	0,510	0,135	1,861	0,340	66,7	0,432	0,431
Sn	0,162	0,090	0,301	0,046	28,4	0,157	0,155
Hg	0,0974	0,0463	0,2051	0,0328	33,7	0,0910	0,0924
Nb	0,0214	0,0016	0,1417	0,0352	164,1	0,0071	0,0099
Sb	0,0154	0,0042	0,0569	0,0130	84,0	0,0103	0,0116

Table A.3: Descriptive statistic for all soil samples.

Element	mean	min	max	SD	RSD	median	geo mean
	[µg/g (dw)]				[%]		
Al	81200	11100	173000	39300	48,5	80600	70400
Fe	54300	6800	117000	22600	41,6	53200	48900
K	25300	3430	53300	11900	47,0	25200	22200
Ca	20000	3110	120000	20600	102,7	12800	14400
Mg	13800	3860	75600	10800	78,4	11600	11900
S	3500	385	9340	1710	48,9	3330	3030
P	1710	363	3730	586	34,2	1700	1600
Na	990	230	2403	359	36,3	980	928
Mn	744	228	2632	344	46,3	651	686
Cl	267	67	846	137	51,3	246	235
V	162	25	386	93	57,5	162	132
Sr	153	30	418	92	60,0	156	125
Zn	137	23	248	51	37,4	135	126,0
Ce	128	21	200	41	32,1	129	119
Cr	104	22	198	47	45,3	103	92
Ni	54,7	11,9	112,9	27,6	50,5	55,6	46,9
Br	36,9	8,1	118,2	21,9	59,3	32,3	31,8
Cu	35,8	7,5	67,8	13,7	38,3	37,3	32,6
Pb	31,5	9,6	52,2	10,6	33,7	30,6	29,5
Y	27,5	8,1	59,3	10,3	37,4	25,3	25,6
As	25,9	3,8	79,4	20,3	78,3	20,1	17,8
Co	21,1	3,4	48,4	8,96	42,6	19,7	19,0
Pr	13,8	2,5	21,2	4,3	31,3	14,1	12,9
Zr	13,0	2,3	21,9	4,3	33,0	13,8	12,0
U	3,47	0,64	33,21	5,45	156,8	1,87	2,34
Mo	1,95	0,40	9,59	1,48	75,9	1,65	1,59
Yb	1,91	0,64	3,86	0,72	37,9	1,75	1,79
Sn	0,910	0,449	2,646	0,283	31,1	0,868	0,877
Tl	0,810	0,219	1,318	0,277	34,2	0,829	0,753
Cd	0,489	0,074	1,533	0,295	60,3	0,415	0,411
W	0,398	0,010	2,448	0,550	138,3	0,193	0,190
Hg	0,155	0,006	0,416	0,083	53,6	0,155	0,124
Sb	0,0800	0,0240	0,3445	0,0441	55,2	0,0682	0,0724

Table A.4: Levels [μg/g] of 11 elements in O- horizon of soil in Svalbard (mean and standard deviation) for 6 different sampling sites.

	Foxdalen	**Jansondalen**	**Jansonhaugen**	**Gasebu**	**Bayelva**	**Leinstranda**
Al	$41{,}1 \pm 8{,}1 \cdot 10^3$	$46{,}9 \pm 10{,}6 \cdot 10^3$	$50{,}3 \pm 10{,}0 \cdot 10^3$	$19{,}1 \pm 2{,}9 \cdot 10^3$	$25{,}7 \pm 9{,}6 \cdot 10^3$	$16{,}3 \pm 10{,}9 \cdot 10^3$
As	$11{,}5 \pm 2{,}9$	$19{,}1 \pm 6{,}5$	$19{,}2 \pm 5{,}1$	$2{,}78 \pm 0{,}70$	$3{,}16 \pm 0{,}75$	$3{,}74 \pm 2{,}21$
Cd	$0{,}246 \pm 0{,}157$	$0{,}195 \pm 0{,}088$	$0{,}157 \pm 0{,}072$	$0{,}161 \pm 0{,}164$	$0{,}318 \pm 0{,}077$	$0{,}252 \pm 0{,}155$
Cu	$21{,}6 \pm 3{,}0$	$18{,}9 \pm 1{,}2$	$20{,}2 \pm 2{,}2$	$10{,}7 \pm 1{,}8$	$12{,}7 \pm 4{,}1$	$7{,}47 \pm 4{,}5$
Fe	$26{,}7 \pm 5{,}4 \cdot 10^3$	$31{,}0 \pm 5{,}3 \cdot 10^3$	$31{,}3 \pm 6{,}6 \cdot 10^3$	$16{,}1 \pm 3{,}2 \cdot 10^3$	$17{,}6 \pm 6{,}1 \cdot 10^3$	$12{,}7 \pm 7{,}6 \cdot 10^3$
Hg	$9{,}94 \pm 2{,}59 \cdot 10^{-2}$	$8{,}16 \pm 2{,}23 \cdot 10^{-2}$	$8{,}86 \pm 1{,}83 \cdot 10^{-2}$	$3{,}943{,}39 \pm 3{,}34 \cdot 10^{-}2$	$6{,}25 \pm 3{,}04 \cdot 10^{-2}$	$1{,}77 \pm 1{,}78 \cdot 10^{-2}$
Mn	379 ± 116	351 ± 108	375 ± 251	263 ± 46	308 ± 82	246 ± 81
Ni	$32{,}0 \pm 6{,}0$	$15{,}9 \pm 4{,}7$	$15{,}8 \pm 6{,}8$	$11{,}4 \pm 1{,}3$	$14{,}2 \pm 4{,}6$	$9{,}11 \pm 5{,}4$
Pb	$13{,}3 \pm 3{,}5$	$15{,}9 \pm 3{,}5$	$15{,}8 \pm 2{,}1$	$11{,}4 \pm 2{,}1$	$14{,}2 \pm 5{,}1$	$9{,}1 \pm 6{,}0$
Zn	$72{,}1 \pm 15{,}9$	$77{,}9 \pm 9{,}3$	$67{,}2 \pm 10{,}2$	$37{,}7 \pm 5{,}0$	$57{,}0 \pm 18{,}4$	$39{,}0 \pm 28{,}4$

Table A.5: Levels (μg/g) of 11 elements in the vegetation cover in Svalbard (mean and standard deviation) for 6 different sampling sites.

	Foxdalen	**Jansondalen**	**Jansonhaugen**	**Gasebu**	**Bayelva**	**Leinstranda**
Al	$13{,}3 \pm \cdot 10^3$	$24{,}4 \pm \cdot 10^3$	$22{,}2 \pm \cdot 10^3$	$6{,}5 \pm \cdot 10^3$	$8{,}4 \pm \cdot 10^3$	$9{,}5 \pm \cdot 10^3$
As	$4{,}06 \pm 1{,}62$	$10{,}3 \pm 5{,}8$	$9{,}61 \pm 2{,}80$	$1{,}07 \pm 0{,}48$	$1{,}29 \pm 0{,}58$	$2{,}32 \pm 1{,}32$
Cd	$0{,}514 \pm 0{,}349$	$0{,}478 \pm 0{,}315$	$0{,}836 \pm 0{,}535$	$0{,}449 \pm 0{,}301$	$0{,}546 \pm 0{,}122$	$0{,}761 \pm 0{,}277$
Cu	$11{,}8 \pm 1{,}5$	$14{,}1 \pm 2{,}5$	$15{,}0 \pm 3{,}5$	$7{,}15 \pm 2{,}17$	$8{,}03 \pm 2{,}40$	$5{,}47 \pm 1{,}05$
Fe	$10{,}5 \pm 5{,}9 \cdot 10^3$	$17{,}3 \pm 7{,}3 \cdot 10^3$	$15{,}4 \pm 3{,}9 \cdot 10^3$	$5{,}82 \pm 3{,}44 \cdot 10^3$	$6{,}79 \pm 3{,}58 \cdot 10^3$	$8{,}91 \pm 5{,}02 \cdot 10^3$
Hg	$9{,}84 \pm 3{,}17 \cdot 10^{-2}$	$9{,}57 \pm 1{,}55 \cdot 10^{-2}$	$13{,}0 \pm 3{,}9 \cdot 10^{-2}$	$8{,}49 \pm 2{,}29 \cdot 10^{-2}$	$7{,}43 \pm 1{,}91 \cdot 10^{-2}$	$6{,}35 \pm 2{,}04 \cdot 10^{-2}$
Mn	170 ± 23	264 ± 145	338 ± 161	204 ± 96	170 ± 57	282 ± 119
Ni	$16{,}3 \pm 4{,}2$	$29{,}0 \pm 8{,}3$	$34{,}3 \pm 13{,}7$	$5{,}27 \pm 2{,}50$	$7{,}26 \pm 2{,}57$	$7{,}06 \pm 2{,}96$
Pb	$5{,}17 \pm 1{,}24$	$8{,}00 \pm 2{,}99$	$8{,}46 \pm 1{,}88$	$9{,}42 \pm 5{,}38$	$7{,}55 \pm 3{,}25$	$8{,}17 \pm 2{,}94$
Zn	$82{,}6 \pm 15{,}3$	$84{,}0 \pm 21{,}1$	$74{,}4 \pm 18{,}1$	$62{,}3 \pm 23{,}5$	$74{,}6 \pm 16{,}4$	$74{,}5 \pm 14{,}4$

Table A.6: Result of the external PCB Analysis for 14 vegetation samples for 7 PCB congers. LOQ was reported as 0,001μg/g. Levels are given in μg/g.

No.	Area	PCB 28	PCB 52	PCB 101	PCB 118	PCB 138	PCB 153	PCB 180
6BV	(2)	<0,001	**0,0086**	<0,001	<0,001	<0,001	<0,001	<0,001
8AV	(2)	<0,001	**0,0097**	<0,001	<0,001	<0,001	<0,001	<0,001
11AV	(2)	**0,0036**	**0,0027**	<0,001	<0,001	<0,001	<0,001	<0,001
18BV	(2)	<0,001	**0,0056**	<0,001	<0,001	<0,001	<0,001	<0,001
19BV	(2)	<0,001	**0,0043**	<0,001	<0,001	<0,001	<0,001	<0,001
22BV	(3)	<0,001	**0,0061**	<0,001	<0,001	<0,001	<0,001	<0,001
24AV	(3)	<0,001	**0,0041**	<0,001	<0,001	<0,001	<0,001	<0,001
27AV	(4)	<0,001	<0,001	<0,001	<0,001	<0,001	<0,001	<0,001
28 BV	(5)	**0,0067**	<0,001	<0,001	<0,001	<0,001	<0,001	<0,001
33AV	(5)	<0,001	<0,001	<0,001	<0,001	<0,001	<0,001	<0,001
34AV	(5)	<0,001	<0,001	<0,001	<0,001	<0,001	<0,001	<0,001
35AV	(4)	<0,001	<0,001	<0,001	<0,001	<0,001	<0,001	<0,001
37AV	(4)	<0,001	<0,001	<0,001	<0,001	<0,001	<0,001	<0,001
38AV	(6)	<0,001	<0,001	<0,001	<0,001	<0,001	<0,001	<0,001
39BV	(6)	<0,001	<0,001	<0,001	<0,001	<0,001	<0,001	<0,001

Table A.7: Result of the external PCB Analysis for 25 soil samples for 7 PCB congers. LOQ was reported as 0,001μg/g. Levels are given in μg/g.

No.	Area	PCB 28	PCB 52	PCB 101	PCB 118	PCB 138	PCB 153	PCB 180
1B	(1)	<0,001	**0,0029**	<0,001	<0,001	<0,001	<0,001	<0,001
3B	(1)	<0,001	**0,0035**	<0,001	<0,001	<0,001	<0,001	<0,001
9A	(2)	<0,001	**0,0017**	<0,001	<0,001	<0,001	<0,001	<0,001
10B	(2)	<0,001	**0,0025**	<0,001	<0,001	<0,001	<0,001	<0,001
11A	(2)	<0,001	**0,0013**	<0,001	<0,001	<0,001	<0,001	<0,001
14A	(2)	<0,001	**0,0018**	<0,001	<0,001	<0,001	<0,001	<0,001
16A	(2)	<0,001	**0,0022**	<0,001	<0,001	<0,001	<0,001	<0,001
17A	(2)	<0,001	**0,0029**	<0,001	<0,001	<0,001	<0,001	<0,001
19B	(2)	<0,001	**0,0029**	<0,001	<0,001	<0,001	<0,001	<0,001
22B	(3)	<0,001	**0,0036**	<0,001	<0,001	<0,001	<0,001	<0,001
23B	(3)	<0,001	**0,0030**	<0,001	<0,001	<0,001	<0,001	<0,001
24A	(3)	<0,001	**0,0054**	<0,001	<0,001	<0,001	<0,001	<0,001
25B	(3)	<0,001	**0,0055**	<0,001	<0,001	<0,001	<0,001	<0,001
26A	(3)	<0,001	<0,001	<0,001	<0,001	<0,001	<0,001	<0,001
28B	(4)	<0,001	<0,001	<0,001	<0,001	<0,001	<0,001	<0,001
30A	(5)	<0,001	**0,0032**	<0,001	<0,001	<0,001	<0,001	<0,001
33A	(5)	<0,001	**0,0025**	<0,001	<0,001	<0,001	<0,001	**0,0056**
34A	(5)	<0,001	<0,001	<0,001	<0,001	<0,001	<0,001	<0,001
35A	(5)	<0,001	<0,001	<0,001	<0,001	<0,001	<0,001	<0,001
36A	(5)	<0,001	<0,001	<0,001	<0,001	<0,001	<0,001	<0,001
37A	(4)	<0,001	<0,001	<0,001	<0,001	<0,001	<0,001	<0,001
38A	(4)	<0,001	<0,001	<0,001	<0,001	<0,001	<0,001	<0,001
40A	(6)	<0,001	<0,001	<0,001	<0,001	<0,001	<0,001	**0,0049**
41A	(6)	<0,001	<0,001	<0,001	<0,001	<0,001	<0,001	**0,0037**
42B	(6)	<0,001	<0,001	<0,001	<0,001	<0,001	<0,001	**0,0055**

Table A.9: Loadings of the variables on the seven factors, which are obtained by varimax rotation. Positive loadings >0,4 and negative loadings <-0,4 are marked with bold letters.

	Component						
	1	2	3	4	5	6	7
Variance [%]	44,72	13,384	12,22	5	4,51	3,59	3,16
Y	0,126	0,199	**0,892**	0,106	-0,172	0,136	-0,003
Zr	**0,865**	0,099	0,117	-0,131	-0,024	-0,031	0,133
Cd	-0,265	**0,716**	-0,141	0,138	0,096	0,117	0,287
Mo	0,138	0,224	-0,190	-0,041	**0,888**	-0,026	0,042
Sn	0,205	0,012	0,248	0,074	0,050	**0,784**	0,347
Ce	**0,676**	**-0,408**	**0,481**	-0,111	-0,152	0,181	-0,011
Pr	**0,593**	-0,270	**0,664**	-0,071	-0,203	0,135	-0,024
Yb	-0,103	-0,072	**0,909**	0,205	-0,187	0,170	0,120
W	**-0,590**	-0,056	-0,370	-0,114	0,151	0,069	0,017
Hg	**0,681**	**0,577**	-0,049	-0,198	-0,051	-0,056	0,071
Tl	**0,926**	-0,107	0,175	0,040	0,048	0,067	0,168
Pb	**0,795**	-0,111	0,224	0,195	-0,220	0,097	0,251
U	-0,204	0,227	0,134	0,063	0,054	0,182	**0,780**
Na	**0,713**	0,075	-0,005	0,240	**-0,454**	0,005	0,017
Mg	0,146	-0,148	0,201	**0,930**	-0,064	0,085	-0,067
Al	**0,965**	-0,172	-0,033	-0,069	-0,051	0,063	-0,021
P	**0,402**	**0,609**	0,045	0,011	0,340	0,342	0,277
S	**0,556**	0,238	-0,204	-0,188	0,325	-0,332	**0,421**
Cl	0,057	**0,722**	0,262	0,021	0,140	0,184	-0,186
K	**0,921**	-0,249	0,041	0,011	-0,087	0,135	0,066
Ca	-0,323	0,165	0,057	**0,883**	0,049	0,005	0,106
V	**0,953**	-0,047	-0,067	-0,129	0,045	0,035	-0,141
Cr	**0,977**	-0,063	-0,016	-0,075	0,011	0,049	-0,062
Mn	0,308	0,241	0,082	-0,009	-0,027	**0,862**	-0,070
Fe	**0,914**	-0,206	0,037	-0,057	-0,066	0,246	-0,071
Co	**0,858**	-0,043	0,135	-0,092	0,024	0,201	-0,127
Ni	**0,917**	0,012	-0,026	-0,123	0,110	0,124	-0,201
Cu	**0,922**	0,163	0,161	-0,055	0,019	0,164	-0,077
Zn	**0,823**	0,125	0,132	0,185	-0,195	0,252	-0,136
Sr	**0,832**	0,235	-0,110	-0,157	0,006	-0,063	-0,201
Sb	-0,276	0,257	-0,279	0,110	**0,790**	0,060	0,045
As	**0,878**	-0,248	-0,238	-0,143	0,116	0,092	-0,068
Br	-0,249	0,357	**0,496**	**0,458**	0,087	-0,164	0,154
TOC	-0,356	**0,735**	-0,058	-0,065	0,341	-0,121	0,287

Table A.8: Shapiro Wilk test for normal distribution. For soil and vegetation samples. Samples with p>0,05 show a normal disribution.

Element	soil	vegetation
Y	*	p>0,05
Zr	p>0,05	
Cd	*	*
Mo	p>0,05	**
Sn	p>0,05	*
Ce	p>0,05	
Pr	p>0,05	
Yb	*	
W	*	**
Hg	p>0,05	p>0,05
Tl	p>0,05	
Pb	p>0,05	*
U	**	**
Na	*	p>0,05
Mg	**	p>0,05
Al	p>0,05	p>0,05
P	p>0,05	*
S	p>0,05	p>0,05
Cl	p>0,05	p>0,05
K	p>0,05	p>0,05
Ca	**	
V	p>0,05	
Cr	*	p>0,05
Mn	p>0,05	p>0,05
Fe	p>0,05	p>0,05
Co	p>0,05	
Ni	p>0,05	*
Cu	p>0,05	p>0,05
Zn	p>0,05	p>0,05
Sr	p>0,05	
Sb	*	*
As	*	*
Br	p>0,05	

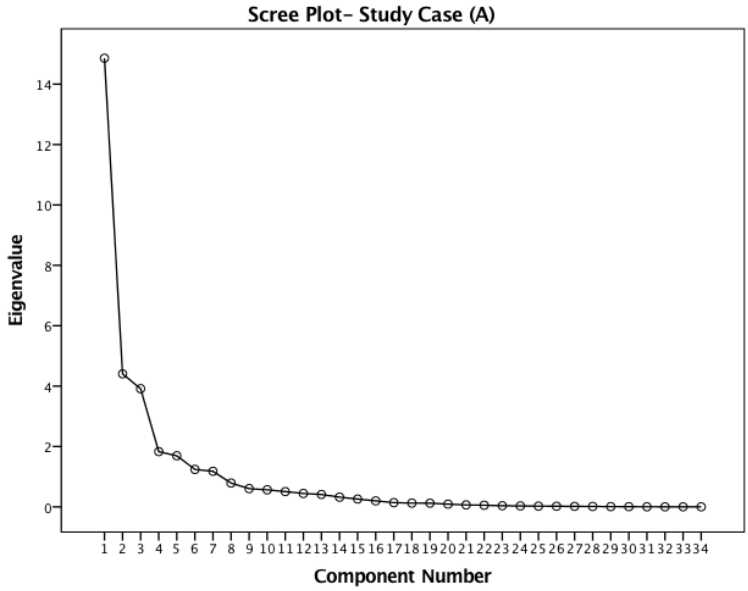

Figure A.1: Scree plot for the factor analysis of the study case (A) more described in chapter 5.4.

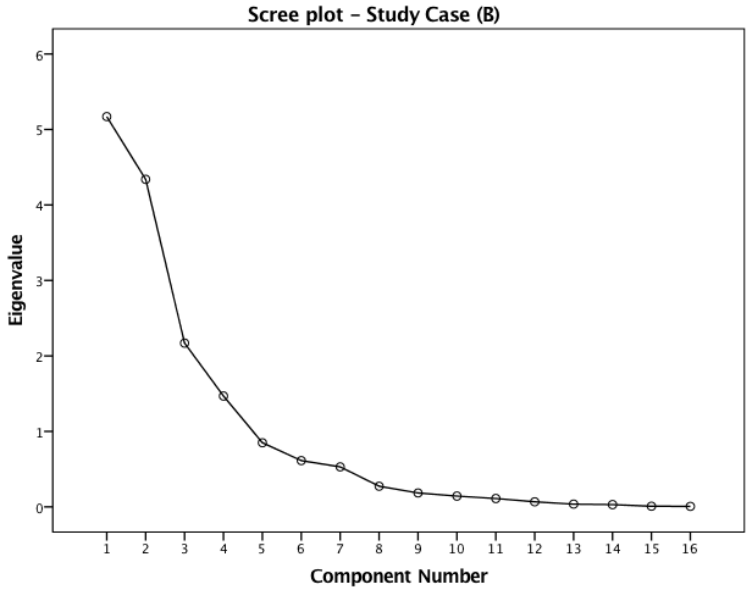

Figure A.2: Scree plot for the factor analysis of the study case (B) more described in chapter 5.4.

	Y	Zr	Cd	Mo	Sn	Ce	Pr	Yb	W	Hg	Tl	Pb	U	Na	Mg	Al	P	S	Cl	K	Ca	V	Cr	Mn	Fe	Co	Ni	Cu	Zn	Sr	Sb	As	Br	LOI
Y		,194	,025	-,257	,370	,439	,663	,888	-,374	,125	,259	,319	,147	,214	,296	,062	,199	-,168	,301	,130	,158	,063	,109	,259	,136	,251	,089	,334	,357	,081	-,355	-,206	,421	-,005
Zr	,051		-,159	,131	,255	,608	,542	-,012	-,472	,642	,860	,742	-,148	,639	-,031	,815	,452	,534	,116	,768	-,371	,765	,851	,264	,760	,731	,778	,799	,699	,656	-,296	,681	-,088	-,204
Cd	,418	,092		,304	,058	-,504	-,412	,057	,215	,189	-,269	-,147	,402	-,156	-,078	-,400	,378	,120	,366	-,398	,328	-,356	-,344	,147	-,424	-,234	-,257	-,170	-,046	-,172	,442	-,401	,276	,726
Mo	,015	,136	,005		,006	,231	-,288	-,359	,079	,164	,152	-,133	,037	-,219	-,167	,044	,479	,463	,194	,018	,026	,145	,128	,046	,008	,097	,228	,149	,065	,143	,740	,173	-,036	,456
Sn	,001	,015	,313	,479		,366	,359	,381	-,140	,125	,355	,344	,326	,167	,187	,219	,499	,022	,188	,307	,098	,164	,223	,699	,328	,254	,166	,304	,316	,092	-,020	,145	,035	-,078
Ce	,000	,000	,000	,025	,001		,954	,422	-,531	,244	,727	,758	-,187	,496	,186	,736	,035	,097	,091	,784	-,359	,623	,673	,302	,768	,699	,619	,633	,643	,404	-,514	,608	-,197	-,619
Pr	,000	,000	,000	,007	,001	,000		,601	-,558	,247	,659	,709	-,131	,488	,230	,618	,069	,043	-,007	,669	-,259	,537	,583	,284	,659	,640	,524	,612	,634	,378	-,547	,429	-,040	-,510
Yb	,000	,462	,317	,001	,000	,000	,000		-,284	,180	,108	,264	,230	,065	,390	,119	-,021	-,353	,131	,012	,261	-,206	-,130	,158	-,015	,046	-,170	,054	,152	-,272	-,346	-,351	,467	-,124
W	,001	,000	,035	,254	,120	,000	,000	,008		-,478	-,586	-,511	-,017	-,481	-,263	-,526	-,228	-,179	-,146	-,531	,077	-,509	-,535	-,242	-,543	-,452	-,482	-,581	-,505	-,447	,350	-,412	-,069	,357
Hg	,147	,000	,056	,084	,148	,019	,018	,065	,000		,545	,431	-,002	,437	-,148	,580	,641	,599	,400	,494	-,271	,633	,639	,911	,321	,859	,795	,824	,879	,744	,652	-,304	,769	-,148	-,380
Tl	,014	,000	,011	,102	,001	,001	,000	,183	,000	,000		,827	-,055	,665	,206	,903	,387	,490	,027	,909	-,260	,840	,911	,321	,859	,795	,824	,879	,744	,652	-,304	,769	-,148	-,380
Pb	,003	,000	,108	,132	,002	,000	,000	,013	,000	,000	,000		-,001	,707	,351	,779	,242	,311	,011	,837	-,104	,643	,730	,297	,774	,723	,619	,713	,774	,455	-,419	,622	-,036	-,358
U	,109	,107	,000	,378	,003	,058	,136	,026	,442	,493	,323	,497		-,154	-,007	-,235	,306	,112	,185	-,145	,245	-,280	-,254	,091	-,220	-,194	-,268	-,104	-,199	-,300	,202	-,270	,315	,420
Na	,036	,000	,095	,032	,081	,000	,000	,293	,000	,000	,000	,000	,098		,303	,678	,179	,196	,026	,679	-,064	,605	,671	,244	,636	,561	,567	,657	,709	,544	-,456	,448	-,098	-,332
Mg	,006	,398	,256	,081	,058	,058	,026	,000	,013	,107	,041	,001	,476	,005		,108	,010	-,220	,007	,206	,762	,030	,085	,091	,143	,088	,022	,103	,345	-,061	,092	-,002	,368	-,285
Al	,303	,000	,000	,358	,033	,000	,000	,160	,000	,000	,000	,000	,023	,000	,184		,269	,443	,027	,975	-,414	,949	,975	,298	,944	,831	,897	,875	,770	,754	-,340	,921	-,355	-,482
P	,047	,000	,001	,000	,000	,385	,283	,429	,027	,000	,000	,020	,004	,066	,467	,011		,484	,434	,221	,035	,346	,371	,567	,298	,319	,369	,502	,388	,413	,287	,230	,211	,450
S	,079	,000	,158	,000	,427	,209	,360	,001	,066	,000	,000	,004	,175	,049	,032	,000	,000		,035	,362	-,222	,502	,484	-,076	,314	,344	,427	,408	,220	,601	,155	,493	-,100	,251
Cl	,005	,165	,001	,051	,057	,223	,476	,136	,110	,000	,411	,462	,059	,414	,476	,412	,000	,386		-,047	,113	,036	-,029	,076	,110	,246	,146	,152	,228	-,093	,343	,442	
K	,139	,000	,000	,439	,004	,000	,000	,462	,000	,000	,000	,000	,113	,000	,041	,000	,031	,001	,347		-,332	,877	,927	,323	,935	,800	,829	,841	,759	,638	-,373	,870	-,323	-,521
Ca	,093	,001	,002	,413	,207	,001	,014	,013	,259	,011	,014	,191	,019	,298	,000	,000	,387	,031	,172	,002		-,435	-,402	-,081	-,398	-,370	-,412	-,310	-,124	-,344	,231	-,464	,528	,238
V	,300	,000	,001	,112	,084	,000	,000	,041	,000	,000	,000	,000	,009	,000	,402	,000	,001	,000	,381	,000	,000		,972	,299	,910	,842	,922	,896	,757	,882	-,239	,906	-,367	-,391
Cr	,181	,000	,002	,142	,030	,000	,000	,138	,000	,000	,000	,000	,016	,000	,239	,000	,001	,000	,413	,000	,000	,000		,319	,927	,833	,919	,917	,789	,820	-,285	,890	-,310	-,412
Mn	,014	,012	,109	,350	,000	,005	,008	,092	,020	,009	,003	,006	,224	,020	,223	,005	,000	,264	,002	,003	,248	,005	,003		,467	,444	,413	,471	,495	,263	,063	,291	,035	,092
Fe	,127	,000	,000	,473	,002	,000	,000	,450	,000	,000	,000	,000	,032	,000	,116	,000	,006	,004	,404	,000	,000	,000	,000	,000		,858	,864	,864	,802	,713	,360	,886	,325	,545
Co	,017	,000	,024	,209	,016	,000	,000	,352	,000	,000	,000	,000	,051	,000	,231	,000	,003	,002	,263	,000	,001	,000	,000	,000	,000		,887	,873	,821	,710	,274	,768	,258	,355
Ni	,229	,000	,015	,027	,081	,000	,000	,077	,000	,000	,000	,000	,011	,000	,427	,000	,001	,000	,179	,000	,000	,000	,000	,000	,000	,000		,912	,772	,815	,185	,866	,326	,336
Cu	,002	,000	,077	,106	,005	,000	,000	,326	,000	,000	,000	,000	,193	,000	,196	,000	,000	,000	,019	,000	,004	,000	,000	,000	,000	,000	,000	,830	,807	,240	,751	,173	,239
Zn	,001	,000	,350	,293	,003	,000	,000	,102	,000	,000	,000	,000	,047	,000	,002	,000	,000	,032	,111	,000	,150	,000	,000	,000	,000	,000	,000	,000	,665	,327	,623	,126	,337
Sr	,248	,000	,075	,115	,222	,000	,001	,010	,000	,000	,000	,000	,005	,000	,305	,000	,000	,000	,102	,000	,002	,000	,000	,013	,000	,000	,000	,000	,000	,177	,731	,279	,162
Sb	,001	,006	,000	,000	,432	,000	,000	,001	,001	,323	,005	,000	,044	,000	,220	,002	,007	,097	,027	,001	,025	,021	,008	,299	,001	,010	,060	,021	,003	,068		,172	,104	,568
As	,041	,000	,000	,074	,113	,000	,000	,001	,000	,000	,000	,000	,011	,000	,493	,000	,026	,000	,219	,000	,000	,000	,000	,007	,000	,000	,000	,000	,000	,000	,074		,456	,479
Br	,000	,231	,009	,380	,387	,048	,369	,000	,281	,160	,107	,382	,004	,205	,001	,001	,038	,202	,002	,003	,000	,001	,004	,386	,003	,014	,003	,073	,145	,009	,192	,000		,343
LOI	,483	,042	,000	,000	,257	,000	,000	,150	,001	,072	,000	,001	,000	,002	,008	,000	,000	,017	,000	,000	,022	,000	,000	,220	,000	,001	,002	,022	,002	,088	,000	,000	,002	

Figure A.3: Pearson correlation for all measured elements in surface soil samples. The upper half shows the pearson correlation, while the lower part shows the significance of the correlation. High correlated elements (r>0,8) are highlighted grey. Correlation coefficients with no significance (p>0,05) are in grey letters.

	Y	Zr	Cd	Mo	Sn	Ce	Pr	Yb	W	Hg	Tl	Pb	U	Na	Mg	Al	P	S	Cl	K	Ca	V	Cr	Mn	Fe	Co	Ni	Cu	Zn	Sr	Sb	As	Br
Y		-,008	0,046	-,120	,441	,221	,489	,943	-,260	,118	,078	,078	,310	,093	,341	-,027	,156	-,155	,429	,017	,427	,010	-,007	,332	-,004	,131	,071	,226	,210	,045	-,254	-,113	,554
Zr	,946		-,114	,481	,116	,500	,347	-,129	-,483	,574	,815	,669	-,093	,673	,433	,806	,289	,535	-,009	,770	-,419	,757	,818	,236	,734	,652	,744	,670	,585	,657	-,144	,753	-,246
Cd	,698	,335		,133	-,069	-,526	-,478	,070	,176	,164	-,215	-,118	,243	-,119	-,174	-,330	,381	,154	,488	-,337	,563	-,335	-,321	,255	-,361	-,144	-,191	-,118	,089	-,097	,374	-,321	,300
Mo	,308	,000	,258		,049	,054	-,055	-,270	-,460	,516	,531	,181	-,155	,170	,116	,455	,712	,656	,311	,380	-,181	,474	,514	,301	,453	,489	,580	,582	,367	,549	,489	,560	-,008
Sn	,000	,324	,558	,678		,314	,326	,488	-,081	-,003	,229	,187	,290	,050	,287	,110	,009	-,038	,134	,189	,238	,055	,095	,206	,171	,125	,063	,148	,132	,018	,085	,047	,230
Ce	0,06	,000	,000	,648	,006		,917*	,152	-,378	,122	,638	,685	-,056	,483	,582	,698	-,211	,046	-,322	,759	-,509	,633	,642	,243	,721	,640	,578	,521	,532	,318	-,413	,628	-,341
Pr	,000	,000	,000	,643	,005	,000		,392	-,420	,111	,507	,573	-,035	,436	,599	,560	-,171	-,019	-,178	,620	-,300	,542	,517	,239	,581	,556	,475	,486	,502	,296	-,491	,462	-,142
Yb	,000	,272	,554	,020	,000	,195	,000		-,080	-,027	-,042	-,002	,472	-,041	,272	-,189	,038	-,305	,383	-,116	,517	-,180	-,174	,247	-,159	-,060	-,113	,046	,048	-,183	-,200	-,269	,579
W	,025	,000	,133	,000	,493	,000	,000	,497		-,534	-,710	-,452	,285	-,569	-,577	-,677	-,365	-,389	-,113	-,648	,269	-,717	-,711	-,347	-,633	-,572	-,677	-,772	-,567	-,715	,131	-,660	,126
Hg	,316	,000	,163	,000	,977	,301	,348	,821	,000		,511	,370	-,276	,453	,319	,567	,662	,554	,415	,478	-,167	,588	,602	,412	,479	,459	,581	,661	,516	,719	,059	,542	-,070
Tl	,509	,000	,066	,000	,050	,000	,000	,721	,000	,000		,763	-,095	,713	,640	,899	,273	,484	-,063	,908	-,437	,841	,900	,340	,849	,757	,817	,833	,658	,650	-,144	,849	-,283
Pb	,510	,000	,318	,122	,111	,000	,000	,986	,000	,000	,000		-,034	,767	,700	,788	,036	,283	-,120	,840	-,306	,713	,728	,383	,774	,689	,633	,610	,733	,492	-,321	,718	,203
U	,007	,429	,037	,188	,012	,634	,765	,000	,014	,017	,423	,775		-,213	-,041	-,342	,020	-,072	,132	-,245	,571	-,431	-,332	-,127	-,353	-,352	-,353	-,285	-,307	-,527	,005	-,382	,506
Na	,430	,000	,313	,148	,671	,000	,000	,728	,000	,000	,000	,000	,069		,718	,772	,135	,296	-,056	,795	-,248	,736	,750	,351	,721	,614	,659	,674	,718	,647	-,325	,671	,214
Mg	,003	,000	,137	,325	,013	,000	,000	,019	,000	,006	,000	,000	,731	,000		,670	,080	,072	,038	,730	,067	,657	,642	,394	,652	,560	,588	,640	,676	,437	-,284	,601	,014
Al	,820	,000	,000	,000	,351	,000	,000	,107	,000	,000	,000	,000	,000	,000	,000		,197	,430	,153	,978	-,591	,973	,980	,379	,956	,843	,898	,849	,756	,773	,226	,950	-,404
P	,186	,013	,000	,000	,939	,073	,149	,751	,000	,000	,019	,760	,869	,256	,501	,095		,519	,617	,122	,216	,244	,274	,418	,191	,239	,315	,437	,309	,414	,368	,228	,289
S	,187	,000	,190	,000	,748	,695	,871	,008	,000	,000	,000	,015	,540	,010	,544	,000	,000		,129	,345	,098	,458	,467	,012	,349	,367	,442	,400	,241	,658	,134	,489	,058
Cl	,000	,943	,000	,007	,259	,005	,133	,000	,343	,000	,595	,311	,267	,638	,752	,196	,000	,277		,179	,463	,109	,124	,305	,162	,004	,017	,166	,095	,081	,296	,155	,592
K	0,88	,000	,000	,000	,107	,000	,000	,325	,000	,000	,000	,000	,036	,000	,000	,000	,304	,000	,130		-,546	,926	,945	,386	,949	,826	,849	,820	,762	,677	-,260	,909	-,387
Ca	,000	,000	,000	,123	,041	,000	,009	,000	,020	,155	,000	,008	,000	,033	,572	,000	,066	,405	,000	,000		-,562	-,574	,027	-,581	-,457	-,488	-,380	-,239	-,333	,154	-,610	,697
V	0,93	,000	,000	,000	,644	,000	,000	,126	,000	,000	,000	,000	,000	,000	,000	,000	,037	,000	,359	,000	,000		,970	,357	,938	,847	,903	,845	,746	,846	-,205	,941	-,371
Cr	0,95	,000	,005	,000	,420	,000	,000	,138	,000	,000	,000	,000	,000	,000	,000	,000	,019	,000	,296	,000	,000	,000		,351	,935	,812	,900	,867	,735	,797	-,173	,936	-,377
Mn	,000	,043	,028	,009	,078	,037	,041	,034	,000	,000	,000	,000	,282	,000	,000	,000	,000	,917	,009	,000	0,82	,000	,000		,467	,590	,517	,569	,652	,325	,063	,383	,084
Fe	0,98	,000	,000	,000	,144	,000	,000	,176	,000	,000	,000	,000	,000	,000	,000	,000	,000	,106	,000	,172	,000	,000	,000	,000		,871	,862	,819	,787	,731	-,183	,929	-,378
Co	0,27	,000	,220	,000	,287	,000	,000	,614	,000	,000	,000	,000	,000	,000	,000	,000	,000	,042	,000	,970	,000	,000	,000	,000	,000		,883	,830	,816	,704	-,125	,832	-,265
Ni	0,55	,000	,103	,000	,594	,000	,000	,338	,000	,000	,000	,000	,000	,000	,000	,000	,000	,007	,000	,889	,000	,000	,000	,000	,000	,000		,900	,760	,789	-,062	,899	-,300
Cu	0,05	,000	,316	,000	,208	,000	,000	,699	,000	,000	,000	,000	,014	,000	,000	,000	,000	,000	,000	,161	,000	,000	,000	,000	,000	,000	,000		,758	,747	-,051	,816	-,178
Zn	0,07	,000	,449	,000	,261	,000	,000	,683	,000	,000	,000	,000	,008	,000	,000	,000	,000	,008	,039	,423	,000	,040	,000	,000	,000	,000	,000	,000		,663	-,122	,705	-,182
Sr	0,7	,000	,412	,000	,877	,006	,011	,118	,000	,000	,000	,000	,000	,000	,000	,000	,000	,000	,000	,496	,000	,000	,000	,005	,000	,000	,000	,000	,000		-,045	,791	-,229
Sb	0,03	,221	,000	,000	,472	,000	,000	,087	,266	,620	,220	,005	,966	0,01	,014	,053	,000	,254	,011	,025	,190	,079	,141	,591	,118	,288	,599	,668	,300	,706		-,083	,200
As	0,34	,000	,005	,000	,690	,000	,000	,020	,000	,000	,000	,000	,000	,000	,000	,000	,052	,000	,190	,000	,000	,000	,000	,000	,000	,000	,000	,000	,000	,000	,480		-,378
Br	,000	,034	,009	,946	,048	,000	,229	,000	,285	,554	,015	,083	,000	0,07	,904	,000	,013	,622	,000	,000	,000	,000	,000	,478	,000	,023	,009	,129	,120	,050	,088	,000	

Figure A.4: Spearman rank correlation for all measured elements in surface soil samples. The upper half shows the correlation (Spearman ρ), while the lower part shows the significance of the correlation. High correlated elements (ρ>0,7) are highlighted grey. Correlation coefficients with no significance (p>0,05) are in grey letters.